THESIS FOR THE DEGREE OF DOCTOR OF PHILOSOPHY

Numerical analysis of geostructures stabilised with lime-cement columns in soft clays

SINEM BOZKURT

Department of Architecture and Civil Engineering

Division of Geology and Geotechnics

CHALMERS UNIVERSITY OF TECHNOLOGY

Gothenburg, Sweden 2025

Numerical analysis of geostructures stabilised with lime-cement columns in soft clays
SINEM BOZKURT
ISBN 978-91-8103-280-2

Doktorsavhandlingar vid Chalmers tekniska högskola
Ny serie nr. 5738
ISSN 0346-718X
Department of Architecture and Civil Engineering
Division of Geology and Geotechnics
Chalmers University of Technology
SE-412 96 Gothenburg
Sweden
Telephone: +46 (0)31-772 1000

Chalmers Digitaltryck
Gothenburg, Sweden 2025

Numerical analysis of geostructures stabilised with lime-cement columns in soft clays
Thesis for the degree of Doctor of Philosophy
SINEM BOZKURT
Department of Architecture and Civil Engineering
Division of Geology and Geotechnics
Chalmers University of Technology

ABSTRACT

Urban infrastructure is increasingly built on soft natural clays with high compressibility due to the limited availability of land in congested areas, while existing transport infrastructure faces increasing maintenance costs due to excessive displacement. Dry Soil Mixing (DSM) is a widely used soil improvement solution for road embankments and deep excavations especially in Scandinavian countries, where stabilising agents, such as lime, cement, or alternative binders, are mixed into *in situ* soil as dry powders. Although DSM offers a cost-effective and rapid application, it is associated with high carbon emissions mainly due to the energy-intensive production of lime and cement. Current practices for the numerical analysis of geostructures (i.e. road embankments and excavations) stabilised with DSM rely on simplified semi-empirical methods, which do not realistically capture the time-dependent behaviour of the stabilised system and disregard the inherent three-dimensional (3D) interaction effects as well as installation effects. Consequently, more accurate and computationally efficient methods are needed to optimise designs with DSM for serviceability.

This research investigates the hydromechanical response of soft natural clays stabilised with lime-cement columns for deep excavations and embankments using the finite element method. In the first part of the research, installation effects were back-calculated from the field data following the Observational Method. Advanced soil models were employed to represent the elastoplastic behaviour of natural clay and deep-mixed columns in the 2D and 3D simulations. A rate-dependent advanced soil model for the natural clay enabled the calculation of long-term displacement predictions, which were validated against the field measurements.

In the second part, the stress-strain response of the composite system of a stabilised excavation was examined considering the different hydromechanical responses of natural clay and columns, respectively. A new numerical scheme, utilising Volume Averaging Technique (VAT), was developed specifically for excavations. VAT for excavations was implemented in a 2D finite element framework to model the composite behaviour of regularly spaced deep-mixed columns and *in situ* clay. This new formulation is a computationally efficient alternative to true 3D analysis, while proving a comparable response. The robustness of VAT, using the existing formulation for embankments, was demonstrated through global sensitivity analyses of stabilised embankments for long-term deformation predictions. System-level analyses explored optimisation scenarios to minimise climate impact. The results highlight that with VAT the responses of the *in situ* clay and the columns can be accounted for in a plane strain analysis for efficient performance-based design with high fidelity.

Keywords: deep excavation, deep mixing, lime-cement columns, soft clay, volume averaging, numerical modelling, embankments, homogenisation

ACKNOWLEDGEMENTS

The research presented in this thesis was conducted in the Division of Geology and Geotechnics of Chalmers University of Technology, spanning October 2020 to October 2025. The project was funded by Formas (Research Council for Sustainable Development) through grant 2019-00456 and by the Swedish Transport Administration through grants 2020/46703 and 2024/27461 under BIG (Branchsamverkan i grunden) initiative. The work is also a part of the Digital Twin Cities Centre, which is supported by Sweden's Innovation Agency VINNOVA through grants 2019-00041 and 2024-03904. The author would like to extend her gratitude to Jonatan Isaksson from NCC AB for providing the laboratory and field data necessary for this project.

I would like to thank and sincerely acknowledge my supervisor, Minna Karstunen. It has been a privilege to have her continuous support, unwavering positivity, and guidance throughout this research. I am grateful to the seniors in the Geotechnics group, my co-supervisor Ayman Abed, my examiner Jelke Dijkstra, and Mats Karlsson for sharing their expertise and inspiring me to grow as a researcher.

I would like to extend my appreciation to Stefan Larsson from KTH for his valuable contributions to this work and for generously sharing his expertise.

I thank all my former and current colleagues at Chalmers for inspiring discussions, good humour, and your kindness. You made me feel at home, and I will always remember.

Lastly, to my family in Turkey, Germany, and Sweden, thank you for always encouraging my love of learning and growth. Your support during hard times, your joy, and your reminders of what truly matters mean the world to me.

Sinem Bozkurt
Gothenburg, 2025

LIST OF PUBLICATIONS

This thesis consists of an extended summary and the following appended papers:

Paper A Bozkurt, S., Abed, A., & Karstunen, M. (2023b). Finite element analysis for a deep excavation in soft clay supported by lime-cement columns. *Computers and Geotechnics*, *162*, 105687. https://doi.org/10.1016/j.compgeo.2023.105687

Paper B Bozkurt, S., Abed, A., & Karstunen, M. (2023a). 2D & 3D numerical analyses of a deep excavation supported by LC columns. In L. Zdravković, S. Kontoe, D. Taborda, & A. Tsiampousi (Eds.), *Proceedings of the 10th European Conference on Numerical Methods in Geotechnical Engineering* (pp. 1–6). International Society for Soil Mechanics and Geotechnical Engineering. https://doi.org/10.53243/NUMGE2023-188

Paper C Bozkurt, S., Abed, A., & Karstunen, M. (2025b). Homogenisation method for braced excavations stabilised with deep-mixed columns. *Computers and Geotechnics*, *181*, 107095. https://doi.org/10.1016/j.compgeo.2025.107095

Paper D Bozkurt, S., Abed, A., & Karstunen, M. (2025a). Alternative ways of modelling stabilised excavations. *Proceedings of the 19th Nordic Geotechnical Meeting – Göteborg 2024 (SGF Report 1:2025)*, *1*, 160–173. Swedish Geotechnical Society. https://ngm2024.se/program/SGF%20R1-2025%20NGM%20volume%201.pdf

Paper E Bozkurt, S., Dijkstra, J., & Karstunen, M. (2025c). Influential factors on the performance of embankments stabilised on deep-mixed columns. *Transportation Geotechnics*, *55*, 101643. https://doi.org/10.1016/j.trgeo.2025.101643

The author carried the main responsibility for the work presented in the appended papers.

For all papers, this work included developing the methodology, conceptualisation, formal analyses, software development, implementation, visualisation, and writing the original drafts. Co-authors contributed through supervision, reviewing, and editing.

OTHER RELATED PUBLICATIONS

- Bozkurt, S., & Akbas, S. O. (2023). Finite element-based geotechnical risk analysis for anchor-supported deep excavations. *Arabian Journal of Geosciences*, *16*(8), 470. https://doi.org/10.1007/s12517-023-11463-5

TABLE OF CONTENTS

NOTATION

Abbreviations

CAUC	anisotropically consolidated undrained triaxial compression test
CAUE	anisotropically consolidated undrained triaxial extension test
CRS	constant rate of strain
CSS	current stress surface
DOE	Design of Experiments
DSM	deep soil mixing
FE	finite element
FEM	finite element method
GHE	greenhouse gas emissions
ICS	instrinsic compression surface
IL	incrementally loaded oedometer test
LC	lime and cement
NC	normally consolidated
NCS	normal compression surface
OCR	overconsolidation ratio
SPW	sheet pile wall
UCS	unconfined compressive strength test
UDSM	User-Defined Soil Model
VAT	Volume Averaging Technique

Greek symbols

$(\Delta\sigma)^{cor}$	out-of-balance stress between clay and columns
α_0	initial amount of anisotropy
β	relative effectiveness of rotational hardening
χ_0	initial amount of bonding
Δu	incremental nodal displacement vector
$\Delta\sigma$	increments of stress
$\Delta\varepsilon$	increments of strain
$\Delta\sigma^c$	increments of stress in column material
$\Delta\sigma^{eq}$	increments of stress in equivalent material
$\Delta\sigma^s$	increments of stress in clay material
$\Delta\varepsilon^c$	increments of strain in column material
$\Delta\varepsilon^{eq}$	increments of strain in equivalent material
$\Delta\varepsilon^s$	increments of strain in clay material
$\dot{\Lambda}$	rate-dependent viscoplastic multiplier
$\dot{\varepsilon}_d^c$	viscoplastic deviatoric strain
$\dot{\varepsilon}_v^c$	viscoplastic volumetric strain
γ,γ'	unit weight, submerged unit weight
γ_s^{ps}	accumulated deviatoric plastic shear strain
γ_{xy}	shear total strain on the plane normal to the x-axis in the direction of the y-axis
γ_{yz}	shear total strain on the plane normal to the y-axis in the direction of the z-axis
γ_{zx}	shear total strain on the plane normal to the z-axis in the direction of the x-axis
κ	slope of the swelling line
λ_{i}	slope of the intrinsic normal compression line
λ_{i}^*	modified intrinsic compression index
μ	
μ_{i}^*	modified intrinsic creep index
ν	Poisson's ratio
Ω_c	volume fraction of column
Ω_s	volume fraction of clay
ϕ'	effective friction angle
σ'^{ref}	reference effective stress
σ'_1	major principal effective stress
σ'_2	intermediate principal effective stress
σ'_3	minor principal effective stress
σ'_{xx}	normal effective stress acting on the x-axis
σ'_{yy}	normal effective stress acting on the y-axis
σ'_{zz}	normal effective stress acting on the z-axis
τ	reference time
τ_{xy}	shear stress on the plane normal to the x-axis in the direction of the y-axis
τ_{yz}	shear stress on the plane normal to the y-axis in the direction of the z-axis
τ_{zx}	shear stress on the plane normal to the z-axis in the direction of the x-axis
ε_1	major principal total strain
ε_2	intermediate principal total strain
ε_3	minor principal total strain
ε_d^e	elastic deviatoric strain
ε_d^p	plastic deviatoric strain
ε_v^e	elastic volumetric strain

ε_v^p	plastic volumetric strain
ε_{xx}	normal total strain acting on the x-axis
ε_{yy}	normal total strain acting on the y-axis
ε_{zz}	normal total strain acting on the z-axis
η	stress ratio
ω	absolute rate of rotational hardening due to volumetric strain
ω_{d}	relative rate of rotational hardening due to deviatoric strain

Roman lower case letters

a	absolute rate of destructuration due to volumetric strain
b	relative rate of destructuration due to volumetric strain
c	notation for column material
c'	apparent cohesion
c_{u}	undrained shear strength
c_{h}	horizontal coefficient of consolidation
c_{k}	permeability change index
c_{v}	vertical coefficient of consolidation
e_0	initial void ratio
eq	notation for equivalent material
k	hydraulic conductivity
m	extent of stiffness dependency
p'	mean effective stress
p'_m	initial mean effective stress at preconsolidation pressure
p'_{mi}	size of the intrinsic yield surface
p_w	pore pressure
q	deviatoric stress
q_a	asymptotic deviatoric stress
q_f	deviatoric stress at failure
r_c	column radius
s	notation for clay material
s_{ij}	modified deviatoric stress tensor

Roman capital letters

C_α	secondary compression index
C_{c}	compression index
D	elastic constitutive matrix
D^c	elastic constitutive matrix of the column material
D^{eq}	elastic constitutive matrix of the equivalent material
D^s	elastic constitutive matrix of the clay material
E'_{50}	effective secant stiffness from triaxial tests
E'_{oed}	effective oedometric stiffness from triaxial tests
E'_{ur}	effective unloading reloading stiffness from triaxial tests
E_{50}	secant stiffness from UCS
G	shear stiffness
G_{50}^{ref}	reference secant shear stress
G_{ur}^{ref}	reference unloading reloading shear stiffness
I_1	first effective stress invariant
I_2	second effective stress invariant
I_3	third effective stress invariant
K'	drained bulk modulus
K_0	coefficient of earth pressure at rest
K_0^{nc}	coefficient of earth pressure at rest for normally consolidated state
K_f	equivalent bulk modulus
K_u	undrained bulk modulus
M_{c}	stress ratio at critical state in triaxial compression
M_{e}	stress ratio at critical state in triaxial extension
R_f	failure ratio of deviatoric stress
S_1	strain redistribution matrix
S_s	structural matrix
U	average degree of consolidation

Part I
Extended summary

1 Introduction

1.1 Background

Constructions in urban settings often take place on soft or problematic soils, which are characterised by low bearing capacity and high compressibility due to the limited availability of land in densely populated areas. In response to the climate change and the growing concerns about the depletion of non-renewable resources, such constructions demand sustainable ground improvement solutions. Soil improvement in these areas can be carried out using designs that minimise carbon dioxide (CO_2) emissions and cumulative energy demand over the life cycle of infrastructure projects (SS-EN ISO 14067:2018 2018). Consequently, in infrastructure construction on soft clays, methods with less environmental impact, such as stone columns, lime-cement columns, vibro-compaction, and prefabricated vertical drains are increasingly being applied (e.g. Ou et al. 2008; Indraratna et al. 2010; Pothiraksanon et al. 2010; Ignat et al. 2016; Jamsawang et al. 2016a; Marte et al. 2017; Ignat et al. 2020; Pandey et al. 2022) in contrast to piling.

The use of Dry Soil Mixing (DSM) method with individual or overlapping lime-cement (LC) columns has become a common solution to improve soft natural clays for the construction of deep excavations and road embankments, especially in the Nordic countries. The method offers reduced construction costs compared to concrete piles (Zöhrer et al. 2010), along with a rapid application procedure. However, significant amounts of materials and energy required for the construction of LC columns result in considerable anthropogenic greenhouse gas emissions (GHE), mainly due to the carbon-intensive manufacturing of lime (Oates 1998; Simoni et al. 2022) and cement (Taylor 1997; Worrell et al. 2001; IEA 2023). Less carbon-intensive materials and/or replacing CEM I (Ordinary Portland cement) with alternative binders (by-products, i.e. blast furnace slag) have been explored as potential substitutes to mitigate environmental impacts (Åhnberg and Holm 1999; Boehm et al. 2005; Sargent et al. 2016; Hov et al. 2022; Ramírez and Korkiala-Tanttu 2023; Kono and Fujisawa 2024; Forsman et al. 2025). Although the use of such alternatives can contribute to the reduction of CO_2 emissions, their effectiveness remains limited by factors such as material availability, performance requirements, and industry adoption rates (Cheng et al. 2023).

The processes involved in stabilising natural clay with lime and cement are highly complex and entail intricate chemical reactions resulting in time dependent hydromechanical response between the *in situ* clay and the stabilising agents. These complexities make it challenging to obtain accurate predictions of the system response with numerical analyses. Additionally, the field evidence concerning large deformations resulting from installation effects in the mixing process, despite reported scarcely, i.e. O'Rourke and O'Donnell (1997) and Wang and Whittle (2024), necessitates the consideration of these effects either directly using adaptive and innovative techniques, such as the Observational Method (Peck 1969; EN 1997-1 2005; Apoji et al. 2023; Patel 2024) or indirectly incorporating these effects in the simulations through modifying numerical model parameters to match the observed response. Consequently, there is a growing need for more accurate, computationally efficient, methods to predict the displacements, enabling further optimisation of designs with DSM to reduce material use and associated GHE.

In traditional design, a common procedure is to ignore any installation effects (e.g. wished-in-place) and adopt simple semi-empirical solutions to describe the behaviour of deep-mixed columns (EuroSoilStab 2002; Bruce et al. 2013; SGF 2000). However, in numerical modelling,

using simplified methods based on elasticity theory and/or considering only one-dimensional compression mechanisms, represented by uniaxial testing, do not provide a real representation of the deep-mixed column behaviour. The elastoplastic soil response in embankments and excavations supported by DSM columns is a three-dimensional (3D) problem governed by stiffnesses, which depends on effective stress paths and stress history for Serviceability Limit State (SLS). Moreover, the different non-linear elastoplastic responses of the individual materials (*in situ* natural clay and LC columns) in the composite system need to be accounted for in numerical analyses at the system level in order to realistically estimate both horizontal and vertical displacements.

Realistic modelling of a composite system, made of two or more periodically arranged materials, is possible through finite element analysis (FEA) using a well-established homogenisation method (Hill 1963; Hashin 1983; van der Sluis et al. 1999; van Dijk 2016; Edefors et al. 2025) that accounts for the stress–strain responses of the individual materials. Macroscopic stresses and strains in the composite system are calculated by applying known boundary conditions to determine the local fields of displacements, strains, and stresses for each constituent material at the interface.

Volume Averaging Technique (VAT) is a powerful numerical method that employs homogenisation procedures within the context of geotechnical engineering (Schweiger and Pande 1986; Canetta and Nova 1989; Lee and Pande 1998; Omine et al. 1999; Jellali et al. 2005; Vogler and Karstunen 2008) for the numerical analysis of road embankments stabilised with regularly spaced columnar inclusions, such as stone columns and deep mixed columns. VAT enables system-level modelling of the 3D composite system, comprising columns and *in situ* soil, in 2D plane strain analyses. The technique is computationally efficient and thus allows for easy incorporation of optimisation procedures.

This research is motivated by the limitations of existing design methods for the numerical analysis of stabilised geostructures (embankments and excavations) in plane strain analysis. The complex 3D interactions between deep-mixed columns and soft clays are often oversimplified, and the different elastoplastic responses of the constituents of the composite material are neglected. Improving the predictive accuracy and computational efficiency is essential for both performance-based design and sustainability, particularly in reducing CO_2 emissions from lime and cement use through material-efficient designs.

1.2 Aim and Objectives

The aim of this thesis is to investigate the time-dependent stress–strain response of deep excavations and embankments stabilised with LC columns in soft natural clays. To accurately predict the system-level response, the interactions among the substructure (road embankments or braced excavations), soft natural clay, and LC columns will be studied using 2D and 3D finite element analyses.

The 3D problem of an embankment on soft clay on periodic ground improvement with VAT has already been developed (Vogler 2008; Abed et al. 2025). The original contribution of this thesis is to further develop VAT and to implement VAT for 2D plane strain analysis of deep excavations stabilised with LC columns. VAT captures the coupled response of stabilised clay by accounting for the behaviour of individual materials, while also providing a practical tool for accurate and efficient predictions for SLS and enabling optimisation, as demonstrated in the thesis.

The main objectives are listed below:

(i) Investigate the installation effects of LC columns and incorporate these effects to numerical analyses using the Observational Method to estimate the hydromechanical response of a well-documented braced excavation (the West Link railway project, Gothenburg) for SLS through both 2D and 3D simulations.

(ii) Identify the interaction mechanisms (i.e. stress and strain distributions) between the columns and the *in situ* soft clay in the context of braced excavations supported by densely spaced LC columns in the passive side.

(iii) Develop Volume Averaging Technique (VAT) for the equivalent-continuum modelling of deep excavations stabilised with LC columns, and implement the technique to a 2D finite element code, based on the individual material responses identified.

(iv) Compare alternative modelling strategies, including 2D simulations using a simple stiffness/strength averaging method and using VAT, as well as a 3D simulation with discrete columns, in terms of their ability to capture displacements and structural forces for a braced excavation.

(v) Systematically perform sensitivity analyses using the method of Design of Experiments (DOE) in combination with VAT to identify the most influential constitutive parameters governing the time-dependent deformations under embankment loading.

(vi) Explore case-specific optimisation of deep mixing for embankments using VAT, considering column length and configuration, and the relative stiffness between soft clay and LC columns, to minimise lime and cement use and related CO_2 emissions, while meeting the displacement limits for serviceability.

1.3 Limitations

The installation effects resulting from the construction of deep-mixed columns were integrated into numerical analyses by utilising the field-monitoring data collected during the early stages of the construction. As a result, qualitative measures and the direction of the expansive and contractive volumetric strains caused by the installation effects cannot be directly extrapolated to similar projects. The field evidence suggests that the values for the external strains to be integrated should be obtained from case-specific field monitoring data as an integral part of implementing Observational Method.

The time-dependent evolution of strength and stiffness, as well as creep, of the deep-mixed columns was not considered in this study. Additionally, both the stabilised and natural clay were assumed to be fully saturated porous continuous medium, where only macroscopic stresses and strains are considered under quasi-static conditions, excluding any particulate or microscopic-level interactions or existing forces. Any potential effects of partial saturation on the behaviour of deep-mixed columns are left for future research. Finally, the effect of temperature (due to the heat generated during curing) is not taken into account in the numerical simulations.

1.4 Outline

This thesis consists of two parts: Part I - Extended summary and Part II - Appended papers.

The outline of Part I is presented below:

- Chapter 2 *Deep mixing for stabilising geostructures in soft clays*. This chapter presents a focussed literature review on the deep mixing method, the characteristics of soft natural clays, and deep excavations and embankments in soft clay deposits. It is divided into four main sections. The first section provides a brief overview of deep soil mixing. The second section examines the key characteristics and mechanical behaviour of soft natural clays. Finally, the third and fourth sections discuss deep excavations and embankments constructed in soft clays, including field performance and numerical analyses.
- Chapter 3 *Methodology*. This study adopts the following methodological framework. Six sections are outlined: *i)* The first section introduces the homogenisation method which is the key contribution of this research; *ii)* The second section presents the capabilities of the technique in modelling the hydromechanical response of embankments constructed on soft clays stabilised with columnar inclusions, such as stone columns or deep-mixed columns, as demonstrated in previous studies; *iii)* The third section defines a plane strain formulation to represent the stabilised clay with deep-mixed columns in *in situ* soft natural clay by examining the stress-strain distribution of the individual materials using different constitutive models for deep excavations; *iv)* The fourth section briefly describes the constitutive models adopted in this study. The behaviour of the *in situ* soft clay is represented by employing the Creep–SCLAY1S (Sivasithamparam et al. 2015; Gras et al. 2018) and the S–CLAY1S (Koskinen et al. 2002; Karstunen et al. 2005) models, while the deep-mixed columns are represented by the MNhard (Benz 2007) model; *v)* The fifth section discusses robust sensitivity analyses and provides details of the systematic technique known as the Design of Experiments (DOE), which is used to identify the most influential model parameters governing the time-dependent displacements of embankments stabilised with deep-mixed columns; and *vi)* In the final section, additional details are provided on the stress-strain response of the benchmark excavation stabilised using the Scandinavian dry soil mixing method, based on the 2D plane strain and the 3D analyses.
- Chapter 4 *Summary of the appended papers*. A brief summary of each of the five appended papers, including key results and conclusions, is provided.
- Chapter 5 *Conclusions and recommendations*. The main conclusions and possible future aspects of this research are summarised.

2 Deep mixing for stabilising geostructures in soft clays

2.1 Deep soil mixing: a brief background

Ground improvement using deep mixing method with lime and/or cement as cementitious binders has predominantly been used since the late 1970s simultaneously in Japan and Sweden (Broms and Boman 1979; Porbaha et al. 1998; Larsson 1999; Massarsch and Topolnicki 2005). Deep mixing is categorised based on the technique executed, such as rotary- or jet-based methods, auger- or blade-based methods, as well as the type of binder used which can be dry, wet, or modified. The dry soil mixing (DSM) uses cementitious binders in dry form, whereas in the wet mixing (WM) a slurry consisting of water and binder is utilised. Typically, the admixtures used in dry soil mixing (DSM) consist of cement (EN 197-1 2011) and unslaked lime.

DSM is specifically referred to as the 'Nordic Method' since it became widely established in Sweden, Norway, and Finland by the end of the 1980s (Holm et al. 2002), exploiting the high natural water content in sensitive clays. In Sweden, field applications began with the use of DSM and accelerated with large infrastructure projects. The applications of DSM in Sweden are often executed using quicklime (unslaked lime) and Ordinary Portland Cement as mixing agents. Additionally, some applications using WM (Hov et al. 2022; Eriksson et al. 2024; Helvacioglu et al. 2024) and the modified dry mixing (MDM) (Gunther et al. 2004; Eriksson et al. 2005) also exist in the Nordics in order to increase the mixing efficiency, as well as the strength and the uniformity of soils with insufficient water content.

DSM involves the use of a rotating mixing tool driven by compressed air. The tool mixes the admixtures with the soil, and therefore any compaction is achieved solely by the mixing tool itself (Larsson 2003). Various shapes and configurations, such as single columns, panels, grids, blocks, walls, or a combination of these, are used for deep mixing according to its intended purpose (EuroSoilStab 2002; EN 14679 2005). The current design methodologies in Sweden are presented in detail herein (Larsson 1999; Larsson 2003).

The mixing process typically increases the strength and stiffness of the natural soil while reducing its compressibility due to the alteration of soil structure (Porbaha et al. 2000; Åhnberg 2006; Kitazume and Terashi 2013). The properties of stabilised clay improve as a result of the chemical reactions between the clay and the admixtures. Soil stabilisation with the deep mixing method involves the following stages (Brandl 1981; Locat et al. 1990; Bell 1996; Shen et al. 2003a; Larsson et al. 2009): *i)* soil disturbance by the mixing procedure (the application of compressed air, admixture injection, and blade rotation); *ii)* soil fracturing and thixotropy resulting from soil disturbance; *iii)* ion exchange at the soil particle surfaces, within pore water, and at the soil-admixture interface; *iv)* pozzolanic reactions within stabilised soil; and *v)* consolidation (dissolution of entrapped air and dissipation of generated excess pore pressures).

In the following sections, the fundamental features and engineering properties of deep-mixed clays, as well as several factors influencing the strength and stiffness of deep-mixed clay during and after mixing, are discussed.

• Engineering properties of deep-mixed columns

Most of the information on the strength and stiffness of deep mixed materials is based on unconfined compression tests (UCTs) and an empirical relationship between the characteristic value of the unconfined compressive strength (q_{uk}) and the stiffness, although neither embankment nor excavation problems are purely one-dimensional. The undrained shear strength, c_{uk} can be calculated as $q_{uk}/2$. Similarly, the estimation of E_{50}/q_{uk} ranges between 50 and 150, as defined by EuroSoilStab (2002) and SGF (2000). Additionally, EuroSoilStab (2002), Bruce et al. (2013), and Trafikverket (2014) suggest limiting c_u to 100–150 kPa for applications under the embankments. However, under field conditions, particularly in the long term, the target value of c_{uk} is often exceeded by a wide margin (Van Impe et al. 2005; Åhnberg 2006; Kitazume and Terashi 2013; Savila et al. 2025).

The correlation between the strength and stiffness of stabilised clays is well-recognised (Porbaha et al. 2000; Miura et al. 2001; Lee et al. 2005; Åhnberg 2006; Kitazume and Terashi 2013; Hov and Larsson 2023), although it is influenced by several variables. These include the composition of the clay (such as inorganic vs. organic content), the type and composition of the binder, as well as factors like binder dosage (kg/m^3), binder ratio, curing time and conditions, water-to-cementitious material ratio (w/c), and soil-to-cementitious material ratio (s/c). Additionally, the mixing technique (wet or dry) and mixing efficiency (e.g. the number of mixing blades, retrieval rate, and rotation speed) also play a role (Larsson et al. 2005b).

Extensive research, particularly in the Nordics, has examined the stress-strain relationship of dry mixed clay through field and laboratory experiments (i.e. Åhnberg and Holm 1999; Axelsson and Larsson 2003; Paniagua et al. 2021; Paniagua et al. 2022a; Paniagua et al. 2022b; Hov and Larsson 2023; Ramírez and Korkiala-Tanttu 2023; Wong et al. 2024; Hov et al. 2025). Numerous studies internationally focus on Wet Mixing (WM) method (e.g. Mitchell et al. 1965; Bell 1996; Yu et al. 1997; Miura et al. 2001; Lee et al. 2005; Navin and Filz 2005) along with those that specifically examine small-strain behaviour (e.g. Tatsuoka et al. 1997; O'Rourke and McGinn 2004; Massarsch 2005; Van Impe et al. 2005; Puppala et al. 2006; Flores et al. 2010; Madhyannapu et al. 2010; Yao et al. 2020). A key finding across these international studies is that an increase in the binder content enhances both the undrained shear strength c_u and the stiffness, as observed in laboratory tests (uniaxial compression, vane, triaxial) and field assessments (destructive: piezocone, static loading, field vane, column penetration (FKPS/FOPS); nondestructive: bender element, fiber optic sensing, resonant column and seismic downhole tests). However, in dry soil mixing, the scale of fluctuation in the field can be significant (Wong et al. 2024), and it is thus not guaranteed that increased stabilising powder content always results in better functioning columns.

In contrast to natural clays, stabilised clay has significantly higher yield stress than that of untreated natural clay. The stiffness of the stabilised soil is highly non-linear and dependent on strain level similar to that of untreated natural clay (Åhnberg and Holm 1987; Hebib and Farrell 1999; Åhnberg et al. 2001; Shen et al. 2003a; Chew et al. 2004; Åhnberg 2006; Wang and Tanttu 2018). The results of UCTs and triaxial tests performed on stabilised clays showed varied responses in the yield strength and the stiffness, especially at high confining stress levels in triaxial tests (Uddin et al. 1997; Yu et al. 1997; Åhnberg and Holm 1999; Åhnberg 2006; Ignat et al. 2019). Åhnberg (2004) and Åhnberg (2006) state that UCTs may produce misleadingly high results, as the strain rate in UCTs is considerably higher than in the triaxial tests, and the tests do not account for

the confining stress or the degree of saturation. Åhnberg et al. (2001) also performed several conventional laboratory tests, such as IL, triaxial and UCTs, on laboratory mixed samples and investigated the initial load application during the hardening of the mixture. Laboratory tests performed on stabilised Swedish peat to simulate compaction resulting from the application of a fill yielded higher strength values than those without application of a prestress. In the same study, it is also reported that a delay in the prestress application results in a considerable decrease in the strength.

The permeability of stabilised soft clay is affected by the properties of the *in situ* soil, the mixing technique and the laboratory testing procedure. In the past, many researchers (e.g. Carlsten 1996; Åhnberg and Holm 1999; Åhnberg 2003; Broms 2004; Baker et al. 2005) have reported considerably higher permeability values for stabilise clay than that of unstabilised clay. Åhnberg and Holm (1999) showed that the permeability of stabilised gyttja is of the same order as that of untreated soil, while stabilised peat had higher permeability that decreased with time. More recently, Wang and Tanttu (2018) investigated one-dimensional compression behaviour of stabilised soft Otaniemi clay with the DSM method and showed that the k values for the stabilised and natural clay were of the same order of magnitude. A mixture of 50% cement and 50% lime was employed. The impact of different curing periods (ranging from 1 to 28 days) and binder amounts (ranging from 1 to 13%) on various properties, such as the compression index (C_c), yield stress (σ'_{vc}), hydraulic conductivity (k), the coefficient of consolidation (c_v), the coefficient of secondary compression (C_α) and compression modulus (E_s), were systematically examined. The C_c and k values measured did not show any significant difference regardless of the binder proportion and curing duration. The c_v associated with a given k and E_s, however, was projected to continue increasing with a higher admixture proportion.

The hydraulic conductivity k of clays stabilised with lime-cement admixtures is a function of the void ratio (e), the properties of the pore water and the microstructure of pores (sizes and distribution) which are altered during hydration and pozzolanic reactions. During pozzolanic reactions, cementation products fill the intra-aggregate pores and thus the k value starts to decrease with increasing lime and/or cement content (Brandl 1981; Kawasaki et al. 1981; Locat et al. 1996; Chew et al. 2004; Quang and Chai 2015). Investigations on the stabilised marine clays (with the use of WM) revealed the same order of k as that of uncemented clays (O'Rourke and O'Donnell 1997; Uddin et al. 1997; Nagaraj et al. 1998; Miura et al. 2001; Chew et al. 2004; Horpibulsuk et al. 2005).

The mineralogy and organic content of the natural clay can significantly affect the mechanical properties of deep-mixed columns. For example, when soil and/or groundwater contain sulphates, the alumina content in natural soil can lead to ettringite hydration, causing detrimental heave in lime-stabilised soil (Brady 1984; Mitchell and Dermatas 1992). While an increase in silica and alumina content enhances pozzolanic reactions and improves the strength of stabilised inorganic soils, the presence of organic matter inhibits these reactions by reducing the availability of Ca^{2+} ions for cementitious reactions. Laboratory tests on stabilised soils with high organic content (peat, gyttja) with different binders have shown these effects (Hebib and Farrell 1999; Åhnberg et al. 2001; Hov and Larsson 2023).

Larsson and Kosche (2005) and Larsson et al. (2009) compared different mixing methods (dry/wet) using various binder ratios (lime/cement) in kaolin clay and showed that the lower undrained

strength measured by using only cement as a binder was attributed to the low cation exchange capacity of kaolin clay and the repulsive effects of the high concentration of ions (Na^+ and K^+) in the pore water. Similarly, Chew et al. (2004) examined the influence of the kaolinite and illite content of *in situ* on pozzolanic reactions in soft marine clay from Singapore using the WM method, where cement was used as an admixture. The study identified that illite is less involved than kaolinite during pozzolanic reactions. The same relationship was highlighted by several researchers (e.g. Eades and Grim 1960; Wissa et al. 1965; Porbaha et al. 2000). Chew et al. (2004) argues that a high cement content causes a rapid consumption of kaolinite during hydration (short term, 7 days), which prevents pozzolanic reactions from occurring (long term, 28 days). The resulting cementitious products formed are then mainly due to hydration rather than pozzolanic reactions. The study also highlighted that the initial water content of the slurry determined the required cement content in order to obtain the same q_{uk}. A higher initial water content required the use of a higher proportion of cement.

• Installation effects and long-term properties

During deep mixing large amounts of admixture is injected into the clay and the shearing forces through blade rotation cause remoulding of *in situ* clay. Therefore, the mixing process is likely to destroy any *in situ* structure (Tatsuoka and Kobayashi 1983; Yong et al. 1996; Shen et al. 2003b; Shen et al. 2003a; Larsson and Kosche 2005; Larsson et al. 2009). Deep mixed columns are constructed by mixing *in situ* with chemical admixtures using rotating blades. Shen et al. (2003a) and Shen et al. (2003b) argue that the mixing process creates mainly two reactions: volume expansion from injection pressure and shearing from blade rotation. These effects may lead to the generation of excess pore pressures and disturb the natural clay surrounding the stabilised area, forming a plastic zone around the columns. According to Shen et al. (2003a) and Shen et al. (2003b), there is also a consolidation process in the surrounding soil after the installation of deep mixed columns, due to the dissipation of excess pore pressures. After the remoulding, the clay regains some of its strength through ageing and thixotropic hardening. Regardless of the mixing method (dry or wet) and binder type (lime, cement, or lime-cement), the long-term undrained shear strength of the columns increases with time, as shown by Larsson and Kosche (2005) and Larsson et al. (2009) for both DSM and WM, and by Shen et al. (2003b), Shen et al. (2003a), and Liu et al. (2008) for WM.

To investigate the regain of the strength after the installation of deep mixed columns, a deep mixing procedure was performed with cement injection and without cement injection by Shen et al. (2003b). Soft Ariake marine clay was mixed with cement slurry in laboratory conditions. Later, the undrained shear strength was evaluated through the laboratory vane shear test. The ratio of water/cement was 100% for a deep mixed column diameter of 10 cm. The strength regained in the cement-injected case was due to a combination of thixotropic effects and cementation and was fully regained after seven days of curing. In the proximity of the column edge, the regained shear strength reached about 1.5 times the initial strength. In contrast, without cement injection, the strength regained reached 70% of the initial strength after 28 days. This finding indicates that the strength regained during thixotropic recovery is a time-dependent process.

The volume expansion resulting from the disturbance of the soil was investigated by Shen et al. (2003b) and Shen et al. (2003a). The results suggested that the expansion ratio of the soil-mixed

columns can be determined from experimental data. An empirical relationship was suggested by Shen et al. (2003b) and Shen et al. (2003a), which considers the volume of injected slurry, the radius of the hardened column, the nominal radius of the mixing blade and the volume factor (ranging between 0.47-0.70). This proposed relationship takes into account the swelling of the soil and the penetration of the cement slurry into the surrounding soft soil. Nonetheless, the measurement of volume changes in highly heterogeneous columns, and the stress dependency of the hardened column volume within the improved zone into Shen et al. (2003b)'s equation require further research. The volume change resulting from the mixing processes, such as hydration, flocculation-coagulation, pozzolanic reactions, cementation, and drying, is highly dependent on the type of lime used and the choice of high/low alkali cement (as reported by Taylor 1997; Lorenzo and Bergado 2006).

The long-term increase in strength and stiffness of stabilised clay due to ongoing pozzolanic reactions was investigated for DSM (Löfroth 2005; Fritzson et al. 2024; Savila et al. 2025) and for WM (Hayashi et al. 2003; Takahashi et al. 2018). Savila et al. (2025) reported that the unconfined compressive strength of field samples mixed with different binders, collected 1.1 and 3.5 years after construction, exceeded the design strength specified in the Finnish design guidelines by factors of 2 to 9, respectively. Löfroth (2005) has examined the long-term behaviour of the lime-cement columns constructed on organic and soft clays for a cut railway slope at Kungsbacka, Sweden. The results have shown that ongoing strength increment was evident within an observation period of 9.5 years.

• Curing temperature and time

The effects of curing temperature and curing time on the strength and the stiffness of the stabilised soil have been well recognised since 1886 (Unwin 1886). Henceforth, attempts have been made to understand the relationship between curing temperature, curing time, and strength (often obtained from uniaxial tests), referred to as *maturity index* (e.g. Unwin 1886; Ruff and Ho 1965; Åhnberg and Holm 1987; Horpibulsuk et al. 2003; Clare and Pollard 2015; Vervoorn and Barros 2021; Bache et al. 2022). Typically, a higher curing temperature leads to higher strength and stiffness development.

Field measurements suggest temperatures between 11-29°C (from July to October) while the soil-mix hardens (Swedish Transport Administration 2018). An increase in the temperature within stabilised soil results from hydration and pozzolanic reactions, which depend on the binder content and type. Moreover, the temperature affects the rate of the chemical reactions. The effect of heat generation within a small laboratory sample is negligible (Åhnberg 2006). On the other hand, the curing temperature creates a substantial difference in the undrained shear strength and the stiffness of the stabilised soil. Reflecting field conditions might be accomplished by increasing the curing temperature to 20°C as suggested by Vervoorn and Barros (2021) and Bache et al. (2022). The relationship between the time-temperature-binder type/amount and the strength/stiffness is usually derived from 28-day curing in laboratory conditions (Åhnberg and Holm 1987; Bache et al. 2022), thus achieving comparable long-term results in the field conditions, accounting for the temperature changes and pozzolanic reactions, proves to be challenging. Thus, the temperature effects will not be considered in the numerical simulations of this thesis.

2.2 Characteristic features and behaviour of soft natural clays

Soft natural clays in Scandinavia and northern Europe were deposited in the glaciomarine environment during late Weichselian times due to deglaciation (Dennegård 1984; Stevens and Bayard 1994). During this period, the change in climate controlled the depositional environment that later on evolved by isostatic uplift (Stevens et al. 1991; Mitchell and Soga 2005). The glacial and post-glacial lightly overconsolidated soft clay deposits are prone to significant deformations at stresses beyond the apparent preconsolidation pressure and have been exposed to mainly one-dimensional deposition history (i.e. the sedimentation under K_0 gravity conditions). In order to accurately predict the hydromechanical response of soft clays caused by the construction of geostructures, it is therefore essential to account for certain features of soft clays, namely the rate-dependency, anisotropy and degradation of bonding, as well as their effects in the mobilised stiffness with strain.

• State, stress history and structure of soft clays

Mitchell (1956) defined the terminology 'structure' as the combination of the arrangement of particles ('fabric') and the resistance of the fabric (interparticle 'bonding') to alteration by physical, chemical, and electrical means. The structure therefore is a result of the depositional environment, consolidation, ageing, weathering and cementation (Bjerrum and Lo 1963; Bjerrum 1967; Leroueil et al. 1979; Burland 1990; Leroueil and Vaughan 1990).

Leonards and Ramiah (1960) and Bjerrum (1967) demonstrated the effect of geological ageing on the compressibility of normally consolidated ('young') clay. In Figure 2.1, the ageing results in higher apparent preconsolidation under sustained load (i.e. drained creep), causing the soil to behave though it were lightly overconsolidated under subsequent loading.

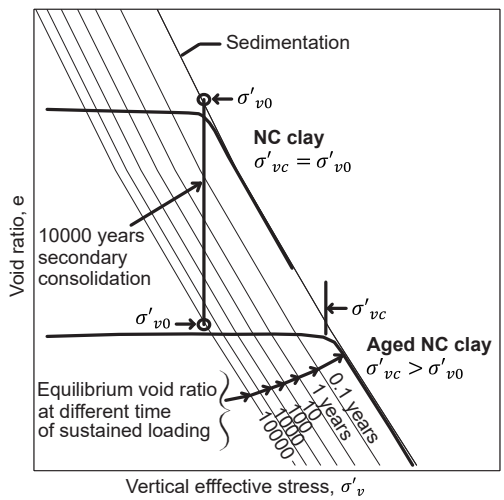

Figure 2.1: *Geological history and compressibility relationship for normally consolidated (NC) clay: sedimentation and ageing (adopted from Bjerrum (1973)).*

It is recognised that the natural soft clays are structured with some apparent bonding between the particles, and thus the mechanical properties of *in situ* clays differ from those at their reconstituted state. Burland (1990) argued that the mechanical properties of the reconstituted state (i.e. intrinsic properties) of soft clay can help explain the progressive loss of structure with irrecoverable straining of natural clays. The intrinsic properties can be obtained by reconsolidating the reconstituted samples one-dimensionally, at a water content, w of between 1 to 1.5 times their liquid limit, w_L. The effect of destructuration on the stress-strain response of soft clays has been discussed by Bjerrum (1973), Leroueil et al. (1982), Leroueil et al. (1985), Burland (1990), Yin and Graham (1994), Yin and Cheng (2006), and Yin et al. (2011) among others, including the effect of leaching and weathering (Bjerrum and Rosenqvist 1956; Løken 1970; Nova et al. 2003; Mitchell and Soga 2005).

The structure not only leads to a higher quasi-preconsolidation pressure but also to a larger yield locus when sheared, for natural soft clays compared to their destructured state (Tavenas and Leroueil 1985; Leroueil and Vaughan 1990), as can be seen in Figure 2.2 in the normalised stress plane $((\sigma'_1+\sigma'_3)/2\sigma'_{vc}, (\sigma'_1-\sigma'_3)/2\sigma'_{vc})$, where σ'_{vc} is the effective apparent preconsolidation stress, and σ'_1 and σ'_3 are the major and minor effective stresses.

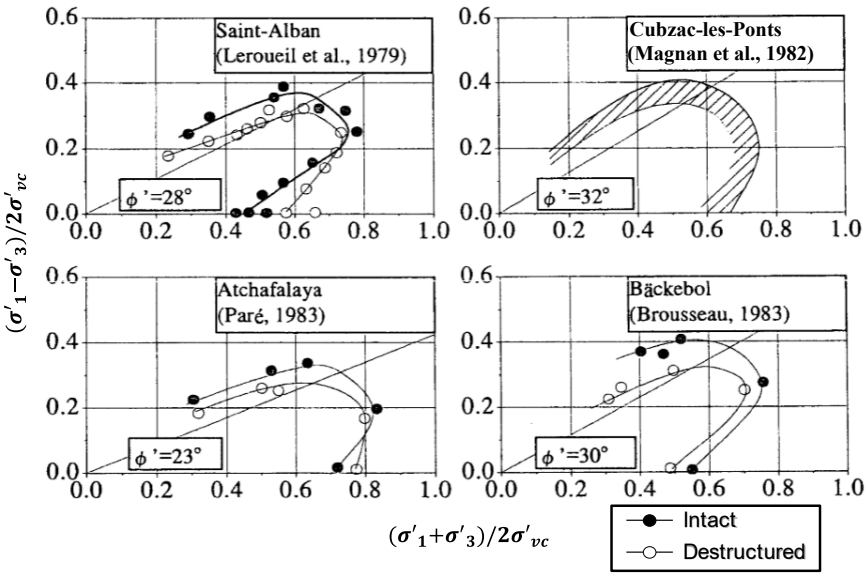

Figure 2.2: *Yield envelops for intact and destructured clays (adopted from Tavenas and Leroueil (1985)).*

Based on experimental evidence, the glacial and post-glacial lightly overconsolidated natural clays exhibit anisotropy (historical and strain-induced) depending on their stress-strain history and deposition process (Leroueil et al. 1979; Pietruszczak and Mróz 1982; Graham and Houlsby 1983; Burland 1990; Kobayashi et al. 2003; Wheeler et al. 2003; Karstunen and Yin 2010). The anisotropy impacts the response of the clays to the direction of applied stresses as well as the stiffness moduli and hydraulic conductivity.

Lo and Morin (1972) demonstrated how sampling affects strength and stiffness, based on isotropically consolidated undrained triaxial tests on soft sensitive marine clay, where block samples were trimmed at various angles relative to the vertical direction. Similarly, Hicher et al. (2000) examined the mechanical properties of clayey materials with a special focus on the micro-structural analysis of inherent and induced anisotropy. Hicher et al. (2000) pointed out that the isotropically consolidated samples (axisymmetric drained compression), cut vertically and horizontally, exhibited higher stiffness and strength when subjected to drained triaxial shearing in a direction perpendicular to the main direction of particle orientation. Additionally, the samples subjected to three-dimensional shearing had a significant decrease in stiffness as the initial loading direction shifted from the principal major stress direction to the intermediate stress direction and finally to the minor stress direction.

• Rate-dependency

Time-dependent deformations in saturated soft clays stem from *(i)* volume changes in relation to viscous deformations in soil skeleton, and *(ii)* volume changes due to pore water dissipation, i.e. the coupled response of the soil skeleton and pore fluid. Viscous deformations compromise the measurable combined effect of irrecoverable straining (Zienkiewicz and Cormeau 1974). The rate-dependent (viscous) shear and/or volumetric strains in the soil skeleton, i.e. creep or 'delayed-secondary compression' (Bjerrum 1967), are dictated by the resistance of the soil structure.

Creep deformations have been investigated through experiments including monotonic loading at various strain rates, monotonic loading at various effective stresses, creep tests at constant effective stress and stress relaxation tests at constant strain. The stress and strain response under sustained load cannot be solely explained by the volume changes in soil (Bjerrum 1973; Anderson and Stokoe 1978). The increase in the stiffness, undrained strength and apparent preconsolidation pressure σ'_{vc} result from the ageing effect, which alters the resistance of the soil structure during creep that progresses at a decreasing rate under further effective stress increase (see Figure 2.3b). Bonding is often related to sensitivity, defined as the ratio of the undisturbed and remoulded undrained strength from vane or fall cone tests at the same water content (Skempton and Northey 1952; Rankka et al. 2004). Therefore, sensitivity is highly dependent on deposition history, mineralogy, pore water composition, and also affected by sample disturbance, all of which have a significant impact on the structure of the soil (Bjerrum and Rosenqvist 1956; Rochelle et al. 1981; Hight et al. 1992; Karlsson et al. 2016).

The effects of creep, stress relaxation, and strain rate effects are governed by the same basic time mechanism, termed "isotach" behaviour (see Figure. 2.3b). The relationship between the stresses and strains is highly rate dependent, i.e. increasing stiffness and undrained shear strength with increasing strain rate (Richardson and Whitman 1963; Leroueil et al. 1982). Beyond σ'_{vc}, irrecoverable straining induces changes in fabric and causes gradual degradation of bonding. The gradual break down of the apparent bonding, called destructuration, has been discussed by Crawford (1960) and Leroueil et al. (1985) among others. In Figure 2.3a the CRS tests in sensitive marine clay show that an increase in the measured pore pressure and structural breakdown can be attributed to a reduction in the strain rate. The higher rates of the applied load led to a higher positive pore pressure development and higher σ'_{vc}, while slower rates, less than 5×10^{-7}, did not cause a significant increase in pore pressures but reduced the apparent σ'_{vc}.

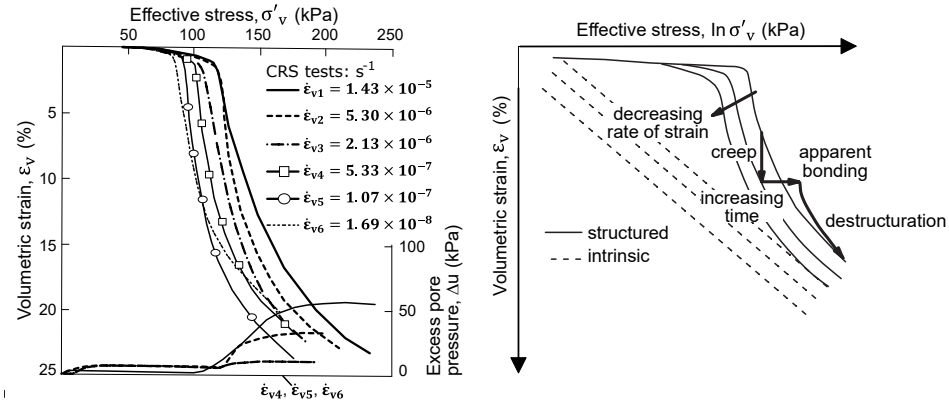

(a) (b)

Figure 2.3: *The effect of strain rate, creep, and structure on one-dimensional compression of soft clay. (a) oedometer tests on soft marine clay (adopted from Leroueil et al. (1985)), (b) structured and intrinsic soft clay under typical oedometer tests.*

The influence of strain rate is demonstrated in Figure 2.4 through CAUC tests with various strain rates on the samples of soft sensitive marine clay that were anisotropically consolidated to their *in situ* effective stress level. A higher strain rate led to a higher deviatoric peak stress, q. In the tests, undrained creep deformations were investigated through relaxation tests while keeping the strain rates at zero (the height of the specimen is constant) rather than subjecting the specimen to a constant (sustained) load as in oedometer tests. The relaxation steps produced undrained creep with reduced q due to an increase in pore pressures. Additionally, in the CAUC tests, various strain rates (step-changed strain rates) were adopted. In the course of the test, sudden changes in the strain rate resulted in changes in the stress-strain response in a manner that followed unique paths, as if the sample was loaded at a specific strain rate from the beginning.

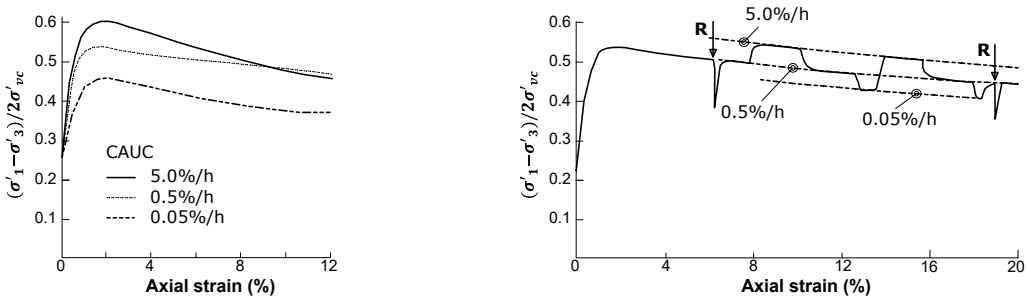

(a) (b)

Figure 2.4: *Stress-strain curves in CAUC tests (adopted from Graham et al. (1983)). (a) constant strain rate, (b) step-changed strain rates and creep relaxation steps denoted as* ***R****.*

2.3 Embankments on stabilised soft clays

The estimation of coupled long-term response of road embankments on soft clays supported by columnar inclusions (e.g. deep-mixed columns) requires taking into account the fundamental characteristics of soil-mixed columns (Bergado et al. 1996; Lorenzo and Bergado 2003; Larsson 2021) as well as soft natural clay (Kitazume 2024). Soft sensitive clay deposits with low permeability are susceptible to large deformations under shearing due to their deposition history and mineralogy (refer to Section 2.2). The stress-strain response of soft natural clays under embankment loading is closely related to the principle stress rotations, historical and stress-induced anisotropy, variation of stiffness, and strain rate effects (i.e. Bjerrum 1973; Ladd and Foott 1974; Smith and Hobbs 1976; Law 1978; Tavenas and Leroueil 1980; Davies and Parry 1985; Leroueil et al. 1990; Li et al. 2002; Zdravkovic et al. 2002; Lehane and Jardine 2003; Karstunen et al. 2005; Lacasse et al. 2011; D'Ignazio et al. 2017).

Time-dependent deformations under embankments have been investigated to account for the magnitude and rate of settlements due to the presence of deep-mixed columns under working load conditions through numerical analyses (Navin and Filz 2006; Krenn and Karstunen 2008; Yao et al. 2016; Filz et al. 2019), and through analytical solutions using the theory of elasticity (Yoshikuni and Nakanodo 1974; Broms and Boman 1979; Alamgir et al. 1996; Baker 2000; Lorenzo and Bergado 2003; Horpibulsuk et al. 2012; Wijerathna et al. 2017). Additionally, slope stability computations for road embankments supported by deep-mixed columns demonstrated varied failure modes including shear, bending or rotation (Inagaki et al. 2002; Kitazume and Maruyama 2006; Kitazume and Maruyama 2007; Al-Naqshabandy and Larsson 2013; Filz et al. 2019).

The commonly used semi-empirical methods (i.e. EuroSoilStab 2002; EN 14679 2005; Bruce et al. 2013; SGF 2000) provide solutions based on the weighted average of the strength, stiffness and permeability of the stabilised clay, i.e. composite material that consists of the stabilised clay and the columns. The deformations in the composite soil can then be computed based on the strain compatibility between the columns and the natural clay, as well as the concept of non-yielding columns (semi-hard columns), as explained by Broms and Boman (1979), Baker (2000), and Broms (2004). The equality of strain dictates that the columns and the natural clay undergo the same total vertical strain while the applied load is distributed between the materials according to the elastic stiffness moduli. The computation implicitly assumes that the soft clay does not provide lateral restraint while the columns ensure lateral support. Thus, in the computation of the average modulus, the constraint modulus, E_{oed} of the soft clay, Young's modulus, E' of the columns, and respective volume ratios of each material are typically incorporated.

The analytical methods provide solutions for determining the consolidation settlements using equations of one-dimensional or radial consolidation (Carrillo 1942; Barron 1948; Hansbo 1979; Balaam and Booker 1981; Hansbo 1981; Barksdale and Bachus 1983; Balaam and Booker 1985; Hird et al. 1992; Chai et al. 2001; Deb 2008). The computations originate from early works of Barron (1948) and Hansbo (1979) that incorporate unit cell concept to estimate the rate of settlement of the reinforced soft clays with stone columns or vertical drains in the absence of lateral movement. The partial differential equation can be written for the three-dimensional flow in a cylindrical saturated soil specimen (axisymmetric) having differing hydraulic conductivity in radial, k_{r} and vertical, k_{v} directions. Equation (2.1) relates the partial degrees of consolidation in the radial and vertical directions to the overall degree of consolidation, and it reduces to Terzaghi's

one-dimensional consolidation equation when k_r equals zero.

$$\frac{\partial u}{\partial t}\left(\frac{a_v}{1+e}\right) = \frac{k_v}{\gamma_w}\left(\frac{\partial^2 u}{\partial z^2}\right) + \frac{k_r}{\gamma_w}\left(\frac{1}{r}\frac{\partial u}{\partial r} + \frac{\partial^2 u}{\partial r^2}\right) \tag{2.1}$$

where u denotes excess pore pressure, t represents time, and a_v (generally denoted as m_v) is the coefficient of compressibility, defining the linear relationship between effective vertical stress and void ratio ($de = -a_v d\sigma'_v$). γ_w is the unit weight of water.

Lorenzo and Bergado (2003) and Wijerathna et al. (2017) investigated consolidation settlement as well as the radial flow of clay stabilised with cement by assuming zero lateral strain for the mixed columns and surrounding clay. In both studies, a unit cell of clay and cement-improved clay was analysed with an analytical method, considering different coefficients of consolidation, c_v and different coefficients of permeability, k for the materials. When subjected to shearing, the column experiences a notable concentration of stress, leading to a simultaneous decrease in stress in the surrounding soil due to differences in rigidity (Barksdale and Bachus 1983). Lorenzo and Bergado (2003) simplified the interaction between the soil and the column into two extreme cases: equal stress and equal strain, and validated the analytical approach developed on a case history of an embankment constructed on soft Bangkok clay. The governing equation was obtained by assuming that the vertical drainage occurred through the radial flow into the column from the surrounding clay due to the higher rate of consolidation resulting from the high rigidity of the columns (i.e. higher c_v). Therefore, Lorenzo and Bergado (2003) disregards vertical drainage through the surrounding soft clay, whereas Wijerathna et al. (2017) incorporates both radial drainage of excess pore pressure from the surrounding clay to the mixed columns and vertical drainage through both the natural clay and the columns, assuming equal straining.

In numerical modelling, true unit cell (3D) and/or axisymmetric unit cell (2D) models have been exploited (Alamgir et al. 1996; Baker 2000; Lorenzo and Bergado 2003; Krenn et al. 2005; Chai et al. 2010; Jiang et al. 2013; Oliveira et al. 2017; Phutthananon et al. 2022) to estimate the deformations under stabilised embankments with deep-mixing method, while a more accurate approximation can be achieved by performing 3D analyses (Krenn and Karstunen 2008; Vogler 2008; Voottipruex et al. 2011; Chai et al. 2015; Jamsawang et al. 2016b). Typical unit cell geometries for axisymmetric finite element analyses is illustrated in Figure 2.5 where d_c and d_e are the diameters of the column and unit cell, respectively (d_e is 1.05, 1.13 and 1.29 times the column spacing for triangular, square and hexagonal arrangements, respectively (Hansbo 1979)).

The 3D analysis, despite its computational demand, enables the incorporation of the true model geometry and modelling distinct mechanical responses of individual materials (i.e. the columns and soft clay). Additionally, plane strain (2D) simulations usually idealise the 3D embankment problem based on linear-elastic assumptions using the composite stiffness/strength or integrating the columns in the form of panels/walls using the estimated equivalent plane-dimension, flexural rigidity (EI) or axial stiffness (EA) based on an area replacement ratio (Bergado et al. 1999; Rampello and Callisto 2003; Ariyarathne et al. 2013; Yapage et al. 2014; Chai et al. 2015). These simplifications, despite being erroneous due to ignoring the highly non-linear elastoplastic constitutive behaviour of the columns and *in situ* clay can work under relatively low embankment

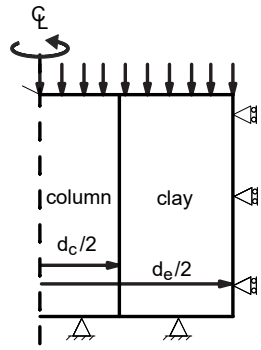

Figure 2.5: *Typical unit cell geometry in axisymmetric analysis.*

heights with a high area replacement ratio with no significant plastic straining. However, employing non-linear elastoplastic constitutive models in 2D FE analyses provides a more realistic representation of the actual response of the soil (e.g. Rampello and Callisto 2003; Yapage et al. 2014) than using linear-elastic considerations.

Similarly, total stress-based analyses often underestimate deformations that become more pronounced as pore pressures dissipate, whereas FOS may be overestimated (for soft clays, medium to low plasticity) or underestimated (for quick clays, low plasticity) due to not accounting for the development of pore pressure at failure, strength anisotropy, and strain rate (Bjerrum 1973; Davies and Parry 1985; Atkinson et al. 1987; Länsivaara et al. 2014). The stiffness and the mobilised strength of stabilised natural clays depend on strain level, stress history, and stress paths rather than being intrinsic soil constants (Jardine et al. 1986; Zdravković et al. 2021). Moreover, the rate at which the strength is mobilised can differ between the deep-mixed columns and the soft natural clay.

2.4 Deep excavations in soft clays

Deep excavations supported by deep-mixed columns are complex system-level problems involving the interaction between the soft clay, supporting wall (e.g. sheet pile, secant and deep-mixed wall) and deep-mixed columns. Thus, there are challenges in accurate predictions of deformation, pore pressures, and structural forces, especially in soft sensitive clays. The permeability of the soft clays is usually low, thus constructions are often assumed to be performed in undrained conditions. During an excavation, various stress paths associated with the stress increments in vertical and horizontal directions are shown in Figure 2.6.

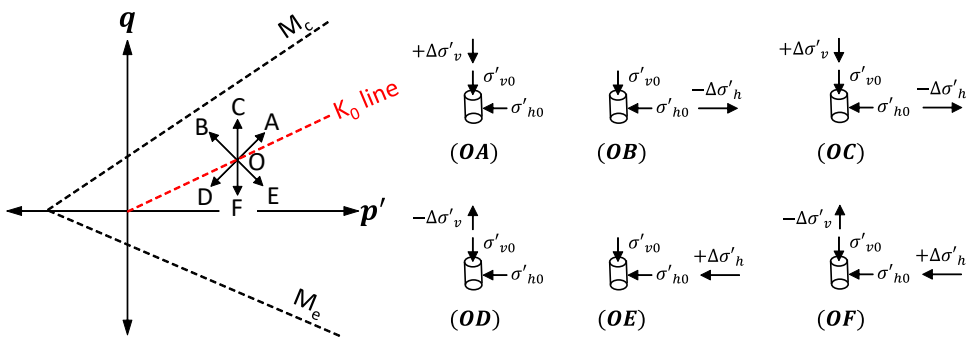

Figure 2.6: *Idealised stress paths for excavations (after Stroh (1974)).*

Due to the low permeability of soft clay, unloading in the undrained conditions results in the development of a negative excess pore pressure (suction) in the bottom of the excavation. The pore pressures immediately after the excavation are typically less than the final state pore pressures, therefore, the factor of safety of retaining walls system will decrease over time (Lambe and Whitman 1991; Atkinson 1993; Freiseder 1998; Ghadrdan et al. 2020).

In order to accurately predict the field response, the fundamental response of soft soils should be incorporated into the analyses (see Section 2.2). The capacity of soft clays to endure shearing forces under undrained conditions, referred to as undrained shear strength (c_u), is dependent on the rate at which the clay reaches failure (Bjerrum 1973). The influence of anisotropy on stress-strain and strength can be attributed to both strain-induced anisotropy and inherent anisotropy of the soil (Bjerrum 1973; Graham and Houlsby 1983; Karstunen et al. 2005). The anisotropy of soils influences the time-dependent performance of excavations in soft soils, impacting the orientation and direction of stresses.

Clough and Lawrence (1981) investigated the basal heave mechanisms and the stress-strain response of a braced excavation supported by struts in soft plastic clays, accounting for the strength anisotropy. The angle of stress reorientation was considered to predict observed deformation and was used to calculate safety against basal heave. An increase in the major principle stress caused a steady decrease in the measured c_u. The calculation of basal heave analysis, based on Terzaghi (1943) and Bjerrum and Eide (1956), was extended by Clough and Lawrence (1981) to account for stress reorientation β in each construction stage, through reevaluating the new modulus and the shear

strength. Figure 2.7 shows the variation of undrained shear strength for different principal stress directions where c_{u0} is the maximum undrained shear strength at $\beta = 0$. The results of Clough and Lawrence (1981) suggest that the basal heave factor of safety for isotropic calculations is overpredicted, whereas the maximum lateral wall deformations and the distribution of strut loads were underestimated. Therefore, simple total stress analysis for excavations in soft clay often yields incorrect results for the prediction of deformations and the ultimate failure (Janbu 1977).

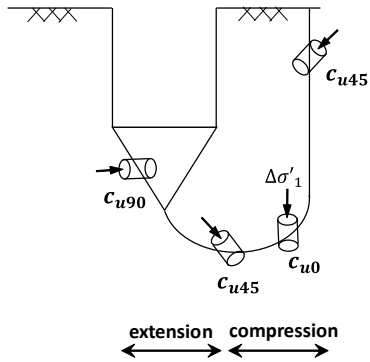

Figure 2.7: *Failure mechanism and principle stress rotation (after Clough and Lawrence (1981)).*

Excavations in soft clays stabilised with deep mixing have been investigated for various column arrangements, such as panels (cross-walls), grids and blocks to increase the passive resistance of the soil or support the excavation as a retaining structure to substitute for concrete or sheet pile walls. The performance of the system has been reported in case studies by Tanaka (1993), O'Rourke and O'Donnell (1997), O'Rourke and McGinn (2004), Ignat et al. (2016), and Wang and Whittle (2024). In order to predict the deformations of the stabilised excavations, 2D and 3D numerical analyses have been performed (Ou et al. 2008; Jamsawang et al. 2016a; Ignat et al. 2020; Waichita et al. 2020a; Zhang et al. 2020; Iorio et al. 2024). Various yield mechanisms and deformations have been investigated through model tests (centrifuge, direct shear box) (Yang et al. 1993; Khan et al. 2009; Larsson et al. 2012; Waichita et al. 2020b) as well as full-scale field tests (O'Rourke and McGinn 2004; Jamsawang et al. 2017; Ignat et al. 2020).

In these studies, very few among them reported on the installation effects due to deep mixing process leading to large deformations (i.e. O'Rourke and O'Donnell 1997; Wang and Whittle 2024). The installation effects are often ignored and indirectly incorporated in the simulations through modifying numerical model parameters in order to match the observed response (field or model tests) through back analysis (Ou et al. 1996; Wang and Whittle 2024). O'Rourke and O'Donnell (1997) investigated the field behaviour of an excavation stabilised by deep soil mixing and jet grouting methods in soft marine clay. The observed deformations after the installation of deep mixed columns were incorporated in the simulations by using the external strain application. The strain field computation methodology followed the precedent study by Finno and Nerby (1989) which is based on calculating the soil strain using data from extensometer and surface-settlement points, assuming plane strain conditions. Resulting strain component $\varepsilon_{\mathrm{hv}}$ was computed by taking the average of the differential horizontal and vertical displacements between the two components (see Figure 2.8 and Equations (2.2)-(2.5)).

$$\varepsilon_{\mathrm{h}} = \left(\frac{u_2 - u_3}{L_{23}} \right) \tag{2.2}$$

$$\varepsilon_{\mathrm{v}} = \left(\frac{v_2 - v_3}{y_2} \right) \tag{2.3}$$

$$\varepsilon_{\mathrm{hv}} = \frac{1}{2} \left(\frac{\partial u}{\partial y} + \frac{\partial v}{\partial x} \right) \tag{2.4}$$

$$\gamma_{\mathrm{hv}} = \left(\frac{\partial u}{\partial y} + \frac{\partial v}{\partial x} \right) \tag{2.5}$$

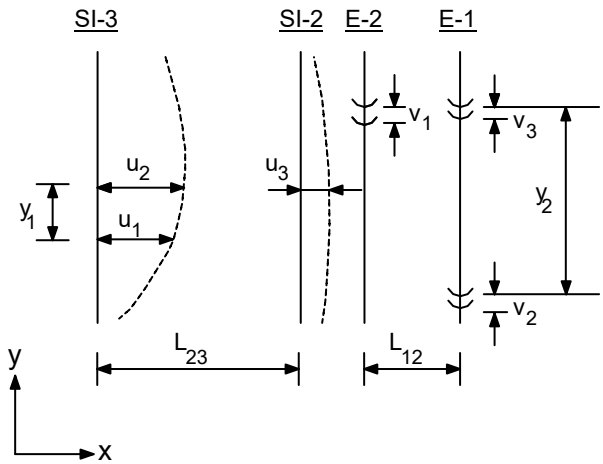

Figure 2.8: *Strain components (after Finno and Nerby (1989)).*

The study by Finno and Nerby (1989) observed lateral wall movements of up to 50 mm during the construction of soil-mixed wall buttresses prior to excavation. It was claimed that the reason behind the lateral movement observed was the insufficient strength and stiffness of the newly installed buttresses to resist lateral earth pressures. This resulted in a reduction of the shear resistance of the soil, causing lateral movement. Deformations due to the deep mixed column installation appear to show similar behaviour to those of pile driving, as seen in Randolph et al. (1979) and Finno et al. (1988). In these studies, pile driving resulted in lateral wall movement away from the excavation and ground surface heave was observed. The strain values calculated by the proposed methodology cannot, however, be extrapolated to other excavations for the calculation of installation effects. Yet, the study by O'Rourke and O'Donnell (1997) provides a more accurate evaluation of soft soil behaviour and stability against basal heave than previous works.

In numerical modelling, the adopted methodology is typically total stress-based. However, incorporating the non-linear stress-strain response of soil in simulations has led to better predictions of

failure mechanisms and deformations. Ou et al. (2008) performed a 3D simulation to investigate the effect of ground improvement with deep mixed columns in the passive side of a braced excavation in soft clay. Total stress analysis was performed in conjunction with the simplified equivalent properties of the stabilised clay, consisting of untreated soil and the columns (i.e. composite material), with the Duncan-Chang hyperbolic model. The results postulated that the corner stiffening effects promote redundancy of the column construction within a distance from the corners.

Ignat et al. (2020) examined a braced excavation and performed a three-dimensional finite element analysis to compare the simulation results with full-scale field test data. Pre-failure and post-failure response of excavations supported by lime-cement (LC) columns were investigated, taking into account strain-induced anisotropy of the natural clay. The stress-strain response of the LC columns (wished-in-place) was simulated using the Hardening Soil (HS) model (Schanz et al. 1999), whereas the soft clay behaviour was represented by the S–CLAY1S model (Koskinen et al. 2002; Karstunen et al. 2005). The LC columns were constructed in the passive side of the excavation using dry soil mixing with a binder mix of 50% quicklime and 50% Portland cement at an amount of 120 kg/m^3. Comprehensive laboratory tests, including isotropically and anisotropically consolidated undrained compression triaxial tests and constant rate of oedometer (CRS) tests, were utilised. Field measurements showed that using c_u calculated from anisotropic tests accurately reflected the failure stress of the columns. Lateral wall deformations and strut forces measured in the field were captured relatively well with the use of advanced soil models.

3 Methodology

3.1 Introduction to Volume Averaging Technique

Ground improvement using stone columns or deep mixed columns is widely used to reduce settlements and increase stability in soft natural clays. To accurately assess the effectiveness of these inclusions in reducing settlements, and to realistically simulate the hydromechanical response of the system, it is crucial to consider an elastoplastic analysis, as the distinct material properties of the constituents may lead to inaccurate results if only elastic perfectly plastic behaviour is considered (Canetta and Nova 1989). The regularly spaced columnar inclusions are stiffer than the *in situ* clay and have relatively small diameters compared to the application area.

Due to the complexity of the interactions between the columns and soil, the stabilised area can be represented by an equivalent material that incorporates the stress-strain response of both soft natural clay and columns. This equivalent material can represent the homogenised medium (a composite system) in which the columns are uniformly and homogeneously distributed. The homogenisation procedure, using Volume Averaging Technique (VAT), can be formulated for plane strain analysis adopting different constitutive models for the two materials, provided that the kinematic and equilibrium constraints are satisfied at the interface between the materials and compatible with the elastic, elastoplastic, or viscoplastic behaviour of the materials involved.

VAT has been successfully applied in numerical analyses to represent the homogenised material for the foundations of embankments under the railway and highway structures (e.g. Schweiger and Pande 1986; Schweiger and Pande 1988; Canetta and Nova 1989; Lee and Pande 1998; Omine et al. 1998; Omine et al. 1999; Jellali et al. 2005; Vogler and Karstunen 2008; Vogler 2008; Becker and Karstunen 2013; Abed et al. 2025), as discussed in Section 3.2.

However, the formulations in these studies primarily focused on loading scenarios and did not account for the stress-strain distributions and boundary conditions present in unloading problems, such as excavations. In this research, see Section 3.3, VAT is also adapted for numerical analysis of braced excavations supported by deep-mixed columns by reformulating the existing algorithm of Vogler (2008) to incorporate the static and kinematic boundary conditions representative of unloading problems. A fully coupled 3D consolidation analysis is performed to assess the interaction between constituents, from which local equilibrium and kinematic constraints are derived, based on a hypothetical braced excavation. These constraints are then used to construct a 2D VAT formulation that incorporates different constitutive models representing the non-linear behaviour of the LC columns and the soft clay, along with the boundary conditions relevant to excavation problems. The technique, implemented in a 2D FE code, ensures computational efficiency and is thus opening opportunities e.g. for optimisation, considering scenarios involving varying column spacing and column lengths, as it eliminates the need for detailed geometric discretisation required in a corresponding 3D model or studies that account for variability.

3.2 Volume Averaging Technique (VAT) for embankments

In order to estimate the elastic moduli of the two-phased homogenised material, namely matrix and inclusion, initially Voigt and Reuss assumptions were utilised. Voigt (1889) assumed that all the elements of the mixture are exposed to the same uniform strains, whereas Reuss (1929) considered that the elements of the composite material are subjected to a uniform stress equal to the applied stress. The rheological analogue of stabilised clay with deep-mixed columns is illustrated based on these assumptions in Figures 3.1a and 3.1b, where the subscripts s and c refer to soil and column, respectively, and the elasticity modulus E, strain ϵ, and stress σ are defined for each constituent in the spring-dashpot models.

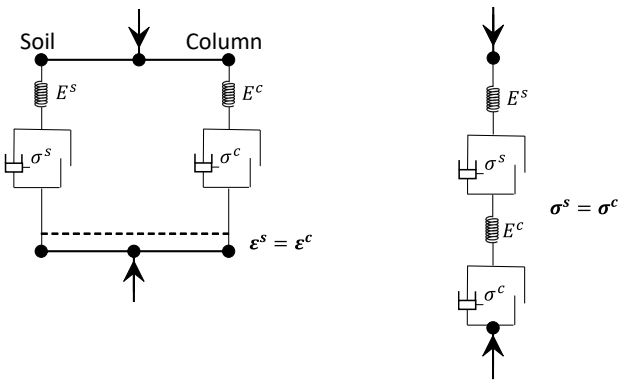

(a) (b)

Figure 3.1: *Stress-strain response of clay/column system (modified from Schweiger and Pande (1986). (a) Voigt estimate , (b) Reuss estimate.*

Omine et al. (1998) and Omine et al. (1999) examined a two-phase mixture model with pile-shaped inclusions to evaluate the strength-deformation properties of stabilised clay. The composite material and its constituents (kaolin clay and cement-mixed columns) were assumed to behave as linear-elastic perfectly plastic materials. Stresses and strains in the stabilised clay were assumed to be distributed based on the volume fractions (i.e. occupied volume) of the inclusion and the *in situ* clay. The stress distribution in the composite material was determined by introducing the stress distribution tensor. The tensor was calculated using a power function that accounts for the ratio of the undrained elasticity modulus between the clay and the inclusion, along with an empirical parameter that depends on the geometry of the inclusion. Omine et al. (1998) demonstrated that the Voigt approximation provides an upper limit, while the Reuss approximation provides a lower limit for the elastic moduli of mixtures.

However, neither soft natural clays nor columns are elastic materials. Schweiger and Pande (1986) and Schweiger and Pande (1988) assumed that the total strains in the clay/column system, which consist of elastic and viscoplastic components, are equal. To preserve the uniform distribution of the radial stresses at the interface between the clay and the column, an auxiliary pseudo-yield criterion was implemented. The criterion depends on the equivalence of radial stresses in the

columns and the surrounding clay. Elastoplastic material behaviour for the *in situ* clay and the column materials was calculated through a viscoplastic algorithm implemented into an FE code for axisymmetric numerical analysis. However, the viscoplastic component of the total strain is more of a correction based on the imposed yield criterion (i.e. the elimination of the stress discontinuity in the radial direction), rather than truly plastic or viscoplastic. Additionally, in the implementation of Schweiger and Pande (1986) and Schweiger and Pande (1988), only the time-independent behaviour was considered.

In order to account for the qualitative effects of the column installation, a radial strain was applied to the surrounding clay prior to the application of external loads. Schweiger and Pande (1988) used the average stiffness for the homogenised material by calculating the weighted average of the stiffnesses of the stone column and the clay (as shown in Equation (3.1), where ρ represents the volume fraction, i.e. the volume proportion of the columns per unit volume, estimated as $\rho = A_{\mathbf{c}}/(/A_{\mathbf{c}} + A_{\mathbf{s}})$, and the stiffness matrix $\mathbf{D}$ for the homogenised material, the stone column, and the *in situ* clay are denoted by subscripts h, c, and s, respectively).

$$D_h = (1 - \rho)D_s + \rho \cdot D_c \tag{3.1}$$

Following on the work by Schweiger and Pande (1988), Lee and Pande (1998) proposed a unit cell approach under axisymmetric conditions to model the elastoplastic stress-strain response of the homogenised media. The viscoplastic algorithm using the methodologies proposed by Schweiger and Pande (1988) and Lee and Pande (1998) maintains the local equilibrium between the individual materials in the integration of non-linear equations at each load (or time) step. However, these formulations include stress corrections based on the imposed criteria that violate initial constraints when plasticity occurs. Therefore, Vogler and Karstunen (2008) and Vogler (2008) extended the main ideas of Schweiger and Pande (1988) and Lee and Pande (1998) by accounting for the redistribution of strains between the constituents after the stress corrections. Vogler (2008) implemented the technique into a 2D FE code for generalised stress states in combination of a coupled consolidation analysis using this technique for embankments.

The main assumptions on the homogenisation technique by Vogler and Karstunen (2008) and Vogler (2008) can be listed as:

- Columns are homogeneously and uniformly distributed over the reinforced region
- The vertical strains in both the column and the *in situ* clay are the same, and slippage is prohibited
- No horizontal and shear stress discontinuity between the *in situ* clay and the columns
- Columns are placed vertically, ensuring that the stiffness matrices are independent of the direction of the stress vector, $\Delta\sigma^{c,s}$

The homogenisation method by Vogler (2008) was implemented into the 2D finite element code PLAXIS version 8.4 (Brinkgreve and Vermeer 2002) for generalised stress states, together with a new solution routine. As suggested by Canetta and Nova (1989), the fundamental assumptions of

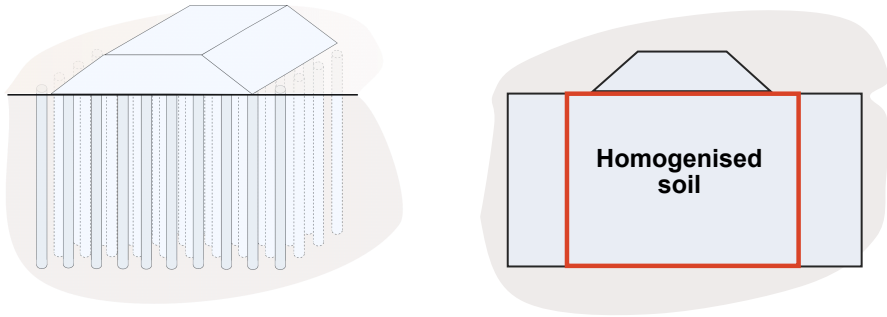

(a) (b)

Figure 3.2: *Numerical simulations of stabilised clay. (a) 3D analysis with discrete columns (Vogler 2008), (b) 2D analysis with VAT.*

the method were verified against a true 3D boundary value problem by Vogler (2008), as illustrated in Figures 3.2a and 3.2b.

The problem in question was investigated using two benchmarks: embankments constructed on soft Vantilla clay and soft Bothkennar clay, both stabilised with deep-mixed cement columns. The benchmark analyses were performed using the full 3D simulations with discrete columns and the 2D simulations with VAT (e.g. Vogler and Karstunen 2008; Vogler 2008; Becker and Karstunen 2013). The performance of the technique is demonstrated by Vogler (2008). The predictions obtained from the full three-dimensional analysis method and the plane strain analysis with VAT were found to be highly comparable. Stress-strain distribution under loading was computed through a sub-iteration procedure, taking into account different soil models for each material.

Local equilibrium is satisfied using Equations (3.2)–(3.5), where the horizontal stresses and the shear stresses between the clay and column materials are assumed to be equal. The global coordinate system is defined as x, z in the horizontal direction and y in the vertical direction.

$$\Delta\sigma_x^{\mathrm{eq}} = \Delta\sigma_x^{\mathrm{c}} = \Delta\sigma_x^{\mathrm{s}} \tag{3.2}$$

$$\Delta\sigma_z^{\mathrm{eq}} = \Delta\sigma_z^{\mathrm{c}} = \Delta\sigma_z^{\mathrm{s}} \tag{3.3}$$

$$\Delta\tau_{xy}^{\mathrm{eq}} = \Delta\tau_{xy}^{\mathrm{c}} = \Delta\tau_{xy}^{\mathrm{s}} \tag{3.4}$$

$$\Delta\tau_{yz}^{\mathrm{eq}} = \Delta\tau_{yz}^{\mathrm{c}} = \Delta\tau_{yz}^{\mathrm{s}} \tag{3.5}$$

The kinematic constraints, based on analogous vertical strains between the clay and columns, are formulated by applying Equations (3.6) and (3.7).

$$\Delta\varepsilon_y^{\mathrm{eq}} = \Delta\varepsilon_y^{\mathrm{c}} = \Delta\varepsilon_y^{\mathrm{s}} \tag{3.6}$$

$$\Delta\gamma_{zx}^{\mathrm{eq}} = \Delta\gamma_{zx}^{\mathrm{c}} = \Delta\gamma_{zx}^{\mathrm{s}} \tag{3.7}$$

The 3D effective stress tensor is denoted by $\boldsymbol{\sigma}'$, and the strain tensor is similarly denoted by $\boldsymbol{\epsilon}$. The stress and strain increments of the equivalent material ($(\boldsymbol{\Delta\sigma^{eq}})'$ and $\boldsymbol{\Delta\epsilon^{eq}}$, respectively) are computed based on the volumetric contribution of each material, with the proportions represented by the volume fractions of clay and columns, Ω_s and Ω_c, respectively (in Equations (3.8)–(3.10)).

$$(\boldsymbol{\Delta\sigma^{eq}})' = \Omega_s(\boldsymbol{\Delta\sigma^{s}})' + \Omega_c(\boldsymbol{\Delta\sigma^{c}})' \tag{3.8}$$

$$\boldsymbol{\Delta\epsilon^{eq}} = \Omega_s\boldsymbol{\Delta\epsilon^{s}} + \Omega_c\boldsymbol{\Delta\epsilon^{c}} \tag{3.9}$$

$$(\boldsymbol{\Delta\sigma^{eq}})' = \mathbf{D^{eq}}\boldsymbol{\Delta\epsilon^{eq}} \tag{3.10}$$

The tensor $\mathbf{D^{eq}}$ represents the elastic stiffness matrix for the homogenised material. By applying averaging rules considering the elastic stiffness matrices of the constituents, along with the appropriate local equilibrium and kinematic constraints, $\mathbf{D^{eq}}$ can be determined analytically.

3.3 Volume Averaging Technique (VAT) for excavations

To accurately assess the effectiveness of the two-material systems, namely in situ clay and the columns, in reducing deformations, the distinct elastoplastic behaviour of each constituent was examined through a full 3D analysis of a 10-meter deep braced excavation case. Considering the stress-strain distribution of the individual materials using different constitutive models, a plane strain VAT formulation was defined to represent the homogenised material.

• Stress-strain response of column and natural clay materials in 3D

In order to examine the hydromechanical response of a clay-column system in deep excavations stabilised with deep-mixed columns, a full three-dimensional (3D), fully coupled consolidation analysis was carried out. The geometry of the model, the boundary conditions, the numerical parameters of the model and the construction stages of the benchmark case are presented in **Paper A** and **Paper B**.

The deep-mixed columns were simulated using separate simplified soil clusters (i.e. overlapping columns), as illustrated in Figure 3.3b, with the MNhard model, while the soft natural clay was represented by the S–CLAY1S model. The mixed columns were assumed to be installed as "wished-in-place".

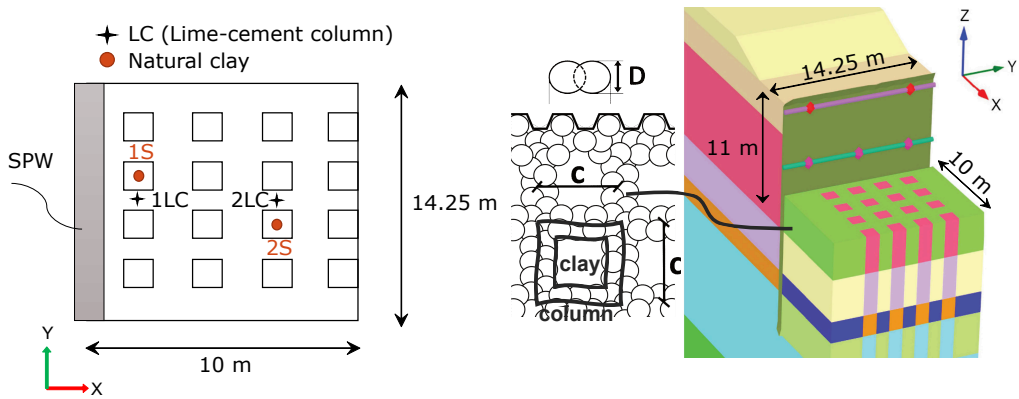

(a) (b)

Figure 3.3: *Sampling points in clay/column system. (a) plan view, (b) 3D analysis.*

To examine the distinct behaviour of the clay/column system, the external strains representing the installation effects due to the construction of deep-mixed columns were not applied in this series of analyses, in contrast to **Paper A** and **Paper B**. In the 3D simulation presented in **Paper B**, only the columns were exposed to the prescribed strains with varied magnitudes along the stabilised zone. The exclusion of the external strains would thus aid in comparing the final stress-strain distribution of the clay and the columns more clearly. This section presents comparisons of stress and strain increments, as well as total values, for the individual materials, without accounting for the installation effects in the final excavation stage.

The success of the homogenisation technique in accurately reflecting the soil response relies significantly on understanding the soil-column interaction. The stress-strain response of the column and the clay were investigated at two different regions projected on the plan view in Figure 3.3a. The increments of stresses and strains in the clay and column materials along the stabilised zone, down to a depth of 22 meters, were examined at two regions: Region 1 (1S and 1LC) and Region 2 (2S and 2LC), where S and LC represent soft clay and LC column materials at the respective locations in Figures 3.4 and 3.5. In 3D analyses, the global coordinate system is defined with x and y as the horizontal directions, and z as the vertical direction.

The high rigidity of the columns compared to the soft natural clay, along with the use of different constitutive soil models, led to varied stress paths within the individual constituents. However, in certain directions, a similar stress-strain response can still be inferred. The results of the simulation for Region 1 and Region 2 highlight that the increments of the vertical strains $\dot{\varepsilon}_{zz}$, the horizontal strains $\dot{\varepsilon}_{xx}$ in the x-axis and the shear strains $\dot{\gamma}_{zx}$ in the zx-plane direction are of the same order. The results presented in Figure 3.4 support the validity of the assumption of perfect bonding between the soil and the columns, based on the benchmark case with densely spaced, overlapping column arrangement.

For the same regions, the stress increments were examined separately in the clay and the columns. The increments of horizontal stress, $\dot{\sigma}_{yy}$, in the y-axis, and shear stresses, $\dot{\tau}_{xy}$ and $\dot{\tau}_{yz}$, in the xy- and yz-planes, respectively, were of the same magnitude. This suggests that no horizontal stress or shear stress discontinuities are expected between the clay and columns in the specified directions, as illustrated in Figure 3.5.

In addition to examining the phase-dependent incremental stress-strain response of the stabilised clay, the total stress-strain distribution at the end of the excavation was also investigated. Similar trends in the incremental stress-strain response are calculated for the total values of the stresses and strains, as shown in Figures 3.6 and 3.7. At the end of the excavation, the final stress and strain developed in both the columns and the clay were of the same order in the identified directions.

Based on the 3D analysis of the benchmark excavation, the unloading mechanism was examined, and the stress-strain response of each constituent was generalised. The fundamental assumptions that form the basis of the homogenisation method for excavations are proposed as:

- Columns are homogeneously and uniformly distributed over the reinforced region in the passive side of the excavation
- The vertical strains, horizontal strains (in the horizontal plane), and shear strains (angular strain in the vertical plane) are equal in both the column and the in situ clay, indicating that no slippage is allowed
- The continuity of the horizontal stress (in the out-of-plane direction) and of the shear stresses (in vertical and horizontal directions) between the clay and the columns are ensured
- Columns are placed vertically

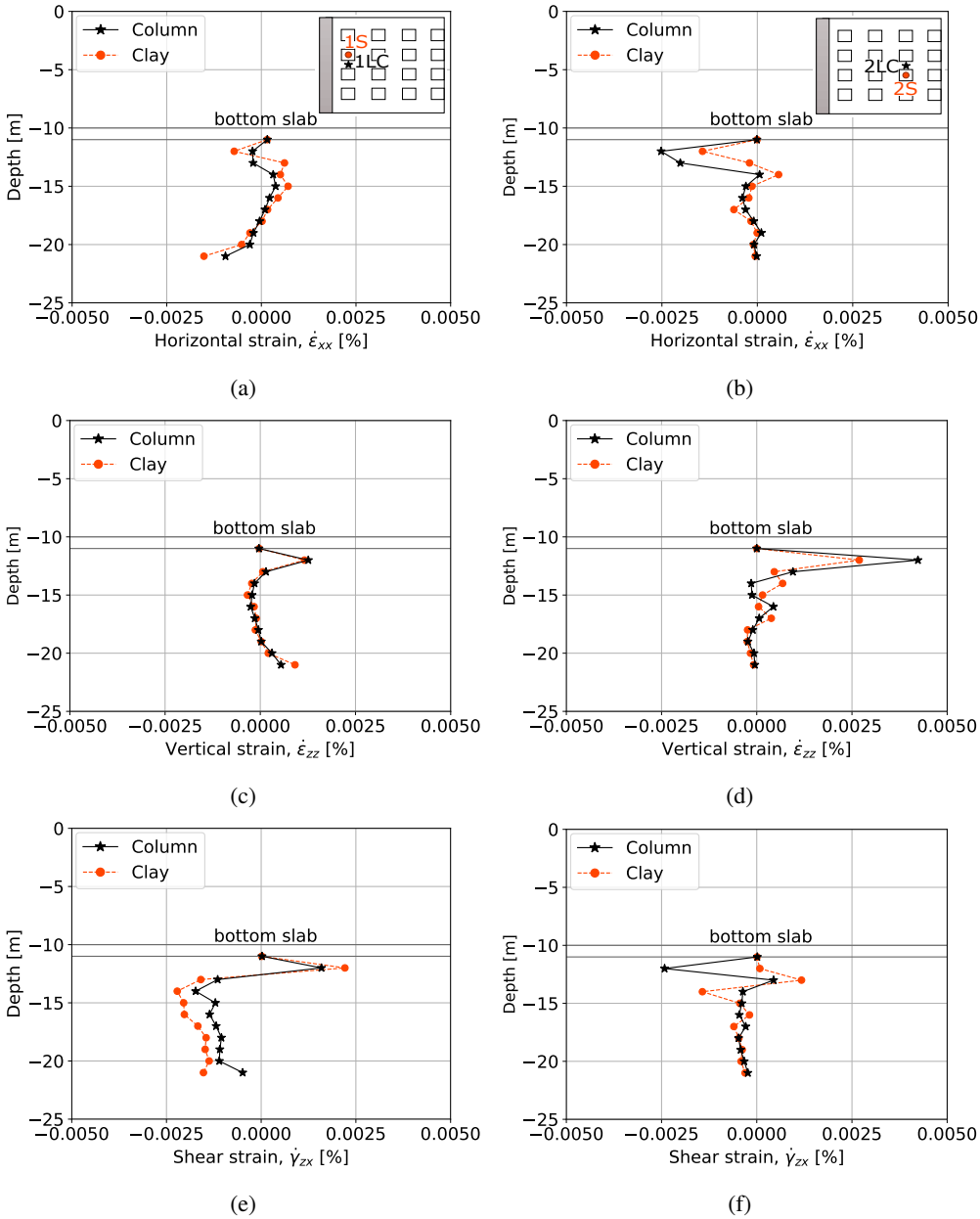

Figure 3.4: *Equal strain increments in clay/column system at the final excavation stage. Region 1: (a) $\dot{\varepsilon}_{xx}$, (c) $\dot{\varepsilon}_{zz}$, (e) $\dot{\gamma}_{zx}$, and Region 2: (b) $\dot{\varepsilon}_{xx}$, (d) $\dot{\varepsilon}_{zz}$, (f) $\dot{\gamma}_{zx}$.*

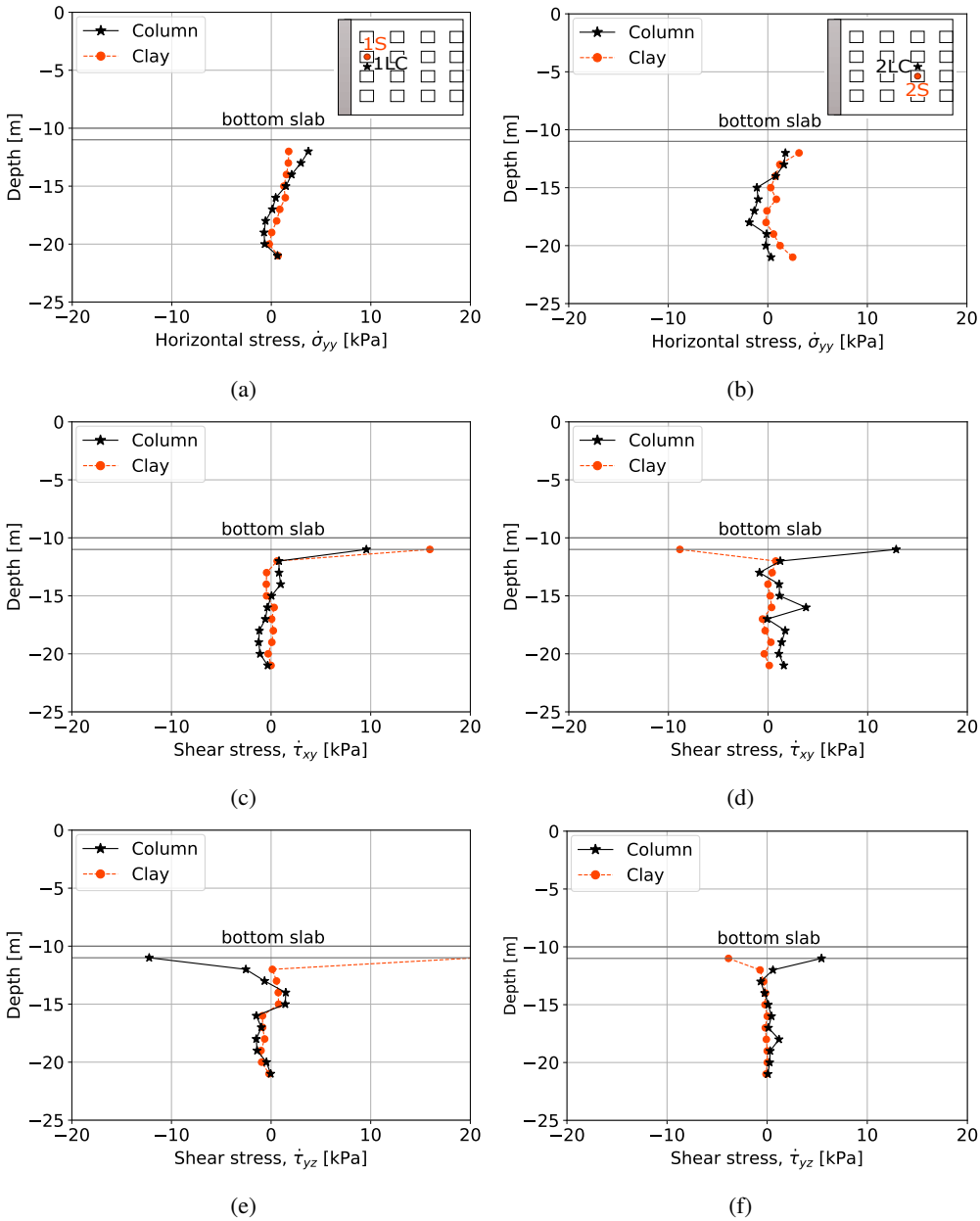

Figure 3.5: *Equal stress increments in clay/column system at the final excavation stage. Region 1: (a) $\dot{\sigma}_{yy}$, (c) $\dot{\tau}_{xy}$, (e) $\dot{\tau}_{yz}$, and Region 2: (b) $\dot{\sigma}_{yy}$, (d) $\dot{\tau}_{xy}$, (f) $\dot{\tau}_{yz}$.*

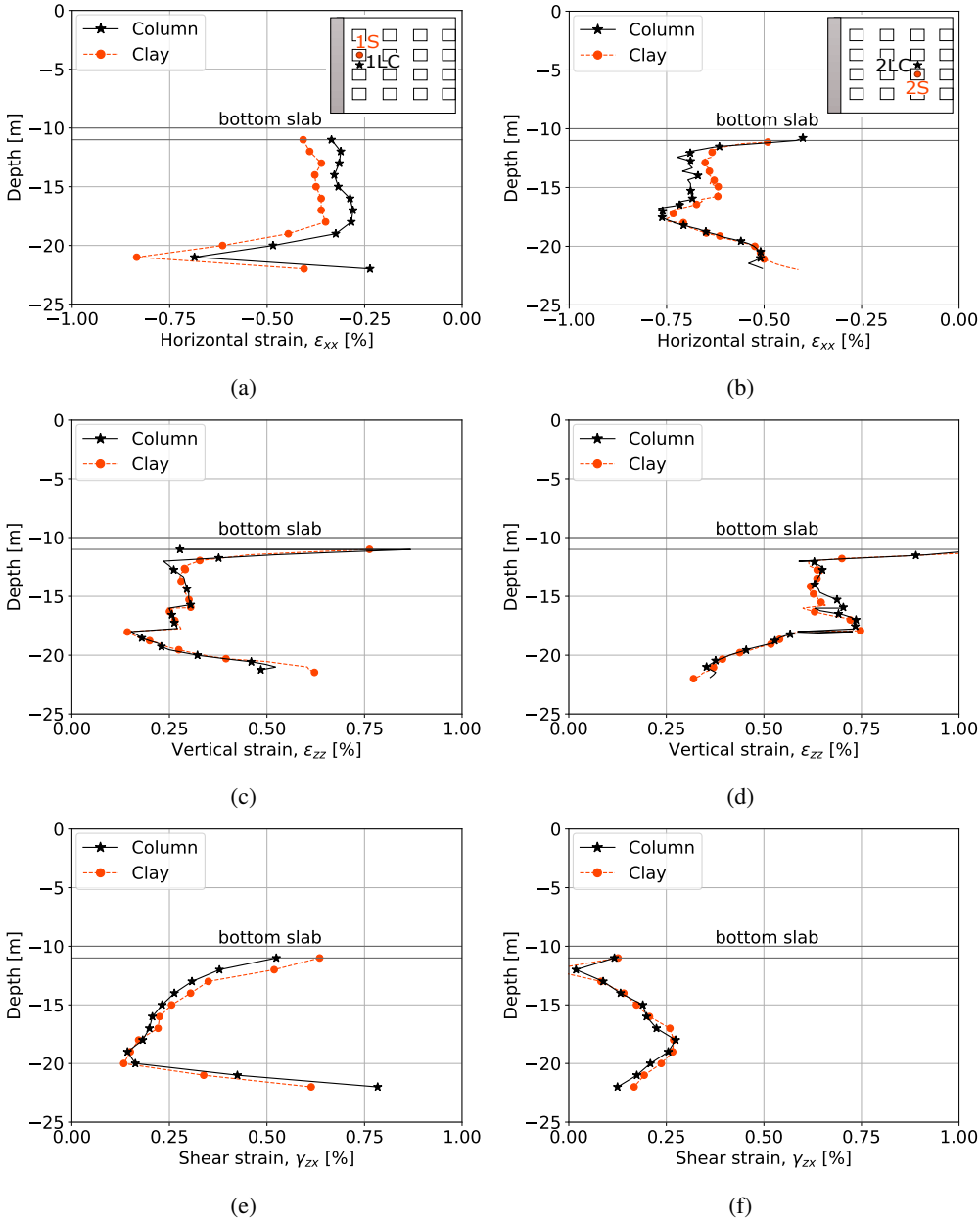

Figure 3.6: *Equal total strain in clay/column system at the final excavation stage. Region 1: (a)* ε_{xx}*, (c)* ε_{zz}*, (e)* γ_{zx}*, and Region 2: (b)* ε_{xx}*, (d)* ε_{zz}*, (f)* γ_{zx}*.*

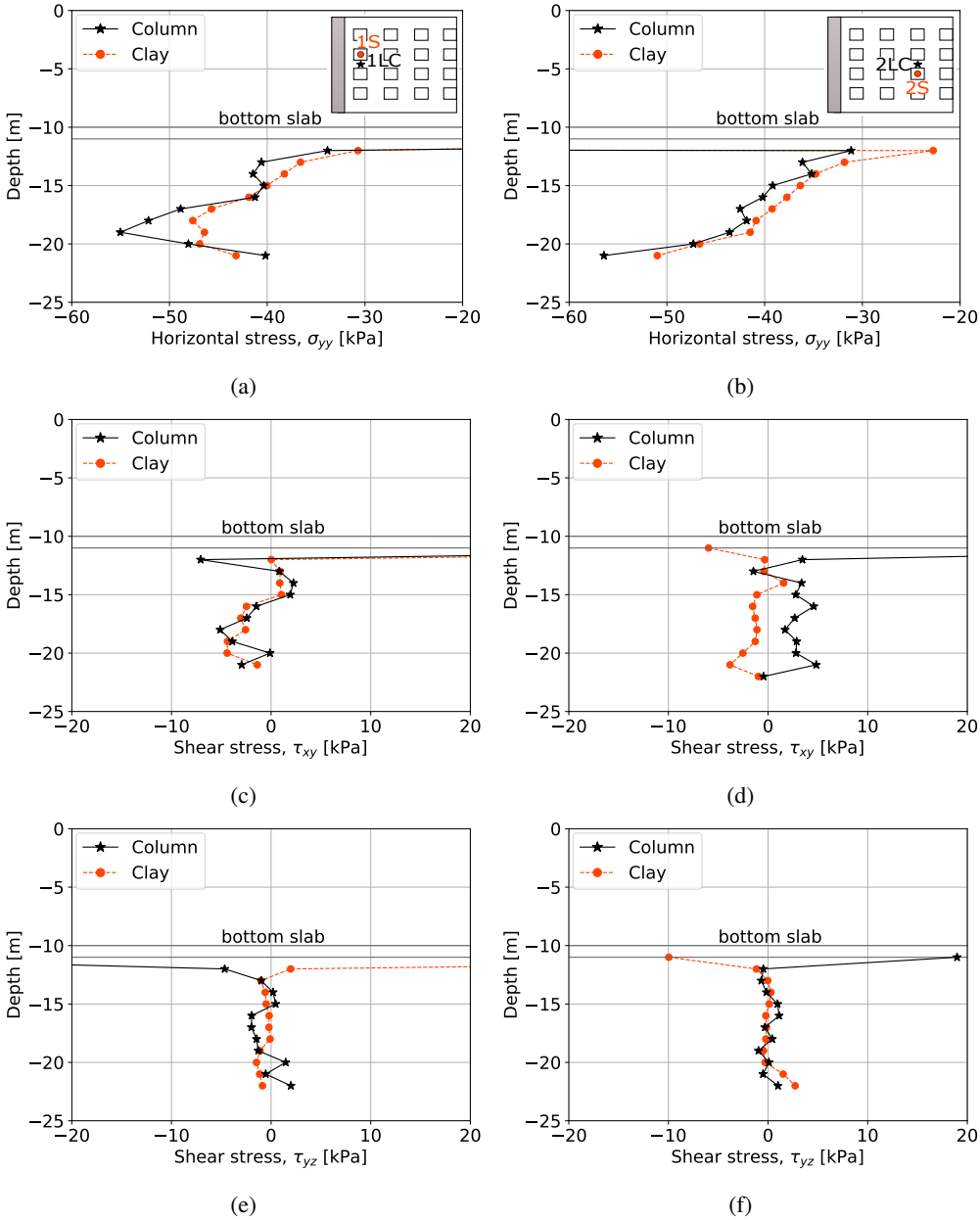

Figure 3.7: *Equal total stress in clay/column system at the final excavation stage. Region 1: (a) σ_{yy}, (c) τ_{xy}, (e) τ_{yz}, and Region 2: (b) σ_{yy}, (d) τ_{xy}, (f) τ_{yz}.*

• Formulation and implementation of VAT for 2D analysis

The full description of VAT, including implementation and verification, is presented in **Paper C**. Therefore, this section will briefly explain some additional details concerning the implementation. The local equilibrium and kinematic constraints of the homogenised medium consisting of deep-mixed columns and *in situ* clay were derived from the 3D numerical simulation. In the following equations, *s*, *c* and *eq* denote *in situ* soft clay, columns and the equivalent material, respectively. In a 2D analysis, the global coordinate system in PLAXIS defines x and z as the horizontal directions and y as the vertical direction. Therefore, the definitions of the y and z axes differ between 2D and 3D analyses and should be inverted. In the equations below, boldface symbols represent tensors.

Local mechanical balance can be imposed as:

$$\Delta\sigma_{zz}^{\mathrm{eq}} = \Delta\sigma_{zz}^{\mathrm{c}} = \Delta\sigma_{zz}^{\mathrm{s}} \tag{3.11}$$

$$\Delta\tau_{yz}^{\mathrm{eq}} = \Delta\tau_{yz}^{\mathrm{c}} = \Delta\tau_{yz}^{\mathrm{s}} \tag{3.12}$$

$$\Delta\tau_{zx}^{\mathrm{eq}} = \Delta\tau_{zx}^{c} = \Delta\tau_{zx}^{\mathrm{s}} \tag{3.13}$$

Kinematic constraints for the case of a stabilised clay can be described as:

$$\Delta\varepsilon_{xx}^{\mathrm{eq}} = \Delta\varepsilon_{xx}^{\mathrm{c}} = \Delta\varepsilon_{xx}^{\mathrm{s}} \tag{3.14}$$

$$\Delta\varepsilon_{yy}^{\mathrm{eq}} = \Delta\varepsilon_{yy}^{\mathrm{c}} = \Delta\varepsilon_{yy}^{\mathrm{s}} \tag{3.15}$$

$$\Delta\gamma_{xy}^{\mathrm{eq}} = \Delta\gamma_{xy}^{\mathrm{c}} = \Delta\gamma_{xy}^{\mathrm{s}} \tag{3.16}$$

The stiffness matrix $\mathbf{D}$ of the equivalent material can be analytically derived from the strain increments in the clay and the columns, taking into account the volume fractions Ω_{s} and Ω_{c}, as well as the stiffness matrices of the representative materials, using the structural matrices $\mathbf{S}^{\mathrm{s}}$ and $\mathbf{S}^{\mathrm{c}}$, respectively ($\mathbf{S^{c,s}} = f(\Omega_{\mathrm{s}}/\Omega_{\mathrm{c}}, \mathbf{D^s}, \mathbf{D^c})$). The computation is given in Equations (3.17)-(3.19) when stress increments in homogenised media are expressed in terms of effective stresses.

$$(\boldsymbol{\Delta\sigma^{eq}})' = \Omega_{\mathrm{s}}(\boldsymbol{\Delta\sigma^{s}})' + \Omega_{\mathrm{c}}(\boldsymbol{\Delta\sigma^{c}})' \tag{3.17}$$

$$\mathbf{D^{eq}}\boldsymbol{\Delta\varepsilon^{eq}} = \Omega_{\mathrm{s}}\mathbf{D^s}\boldsymbol{\Delta\varepsilon^{s}} + \Omega_{\mathrm{c}}\mathbf{D^c}\boldsymbol{\Delta\varepsilon^{c}} \tag{3.18}$$

$$\mathbf{D^{eq}}\boldsymbol{\Delta\varepsilon^{eq}} = \Omega_{\mathrm{s}}\mathbf{D^s}\mathbf{S^s}\boldsymbol{\Delta\varepsilon^{eq}} + \Omega_{\mathrm{c}}\mathbf{D^c}\mathbf{S^c}\boldsymbol{\Delta\varepsilon^{eq}} \tag{3.19}$$

The generalised expression for $\mathbf{D^{eq}}$ yields Equation (3.20).

$$\mathbf{D^{eq}} = \Omega_{\mathrm{s}}\mathbf{D^s}\mathbf{S^s} + \Omega_{c}\mathbf{D^c}\mathbf{S^c} \tag{3.20}$$

When the behaviour of stabilised clay is considered to be non-linear elastoplastic, the stiffness matrix in the system of equations changes during each load step. The use of separate constitutive models for the clay and the columns therefore necessitates a solution strategy that involves the

determination of incremental strain and stresses with a sub-iteration procedure. The formulation of the VAT used in this study follows a similar methodology described in Vogler (2008).

Constitutive stresses are computed following an automatic substepping algorithm (Sloan 1987; de Borst and Heeres 2002). The local integration of the constitutive equations is carried out using a return mapping algorithm, which projects the elastic trial stress $\sigma_{ij}^{\mathrm{tr}}$ back onto the updated yield surface by employing the derivative of the plastic potential, $\frac{\partial g}{\partial \sigma_{ij}}$.

$$\begin{aligned} \sigma_{ij}^{i} &= \sigma_{ij}{}^{i\text{-}1} + \Delta\sigma_{ij}^{tr} \text{ with } \Delta\sigma_{ij}^{tr} = D_{ijkl}\Delta\varepsilon_{kl} \\ \Delta\sigma_{ij}^{i} &= D_{ijkl}^{e}(\Delta\varepsilon_{kl}^{tr} - \Delta\Lambda\frac{\partial g}{\partial\sigma_{ij}}) \end{aligned} \tag{3.21}$$

Trial stress is modified under the consideration of the occurring elastic strains as long as local balance is maintained for the specified error tolerance. The magnitude of the error, in the integration of the constitutive laws, is dependent on the size of the solution increment. In this implementation, the Euler backward (implicit) algorithm employs user-defined *Stepsize* and *Strain Reduction* factors to control internal equilibrium conditions. The calculation of out-of-balance stresses (i.e. local equilibrium) employs a tolerated error of 1×10^{-8} in an increased manner to achieve convergence up to 1×10^{-6} that maintains the restricted limit of 1%.

The implicit algorithm, however, has a limitation by the fact that large *Stepsize* values can accumulate computational errors, necessitating smaller increments for accurate solutions when solving non-linear differential equations. In this implementation, one input parameter, *Stepsize*, has been added to control the size of the trial stain increment within the subroutine, similar to implementations by Wiltafsky (2003) and Vogler (2008). To prevent excessively large strain increments that could create inaccuracies in the simulations, the convergence of the subiterative process was controlled by restricting the Euclidean norm of the six-dimensional strain increment vector, $\|\boldsymbol{\Delta\varepsilon}\|$. Similarly, in case of nonconvergence *Strain Reduction* factor ensures adopting a smaller trial step size, $\boldsymbol{\Delta\varepsilon_{\mathrm{tr}}}$ that will be used to calculate the trial stress, $(\boldsymbol{\Delta\sigma_{\mathrm{tr}}})'$ in the next step.

The implementation of the homogenisation as a User-Defined Soil Model (UDSM) using an Euler backward scheme is summarised in Algorithm 1. The numerical integration was done by updating the stress state at the end of the strain increment by using an iterative solution procedure. The iterative procedure continues until compliance with the dictated local equilibrium is achieved. The VAT continually updates the accumulated stresses and restores the state variables of the soil models adopted for each iteration step.

Additionally, the implementation accounts for both drained and undrained behaviour. Under drained conditions, the soil skeleton alone governs the response, and no excess pore pressure develops; hence, the effective Poisson's ratio ν' is used in the computation. Under undrained conditions, pore pressure increments, Δp_{w}, are computed based on the volumetric strain increments, $\Delta\varepsilon_{\mathrm{v}}$ and the equivalent bulk modulus of the pore fluid-soil system, K_{f}, using Equation (3.22) (see Naylor and Pande (1981) and Potts and Zdravković (1999)).

Algorithm 1: Euler backward (implicit) algorithm for VAT

DECIDE: n_{sub} by *Stepsize* (where n_{sub} = number of substepping)
FIND: $\mathbf{\Delta\varepsilon} \leftarrow \frac{\mathbf{\Delta\varepsilon}}{n_{\text{sub}}}$ and FTOL $= \frac{1.d-8}{n_{\text{sub}}^2}$
GET: User defined values of *Stepsize* and *Strain Reduce*
if Stepsize < 0 **then**
    $n_{\text{sub}} = \left\lfloor \frac{\|\Delta\varepsilon\|}{|(Stepsize/1000)|} \right\rceil$
end if
if *Stepsize* > 0 **then**
    $n_{\text{sub}} = Stepsize$
end if
$\mathbf{\Delta\varepsilon} = \frac{\mathbf{\Delta\varepsilon}}{n_{\text{sub}}}$
for Iteration=1 to n_{sub} **do**
    GET: $\mathbf{D^{eq}}$, $\mathbf{\Delta\varepsilon^{s}_{tr}}$, $\mathbf{\Delta\varepsilon^{c}_{tr}}$
    FTOL $= \frac{1.d-8}{n_{\text{sub}}^2}$
    Convergence=0
    while Convergence $= 0$ **do**
        CALL: MNhard UDSM subroutine
        CALCULATE: $(\mathbf{\Delta\sigma^{c}_{tr}})'$
        if $(f((\sigma^{\mathbf{c}})', \kappa^{\mathbf{c}}) > 0)$ **then**
            CALCULATE: Plastic multiplier, $\mathbf{\Delta\Lambda}$ **from Benz (2007)**
            CALCULATE: $(\mathbf{\Delta\sigma_c})' = \mathbf{D^e_c \Delta\varepsilon^c_{tr}} - \mathbf{\Delta\Lambda D^e_c} \left(\frac{\partial \mathbf{g}(\boldsymbol{\sigma}'_{\mathbf{c}}, \kappa^{\mathbf{c}})}{\partial \boldsymbol{\sigma}'_{\mathbf{c}}} \right)$
        end if
        CALL: S–CLAY1S UDSM subroutine
        CALCULATE: $(\mathbf{\Delta\sigma^{s}_{tr}})'$
        if $(f((\sigma^{\mathbf{s}})', \kappa^{\mathbf{s}}) > 0)$ **then**
            CALCULATE: Plastic multiplier, $\mathbf{\Delta\Lambda}$ **from Karstunen et al. (2005)**
            CALCULATE: $(\mathbf{\Delta\sigma_s})' = \mathbf{D^e_s \Delta\varepsilon^s_{tr}} - \mathbf{\Delta\Lambda D^e_s} \left(\frac{\partial \mathbf{g}(\boldsymbol{\sigma}'_{\mathbf{s}}, \kappa^{\mathbf{s}})}{\partial \boldsymbol{\sigma}'_{\mathbf{s}}} \right)$
        end if
        continue on next page
    end while
end for

Continue Algorithm 1: Euler backward (implicit) algorithm for VAT

for Iteration = 1 to n_{sub} **do**
  while Convergence = 0 **do**
    if Convergence = 0 **then**
      continue from the previous page
      GET: $(\boldsymbol{\sigma}^{\mathbf{c}})'$, $(\boldsymbol{\sigma}^{\mathbf{s}})'$, FTOL, Convergence
      CALL: Local equilibrium subroutine
      CALCULATE: Local equilibrium
      Calculate trial stress correction matrix: $(\boldsymbol{\Delta\sigma}^{\mathbf{c}})^{\mathbf{cor}}$ **from Paper C**
      Calculate trial strain increments $\boldsymbol{\delta\varepsilon}^{\mathbf{c}}_{\mathbf{tr}}$, $\boldsymbol{\delta\varepsilon}^{\mathbf{s}}_{\mathbf{tr}}$
      Reduce trial strain increments by "Strain Reduce" input parameter
      Redistribute trial strain matrices: $\boldsymbol{\Delta\varepsilon}^{\mathbf{c}}_{\mathbf{tr}} = \boldsymbol{\Delta\varepsilon}^{\mathbf{c}}_{\mathbf{tr}} + \boldsymbol{\delta\varepsilon}^{\mathbf{c}}_{\mathbf{tr}}$, $\boldsymbol{\Delta\varepsilon}^{\mathbf{s}}_{\mathbf{tr}} = \boldsymbol{\Delta\varepsilon}^{\mathbf{s}}_{\mathbf{tr}} + \boldsymbol{\delta\varepsilon}^{\mathbf{s}}_{\mathbf{tr}}$
    end if
    if Iteration = 100 **then**
      FTOL = FTOL + FTOL
      counter = 0
      if FTOL $> 1.0 \times 10^{-6}$ **then**
        PRINT: *Tolerance is higher than 1%*
      end if
      if FTOL $> 1.0 \times 10^{-3}$ **then**
        PRINT: *Tolerance is too high, local equilibrium is not found.*
        stop
      end if
      Strain Reduce = *Strain Reduce*/2
      Return initial $\boldsymbol{\Delta\varepsilon}^{\mathbf{c}}_{\mathbf{tr}}$, $\boldsymbol{\Delta\varepsilon}^{\mathbf{s}}_{\mathbf{tr}}$
    end if
    if Convergence = 1 **then**
      Update stresses, $(\boldsymbol{\sigma}^{\mathbf{c}})'$, $(\boldsymbol{\sigma}^{\mathbf{s}})'$, $(\boldsymbol{\sigma}^{\mathbf{eq}})'$
      Update state variables, $\kappa^{\mathbf{c}}$, $\kappa^{\mathbf{s}}$, $\kappa^{\mathbf{eq}}$
    end if
  end while
end for

$$\Delta p_w = K_f \, \Delta\varepsilon_v \tag{3.22}$$

The equivalent bulk modulus K_{f} can be estimated using Equation (3.23), where K_{u} and K' are the undrained and drained bulk moduli, respectively. The bulk modulus K_{u} is calculated using the undrained Poisson's ratio $\nu_{\text{u}} = 0.495$.

$$K_f = K_{\text{u}} - K' = \frac{2G}{3}\left(\frac{1+\nu_u}{1-2\nu_u} - \frac{1+\nu'}{1-2\nu'}\right) \tag{3.23}$$

3.4 Constitutive models employed in numerical analyses

Constitutive models employed in the context of this research are briefly explained in this section. To simulate the stress-strain response of soft natural clay, the Creep–SCLAY1S and S–CLAY1S models were used, while the MNhard soil model was used for the deep mixed columns in the subsequent numerical analyses.

3.4.1 Modelling soft clay

Advanced constitutive soil models describing the soft soil behaviour, frequently recognise the isotropic elastoplastic Modified Cam Clay Model (MCC) (Roscoe and Burland 1968) as a reference model. However, based on experimental evidence, lightly overconsolidated natural clays exhibit anisotropy depending on stress-strain history, deposition process and fabric (Graham and Houlsby 1983; Wheeler et al. 2003; Karstunen and Koskinen 2008). In order to accurately model natural soil response, it is essential to consider strain-induced anisotropy, bonding, and destructuration, along with viscosity (refer to Section 2.2). Destructuration effect on stress-strain response of soft soils has been demonstrated by Leroueil et al. (1985), Burland (1990), Adachi et al. (1998), Yin and Cheng (2006), Karstunen and Yin (2010), and Yin et al. (2011) among others. Beyond apparent consolidation pressure, plastic straining induces changes in fabric and therefore causes gradual degradation of bonding. These typical features of soft soil, namely rate-dependency, destructuration and anisotropy, are taken into account by the Creep–SCLAY1S model. Some of the advantages of using Creep–SCLAY1S are the prediction of swelling on the 'dry' side of the critical state line (Sivasithamparam et al. 2013) and a realistic prediction of K_0 in the normally consolidated region similar to the S–CLAY1 and the S–CLAY1S models. The model takes into account destructuration-induced softening. However, the model formulation above does not account for small-strain stiffness, which was only very recently added (Tahershamsi 2023). Before introducing the key aspects of the viscoplastic Creep–SCLAY1S model, a summary of the preceding hierarchical models is necessary.

The S–CLAY1 model (Wheeler et al. 2003) is a critical state soil model that was developed to describe the behaviour of normally consolidated and lightly overconsolidated soft natural clays in the wet side of the critical state line. This model is an extension of MCC, which accounts for initial (inherent) anisotropy and the evolution of anisotropy defined by a sheared inclined yield surface during plastic straining caused both mechanisms: plastic volumetric strain and plastic shear strain.

Later, the S–CLAY1S (Soft–Clay1 with Structure (Koskinen et al. 2002; Karstunen et al. 2005)) model enabled a better prediction of sensitive natural clay response. The yield surface of the S–CLAY1S model takes into account both *destructuration*, resulting from degradation of inter-particle bonding (slippage and degradation of bonding), and *anisotropy* (rearrangement-realignment of particles and particle contacts) owing to plastic straining. The S–CLAY1S model formulation does not include strain rate effects. Therefore, the model is not capable to simulate the strain rate-dependency of natural clays.

Creep S–CLAY1S

The Creep–SCLAY1S model is an enhancement to the over-stress models (Perzyna 1966) that accounts for rate effects (Sivasithamparam et al. 2013; Sivasithamparam et al. 2015; Gras et al. 2018). According to Perzyna (1966)'s overstress theory, the total strain rate is the sum of the elastic and viscoplastic (creep) strain rates (in Equations (3.24) and (3.25)). However, in contrast to the "pure" overstress models, Creep–SCLAY1S does not have a purely elastic range.

$$\dot{\varepsilon_v} = \dot{\varepsilon}_v^e + \dot{\varepsilon}_v^c \tag{3.24}$$

$$\dot{\varepsilon_q} = \dot{\varepsilon}_q^e + \dot{\varepsilon}_v^c \tag{3.25}$$

where $\dot{\varepsilon}_{\mathrm{v}}$ and $\dot{\varepsilon}_{\mathrm{q}}$ denote the volumetric and deviatoric strain rates, respectively.

The three hardening laws incorporated into the Creep S–CLAY1S model define the changes in *sheared ellipse* in terms of size, rotation, and progressive loss of bonding with volumetric ($\varepsilon_{\mathrm{v}}^{\mathrm{c}}$) and deviatoric ($\varepsilon_{\mathrm{d}}^{\mathrm{c}}$) creep strains. The creep strains represent the combined viscous and plastic (irrecoverable) effects. The Normal Compression Surface (NCS) can be expressed with Equation (3.26) in triaxial stress space. An illustration of the surfaces of the model for this simplified case has been visualised in Figure 3.8.

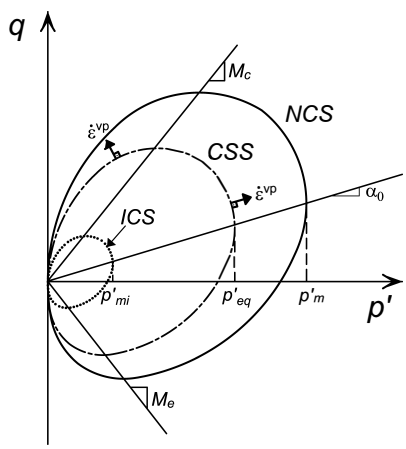

Figure 3.8: *Model surfaces in triaxial stress space (adopted from Bozkurt et al. (2023b)).*

$$f_{NCS} = (q - \alpha p')^2 - (M(\theta)^2 - \alpha^2)(p'_m - p')p' = 0 \tag{3.26}$$

where deviator stress $q = (\sigma'_1 - \sigma'_3)$ and mean effective stress $p' = (\sigma'_1 + \sigma'_2 + \sigma'_3)/3$, $M(\theta)$ is the Lode angle dependent stress ratio at the critical state, f_{NCS} represents the size of NCS, the boundary between large and small creep strains. A vertical tangent to NCS gives the initial isotropic preconsolidation pressure, p'_{m}. The current stress surface (CSS) defines the current state

of effective stress (p'_{eq}) projected to the isotropic axis, and α defines the orientation of the model surfaces, as illustrated in the triaxial stress space in Figure 3.8.

In the generalised version of the model, invariants cannot be used, thus the formulation is expressed as follows:

$$f_{NCS(3D)} = \underbrace{\frac{3}{2}\left(\left\{\sigma'_d - p'\alpha_d\right\}^T \left\{\sigma'_d - p'\alpha_d\right\}\right)}_{q^2} - \left(M(\theta)^2 - \underbrace{\frac{3}{2}\left\{\alpha_d\right\}^T \left\{\alpha_d\right\}}_{\alpha^2}\right)\left(p'_m - p'\right)p' = 0 \tag{3.27}$$

where $q^2 = 3/2\left(\left\{\sigma'_{\mathrm{d}} - p'\alpha_{\mathrm{d}}\right\}^{\mathrm{T}}\left\{\sigma'_{\mathrm{d}} - p'\alpha_{\mathrm{d}}\right\}\right)$ is the scalar value of the modified deviatoric stress tensor. The scalar value of the fabric tensor, denoted by α, is computed as $\alpha^2 = 3/2\left(\alpha_{\mathrm{d}}^{\mathrm{T}} : \alpha_{\mathrm{d}}\right)$. The deviatoric stress tensor and the deviatoric fabric tensor are defined by Equations (3.28) and (3.29), respectively.

$$\sigma'_d = \begin{bmatrix} \sigma'_x - p' \\ \sigma'_y - p' \\ \sigma'_z - p' \\ \sqrt{2}\tau_{xy} \\ \sqrt{2}\tau_{yz} \\ \sqrt{2}\tau_{zx} \end{bmatrix} \tag{3.28}$$

$$\alpha_d = \begin{bmatrix} \frac{1}{3}\left(\left(2\alpha_x - \alpha_y - \alpha_z\right)\right) \\ \frac{1}{3}\left(\left(-\alpha_x + 2\alpha_y - \alpha_z\right)\right) \\ \frac{1}{3}\left(\left(-\alpha_x - \alpha_y + 2\alpha_z\right)\right) \\ \sqrt{2}\alpha_{xy} \\ \sqrt{2}\alpha_{yz} \\ \sqrt{2}\alpha_{zx} \end{bmatrix} \text{with } \frac{1}{3}\left(\alpha_x + \alpha_y + \alpha_z\right) = 1 \tag{3.29}$$

$M\left(\theta\right)$ is the Lode angle-dependent stress ratio at the critical state, as defined by Equation (3.30), where m is the ratio of extension to compression at the critical state ($m = M_{\mathrm{e}}/M_{\mathrm{c}}$).

$$M\left(\theta\right) = M_c\left(\frac{2m^4}{1 + m^4 + \left(1 - m^4\right)\sin 3\theta_\alpha}\right)^{\frac{1}{4}} \tag{3.30}$$

$M(\theta)$ at the critical state is determined in triaxial compression, isochoric shear, and triaxial extension for $\theta_\alpha = -30°$, $\theta_\alpha = 0°$, and $\theta_\alpha = 30°$, respectively. The value of θ_α is defined based on the function of the second and third stress invariants of the modified deviatoric stress tensor ($\hat{s}_{ij}$) in Equation (3.31), as described by Sheng et al. (2000).

$$\sin 3\theta_\alpha = -\left[\frac{3\sqrt{3}}{2}\frac{(J_3)_\alpha}{(J_2)_\alpha^{3/2}}\right] \tag{3.31}$$

The $\hat{s}_{ij}$ is calculated as $(\sigma'_{\mathrm{d}} - p' \cdot \alpha_{\mathrm{d}})$ and the invariants of $\hat{s}_{ij}$ are defined in Equations (3.32)-(3.34).

$$J_1 = \mathbf{tr}\hat{s}_{ij} \tag{3.32}$$

$$J_2 = 1/2\hat{s}_{ij}\hat{s}_{ij} \tag{3.33}$$

$$J_3 = 1/3\hat{s}_{ij}\hat{s}_{jk}\hat{s}_{ki} \tag{3.34}$$

The parameters for the rate-dependency can be determined directly from the experimental data using the concept of a constant viscoplastic multiplier, as described in Grimstad et al. (2010) and Yin et al. (2011). The viscoplastic multiplier is used to formulate the creep strain rate, with the assumption of an associated flow rule (i.e. the viscoplastic strain increment normal to CSS) (Equations (3.35) and (3.36)).

$$\dot{\Lambda} = \frac{\mu_i^*}{\tau}\left(\frac{p'_{eq}}{p'_m}\right)^\beta \left(\frac{M_c^2 - \alpha^2_{K_0^{NC}}}{M_c^2 - \eta^2_{K_0^{NC}}}\right) \text{ with } \beta = \left(\frac{\lambda_i^* - \kappa^*}{\mu_i^*}\right) \tag{3.35}$$

where K_0^{NC} is the coefficient of earth pressure at the critical state calculated from Jaky's formula, η is the stress ratio at the normally consolidated state ($\eta^2_{K_0^{\mathrm{NC}}} = 3(1 - K_0^{\mathrm{NC}})/(1 + 2K_0^{\mathrm{NC}})$), λ_i^* and κ^* are the modified intrinsic compression and swelling indices, respectively; and τ is the reference time corresponding to the duration of the test (most commonly an oedometer test with a load step duration of 24 hours). The additional term, $(M_{\mathrm{c}}^2 - \alpha^2_{K_0^{\mathrm{NC}}})/(M_{\mathrm{c}}^2\eta^2_{K_0^{\mathrm{NC}}})$ ensures the same volumetric strain rate as in the oedometric loading conditions as described in Grimstad et al. (2010).

$$\dot{\varepsilon}_v^c = \dot{\Lambda}\frac{\partial p'_{eq}}{\partial p'} \text{ and } \dot{\varepsilon}_q^c = \dot{\Lambda}\frac{\partial p'_{eq}}{\partial q} \tag{3.36}$$

Deviatoric and volumetric components of elastic strains can be computed as follows:

$$\dot{\varepsilon}_v^e = \frac{\kappa^*}{(1+e)p'}\dot{p}' \text{ and } \dot{\varepsilon}_q^e = \frac{1}{3G}\dot{q} \tag{3.37}$$

The change in size of the surfaces can be defined similarly as in the S–CLAY1, S–CLAY1S, and MCC models with an isotropic hardening law. The size of the Intrinsic Consolidation Surface (ICS) is assumed to be dependent on volumetric creep strains only (Equation (3.38), in ε_v - $\ln p'$ plane).

$$\dot{p}'_{mi} = p'_{mi} \exp\left(\frac{\dot{\varepsilon}_v^c}{\lambda_i^* - \kappa^*}\right) \tag{3.38}$$

The progressive loss of bonding is modelled by adopting an ICS (Gens and Nova 1993), which is analogous to the S–CLAY1S model as described in Koskinen et al. (2002). ICS relates to the reduction in the resistance of natural soil that occurs as a result of the gradual loss of interparticle bonding during irrecoverable straining. The evolution of the size of NCS, p'_m corresponding to the current degree of bonding (χ) can be calculated using Equation (3.39). The parameter χ relates the sizes of ICS and NCS, as illustrated in Figure 3.9, and is defined in Equation (3.39).

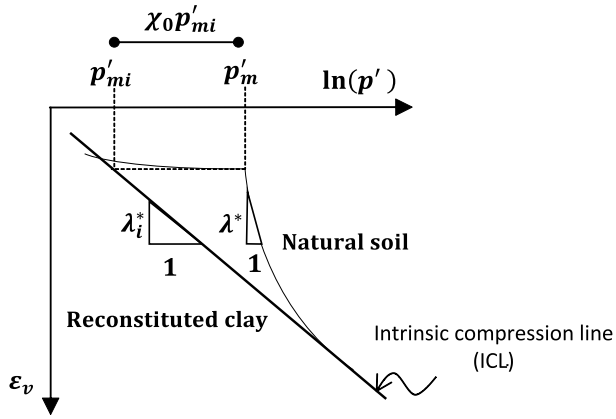

Figure 3.9: *Definition of model surfaces in one-dimensional loading.*

$$\dot{\chi} = -a\chi\left(|\ \dot{\varepsilon}_v^c\ | + b\dot{\varepsilon}_d^c\right) \text{ and } \dot{p}_m = p_{mi}(1+\dot{\chi}) \tag{3.39}$$

where a and b are the soil constants controlling the destructuration. The bonding parameter χ heads towards a target value of zero as a function of the volumetric and deviatoric creep strains.

The rotational hardening law is used to describe the changes in anisotropy expressed with a deviatoric fabric tensor. The orientation of the constitutive ellipses in the $q - p'$ plane, see Figure 3.8, can be determined by the scalar parameter α for a cross-anisotropic sample. The rotational hardening is defined by the increments of the creep strains ($\dot{\varepsilon}_{\mathrm{d}}^{\mathrm{c}}$, $\dot{\varepsilon}_{\mathrm{v}}^{\mathrm{c}}$) and two additional model constants, ω and ω_{d} that define the absolute and the relative effectiveness of creep strains in changing the anisotropy (Equation (3.40)).

$$\dot{\alpha} = \omega \left[\left(\frac{3\sigma'_d}{4p'} - \alpha_d \right) \langle \dot{\varepsilon}_v^c \rangle \; + \; \omega_d \left(\frac{\sigma'_d}{3p'} - \alpha_d \right) \dot{\varepsilon}_d^c \right] \tag{3.40}$$

The Macaulay brackets are used to limit the rotation in the 'dry' side of the critical state, but elsewhere where $\langle \dot{\varepsilon}_{\mathrm{v}}^{\mathrm{c}} \rangle \geq 0$ so that α is heading to a target value between $\frac{3\dot{\eta}}{4}$ and $\frac{\dot{\eta}}{3}$ where $\dot{\eta}$ is the tensorial equivalent of the stress ratio defined as $\eta = \sigma'_{\mathrm{d}}/p'$.

The values for the model constants can be defined using routine laboratory testing: anisotropically consolidated undrained triaxial compression (CAUC) and extension (CAUE) tests, and incrementally loaded (IL) oedometer tests. The recommended calculation procedure for the soil constants and state variables, as well as the optimisation of the parameters, has been described in detail in Gras et al. (2017) and Gras et al. (2018). The model parameters of Creep S–CLAY1S together with the definitions are summarised in Table 3.1.

Table 3.1: Model parameters of Creep-SCLAY1S.

Type	Parameter	Definition
Stiffness	κ^*	Modified swelling index
	λ_i^*	Modified intrinsic compression index
	ν'	Poisson's ratio
Strength	M_{c}	Critical state stress ratio in compression
	M_{e}	Critical state stress ratio in extension
Anisotropy	ω	Absolute effectiveness of rotational hardening
	ω_{d}	Relative effectiveness of rotational hardening
Destructuration	a	Absolute rate due to volumetric strain
	b	Relative rate due to deviator strain
Viscous	μ_i^*	Modified intrinsic creep index
	τ	Reference time (days)
Initialisation	e_0†	Initial void ratio
	σ'_{p}	Apparent preconsolidation pressure (kPa)
	K_0	Coefficient of earth pressure at rest
	α_0	Initial anisotropy
	χ_0	Initial amount of bonding

† e_0 is used to account for the changes in hydraulic conductivity, k in coupled consolidation analyses ($k = k_0 \exp\left((e_0 - e)/c_{\mathrm{k}}\right)$ where k_0 denotes the hydraulic conductivity corresponding to e_0, k is the current hydraulic conductivity at the current void ratio, e and c_{k} is the permeability change index).

3.4.2 Modelling stabilised clay

The elastoplastic mechanical behaviour of geomaterials (Jardine et al. 1986; Nova 1986) similarly characterises the response of stabilised clays. The realistic representation of the response of stabilised clay with cementing agents (i.e. lime and cement) can be achieved by incorporating the fundamental features of soil such as cementation leading to higher apparent preconsolidation pressure, loss of structure (anisotropy and/or bonding) due to irrecoverable straining and strain softening (Leroueil et al. 1979; Locat et al. 1996). In numerical modelling, soil structure was introduced by a strain-softening formulation to capture post peak behaviour based on initial ideas of Gens and Nova (1993), Lagioia and Nova (1995), and Nova et al. (2003) who suggested the use of the same framework for describing both diagenesis (bond development between grains forming sedimentary rocks) and weathering (transforming into residual soil) effects. Since then the numerical modelling of artificially structured soils at some extent incorporated the degradation of cement-soil bond.

In literature, stabilised clay behaviour has been modelled using various constitutive models, including the Extended Mohr-Coulomb model and critical state soil mechanics based models, such as Cam Clay type models, among others. Several studies that employ different modelling considerations to represent the stabilised clay response are given in Table 3.2.

In this research, the hydromechanical response of the deep-mixed columns was modelled in numerical simulations using the MNhard model (Benz 2007). Thus, a brief description of the model is presented in the following section.

Constitutive model	Origin	Example use for deep soil mixing	Comments on the examples
Extended Mohr-Coulomb model	Potts et al. (1990) and Wood (2004)	Yapage et al. (2014)	Linear–elastic model with plastic strain hardening, accounting for variation in stiffness with stress and strain
Cam Clay type models	Roscoe and Burland (1968), Oka (1985), Dafalias and Herrmann (1986), and Gens and Nova (1993)	Kasama et al. (2000), Vatsala et al. (2001), Lee et al. (2004), Liu et al. (2006), Horpibulsuk et al. (2010), Suebsuk et al. (2010), Arroyo et al. (2012), Nguyen et al. (2017), Oliveira et al. (2017), Quiroga et al. (2017), and Xiao et al. (2017)	Critical state base models accounting for fabric effects to an extent, yet the scarcity of rate-effects
Hyperbolic stress-strain relationship	Duncan and Chang (1970) and Schanz et al. (1999)	Rampello and Callisto (2003), Grimstad et al. (2008), Ou et al. (2008), Vogler and Karstunen (2008), and Bozkurt et al. (2023a)	Elastoplastic response, stress-dependent stiffness, and shear hardening/softening
Concrete damage plasticity	Lubliner et al. (1989), Lee and Fenves (1998), Schütz et al. (2011), and Schädlich and Schweiger (2014)	Larsson et al. (2012) and Waichita et al. (2020b)	Degradation in strength and stiffness, and tensile failure

Table 3.2: Various constitutive models representing stabilised clay response.

MNhard model

The Matsuoka-Nakai hardening (MNhard) model, as described in (Benz 2007), has a similar formulation to the well-known Hardening Soil model (HS) (Schanz 1998; Schanz et al. 1999). However, MNhard does not account for volumetric hardening for the sake of simplicity. The isotropic hyperbolic soil model employs the Matsuoka-Nakai (MN) failure criterion (Matsuoka and Nakai 1974; Matsuoka and Nakai 1982). The criterion was initially integrated into the HS model (HSMN) and HS-Small model (HS-Small(MN)) by Benz et al. (2008) and Benz (2007), respectively, as an alternative to the Mohr-Coulomb criterion.

The shear hardening during triaxial primary loading is defined through a cone yield surface. The definition of the accumulated deviatoric plastic shear strain γ_s^{ps} is expressed by $\frac{3}{2}\varepsilon_1^{\mathrm{p}}$ (Benz et al. 2008). Therefore, the yield function can be rewritten as in Equation (3.41).

$$f_s = \frac{3}{4}\frac{q}{E'_{50}}\frac{\frac{1-\sin\phi'_m}{\sin\phi'_m}}{\frac{1-\sin\phi'_m}{\sin\phi'_m} - R_{\mathrm{f}}\frac{1-\sin\phi'}{\sin\phi'}} - \frac{3}{2}\frac{2q}{E'_{ur}} - \gamma_s^{ps} \text{ and } R_{\mathrm{f}} = \frac{q_{\mathrm{f}}}{q_{\mathrm{a}}} < 1.0 \tag{3.41}$$

where E'_{50} and E'_{ur} are the secant and unloading/reloading stress-dependent stiffnesses, respectively (refer to Equation (3.42)). q_{a} is the asymptotic deviatoric stress, as defined in the original Duncan–Chang model, and q_{f} and R_{f} are the deviatoric stress at failure and the failure ratio.

$$E'_{50,ur} = E'^{ref}_{50,\mathrm{ur}}\left(\frac{\sigma'_3 + c'\cot\phi'}{\sigma'^{ref} + c'\cot\phi'}\right)^m \tag{3.42}$$

where $E'^{\mathrm{ref}}_{50,\mathrm{ur}}$ is the reference modulus corresponding to a reference stress σ'^{ref}, σ'_3 is the confining stress, and the exponent of m defines the shape of the yield locus and reflects the amount of stress dependency of the stiffness (Vermeer and Brinkgreve 1998). If the model is to be used for soft clays, the exponent of the power law should be selected as 1 (Schanz et al. 1999). For granular materials, the value ranges between 0.5-1.0 (Benz 2007). In the model, the shear modulus G and the effective Poisson's ratio ν' are used as input parameters. The value of G is calculated based on the principles of elasticity theory.

The yield criterion is determined by the average of mobilised planes in three-dimensional effective stress space (Matsuoka and Nakai 1974; Matsuoka and Nakai 1982). The Spatial Mobilised Plane (SPM) is illustrated in Figure 3.10. The maximum ratio of the normal stress σ'_{SMP} and the shear stress τ_{SMP} on SPM is expressed in Equation (3.43). Using the principal stress σ'_i and the stress tensor σ'_{ij}, the normal and shear stresses acting on the octahedral plane can be defined as follows: the normal stress is given by $p' = 1/3\sigma'_i$, and the shear stress is given by $q = \sqrt{3/2\left(\sigma'_{ij} - p'\delta_{ij}\right)\left(\sigma'_{ij} - p'\delta_{ij}\right)}$, where δ_{ij} is Kronecker's delta.

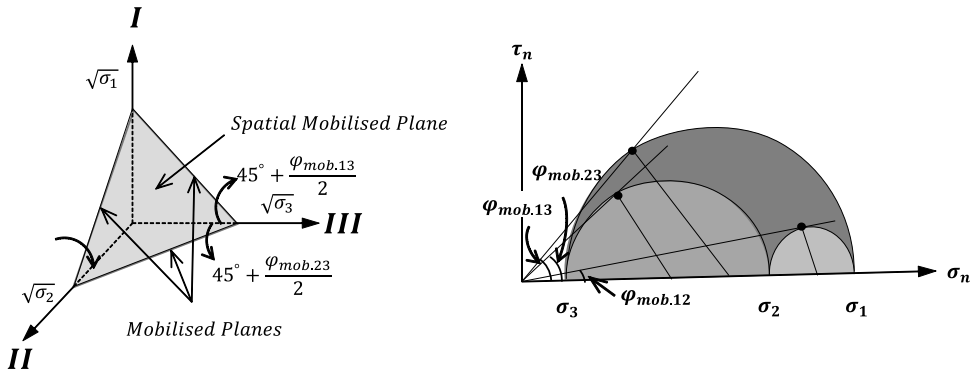

(a) (b)

Figure 3.10: *Spatial Mobilised Plane (SPM) (after Nakai and Matsuoka (1983)). (a) SPM in three-dimensional effective stress space, (b) mobilised planes.*

$$\frac{\tau_{\text{SMP}}}{\sigma'_{\text{SMP}}} = \frac{2}{3}\sqrt{\frac{(\sigma'_1-\sigma'_2)^2}{4\sigma'_1\sigma'_2}+\frac{(\sigma'_2-\sigma'_3)^2}{4\sigma'_2\sigma'_3}+\frac{(\sigma'_3-\sigma'_1)^2}{4\sigma'_3\sigma'_1}} \tag{3.43}$$

In triaxial compression, the hexagonal-shaped MC failure criterion coincides with the smoother yield surface represented by the octahedral plane. The success of the MNhard yield criterion in accurately predicting soil behaviour has been demonstrated by Matsuoka and Nakai (1985), Benz (2007), Benz et al. (2008), and Vogler (2008). These studies have reported a good agreement with the experimental yield surfaces. Upon reaching the failure condition, the ratio of shear stress to mean effective stress corresponds to the limiting value as defined in Equation (3.44).

$$\frac{I_1 I_2}{I_3} = c \quad \text{with } c = \frac{9-\sin\phi'^2}{-1+\sin\phi'^2} \tag{3.44}$$

The first, second, and third effective stress invariants are represented by I_1, I_2, and I_3, respectively (in Equation (3.45)).

$$\begin{aligned} I_1 &= \sigma'_{ii} \\ I_2 &= \frac{1}{2}\left(\sigma'_{ij}\sigma'_{ij}-\sigma'_{ii}\sigma'_{jj}\right) \\ I_3 &= \frac{1}{6}\left(\sigma'_{ii}\sigma'_{jj}\sigma'_{kk}+2\sigma'_{ij}\sigma'_{jk}\sigma'_{ki}-3\sigma'_{ij}\sigma'_{ji}\sigma'_{kk}\right) \end{aligned} \tag{3.45}$$

The shear hardening function can be rewritten in terms of the mobilised friction, ϕ'_{m}, in triaxial compression (Equation (3.46)) when the MNhard yield criterion is incorporated.

$$\sin \phi'_m = \sqrt{\frac{9 - \frac{I_1 I_2}{I_3}}{1 - \frac{I_1 I_2}{I_3}}} \tag{3.46}$$

The plastic potential to the cone-type yield surface is defined using Equation (3.47) with the non-associated flow rule.

$$g = \left(p' + c' \cot \psi'\right) \frac{6 \sin \psi'_m}{3 - \sin \psi'_m} \tag{3.47}$$

The mobilised dilatancy angle ψ'_{m} can be calculated using the stress dilatancy theory by Rowe (1962) as in Equations (3.48) and (3.49). Due to the highly contractive behaviour at low friction angles, the mobilised dilatancy angle $\sin \psi'_{\mathrm{m}}$ is set to greater than zero (Benz et al. 2008).

$$\sin \psi'_m = \frac{\sin \phi'_m - \sin \phi'_{cv}}{1 - \sin \phi'_m \sin \phi'_{cv}} \geq 0 \tag{3.48}$$

$$\sin \phi'_{cv} = \frac{\sin \phi' - \sin \psi'}{1 - \sin \phi' \sin \psi'} \tag{3.49}$$

3.5 Global sensitivity analysis

In numerical modelling, sensitivity analyses are performed in order to determine the effect of the variability in input parameters on a specific model output. In deterministic analyses, the assessment is often done with a one factor at a time (OFAT) approach for an arbitrarily selected set of soil model parameters based on engineering judgement. The OFAT approach has traditionally been utilised in geotechnical engineering (Alamgir et al. 1996; Jamsawang et al. 2019; Zhang et al. 2020; Pandey et al. 2022) to explore the effect of individual factors on the model output (i.e. maximum settlement, factor of safety) by changing an individual factor while keeping other factors fixed (i.e. local sensitivity). However, OFAT is valid only when the model is linear, or when the input space is small enough that the model behaves approximately linearly within that region. Additionally, the OFAT approach cannot guarantee the possible correlation effects between different factors when they are at different levels (i.e. maximum and minimum values of each factor).

Deterministic evaluations of settlements and slope stability usually ignore the soil variability, which in the case of stabilised clay included both the columns and the *in situ* clay. Probabilistic methods have been incorporated in the 2D FE analyses for stabilised soils with deep-mixed columns to investigate the failure mechanisms (Honjo 1982; Navin and Filz 2006; Al-Naqshabandy and Larsson 2013; Kasama et al. 2019; Wijerathna and Liyanapathirana 2019) and allowable settlements (Huang et al. 2015; Spross et al. 2021; Phutthananon et al. 2022) in embankments, as well as in excavations (Wu et al. 2014; Pan et al. 2018) using the reliability concept and the Observational Method (Peck 1969; Nicholson et al. 1999; EN 1997-1 2005).

These studies accounted for the high variability in the strength and deformation properties of the mixed columns as the overall uncertainty in the design soil property, thereby contributing to the overall variability in the output. However, the reliability assessment adopted often treats the limit state function (i.e. serviceability limit state) based on simple stiffness averaging and/or linear-elastic perfectly-plastic solutions as absolute. The transformation uncertainties arising from numerical or analytical model assumptions strongly affect the predicted soil response (Phoon and Kulhawy 1999; Phoon et al. 2003). Besides, the performance of the system is not solely dependent on a single number (e.g. maximum settlement or FOS). Therefore, numerical and analytical tools integrated into performance-based analyses are expected to appropriately capture the coupled hydromechanical response of the stabilised clay as well as the soft natural clay (Kitazume 2024).

The complex interaction of the geostructures considered (embankment or braced excavation), soft natural clay, and the deep-mixed columns, necessitates accurate representations of the columns and the clay in numerical analyses at a system level. To accurately represent the relations between the stresses and strains in stabilised soil, advanced constitutive models are increasingly being employed that provide realistic representations of *in situ* and evolving soil parameters (e.g. stress-dependent stiffness, mobilised strength and hydraulic conductivity). However, a large number of soil parameters adopted can lead to greater computational effort in the numerical analyses. Therefore, a systematic approach is needed to identify a few important factors in models with many factors (Campolongo et al. 2007).

The Design of Experiments (DOE) is a powerful tool that accounts for changes in multiple factors at different levels and their interactions on a response variable (Box et al. 2005; Montgomery 2020; Wu and Hamada 2021). DOE allows for identifying dominant model parameters governing

the system response in order to evaluate the system performance and to integrate optimisation procedures realistically.

In this research, VAT was utilised to simulate the stabilised clay using advanced constitutive models with many model parameters for each material, including the soft natural clay (S–CLAY1S) and the deep-mixed columns (MNhard). Thus, a systematic approach, DOE, was adopted to identify the most important model parameters affecting the hydromechanical response of the stabilised clay with deep-mixed columns due to embankment load. The evolution of time-dependent deformations were investigated considering a range of model parameters. Note that in this study, the sensitivity analyses do not seek to investigate the natural variability of the materials.

Design of experiments (DOE)

The framework of DOE involves assessing the impact of factors on a response variable through all possible combinations of factors using a full factorial design or the main effects (i.e. primary factors) and low-order interactions using a fractional factorial design. If each of the k factors has n levels, the total number of experimental runs (i.e. realisations) is n^k. While this approach offers detailed insights, it can become computationally expensive and time-consuming when the number of factors increases. The standard design matrix of a 2^2 full factorial design, where each factor is run at two levels, is shown in Table 3.3.

Table 3.3: 2^2 full factorial design table of contrasts.

Factor		Interaction	Factor combination	Simulation result
A	B	AB		
−	−	+	A low, B low	y_1
+	−	−	A high, B low	y_2
−	+	−	A low, B high	y_3
+	+	+	A high, B high	y_4

The effects can be computed for a 2^2 design as shown in Equation (3.50). The main effect of a factor is the average difference between the high and low levels of the same factor, while the interaction effects are the average difference between the effects of the factors at the high level of one factor and those at the low level of the same factor. The main and interaction effects of factors A and B are denoted as A_{main}, B_{main}, and $AB_{\text{interaction}}$, respectively.

$$\begin{bmatrix} A_{\text{main}} \\ B_{\text{main}} \\ AB_{\text{interaction}} \end{bmatrix} = \frac{1}{n_{\text{run}}/2} \begin{bmatrix} -1 & -1 & +1 \\ +1 & -1 & -1 \\ -1 & +1 & -1 \\ +1 & +1 & +1 \end{bmatrix}^{\text{T}} \begin{bmatrix} y_1 \\ y_2 \\ y_3 \\ y_4 \end{bmatrix} \tag{3.50}$$

Fractional factorials are usually employed as screening designs in the initial stage. Each factor is studied at two levels, but only a fraction of all factor-level combinations is analysed, thereby reducing a relatively large list of factors to a manageable number. A fractional factorial design is

generally represented in the form 2^{k-p}, where k is the number of factors and $1/2^p$ indicates the fraction of the full factorial 2^k (Box et al. 2005).

Fractional factorial designs vary in resolution levels, which determine the extent of confounding between the main effects and interactions. Designs below resolution *III* are ineffective, as lower levels lead to complete confounding that makes it hard to distinguish the effect of a particular factor or interaction from that of another factor or interaction. The most common resolutions of *III*, *IV*, and *V* differ in how well they separate effects such that the lower-order effects are not confounded with higher-order effects, which are usually assumed to be negligible (Box et al. 2005). When multiple variables are involved, the system or process is typically influenced mainly by a few primary effects and low-order interactions (Box and Meyer 1986; Montgomery 2020) that allows for the efficient identification of significant factors using a fractional factorial design with a reduced number of simulations.

In geotechnical engineering, screening designs within the DOE framework have been employed to effectively quantify uncertainties arising in the mixing process (Larsson et al. 2005a; Larsson et al. 2005b). Larsson et al. (2005a) and Larsson et al. (2005b) investigated multiple influencing factors, including retrieval rate, number of mixing blades, rotational speed, and air pressure, through two-level and 2^k factorial experiments. Later, Larsson et al. (2005c) employed DOE to examine the spatial correlation structure of horizontal variability in deep-mixed columns using penetrometer test data as an indicator of the mixing quality. Additionally, the method has been integrated into the calibration of soil model parameters, demonstrating the non-stationary nature of factor screening in time-dependent processes by utilising both the methods of DOE and Sobol (Tahershamsi and Dijkstra 2022).

As opposed to the screening designs when optimisation is the goal, the methodology of DOE can be used in combination with regression or inverse analysis to improve the predictive capabilities of geotechnical models. Some examples can be seen in studies such as those by Miro et al. (2014), Khaledi et al. (2016), Kolivand and Rahmannejad (2018), Müthing et al. (2018), Lafifi et al. (2019), Bak et al. (2021), and Martinelli et al. (2024), using the Taguchi's design of experiments (Taguchi 1987; Roy 2010), response surface methodology (Myers 1999; Borror et al. 2002) and Sobol method (Sobol' 1993; Saltelli et al. 2008).

3.6 Benchmark excavation supported by lime-cement columns

Comparison of the 2D and 3D simulations of the benchmark

In order to compare the stress-strain response of stabilised clay in plane strain (2D) and the 3D analyses, the predicted effective stress paths were compared. Sampling points were selected at specific locations within the excavation, including Point A and Point B inside the active wedge behind the sheet pile wall, and Point C inside the passive wedge beneath the bottom of the excavation, as can be seen in Figure 3.13. The results were taken from the mid-span in the 3D analysis. The construction stages and the prescribed strain quantities used to represent the installation effects resulting from lime-cement (LC) column construction were kept consistent throughout the analyses.

The analysed geometries in the 2D and 3D analyses are presented in Figure 3.11. The model geometry, boundary conditions, mesh discretisation, numerical model parameters, and construction stages of the case study are presented in **Paper A** and **Paper B**. The same construction stages were followed in the 2D and 3D analyses.

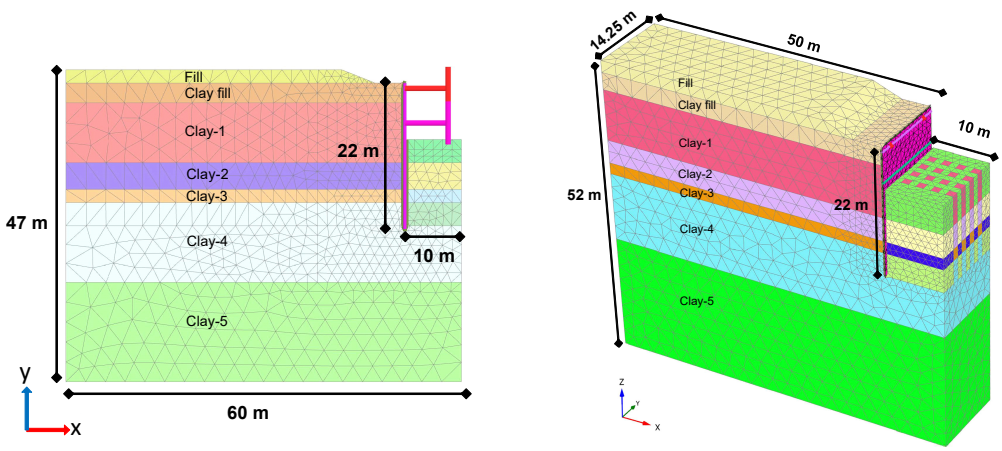

(a) (b)

Figure 3.11: *Mesh discretisation and geometric limits of the simulations. (a) 2D, (b) 3D.*

The primary difference between the analyses is the external strain application. In the 2D analysis, prescribed strains were applied over the entire excavation area, using a simple stiffness averaging method for the stabilised clay with LC columns. In contrast, in the 3D analysis, only the LC columns, which were modelled separately, were subjected to external strains. To account for the variable strut spacing, the average values of the spacings were employed to simplify the geometry. The 3D simulation focused on the mid-span section, where the field instrumentation was installed, and thereby did not account for the stiffening effects at the corners.

The soil response was investigated in the untreated soft clay simulated using the Creep–SCLAY1S model. The inspection points are located in the soft natural clay layers: Clay-1 for Point A, and Clay-4 for Point B and C. The convexity of the NCS, as well as the CSS, is determined by the layer-specific m values ($m = M_e/M_c$), resulting in analogous convexity for Point B and Point C. The yield surfaces change gradually with increasing m, and a value of $m = 1$ corresponds to a circular Drucker-Prager failure surface. Irrecoverable strain-induced anisotropy is affected by volumetric and deviatoric creep straining, therefore the initial anisotropy (α_0) was gradually reduced to α_f in the last construction phase as shown in Figures 3.12a and 3.12b.

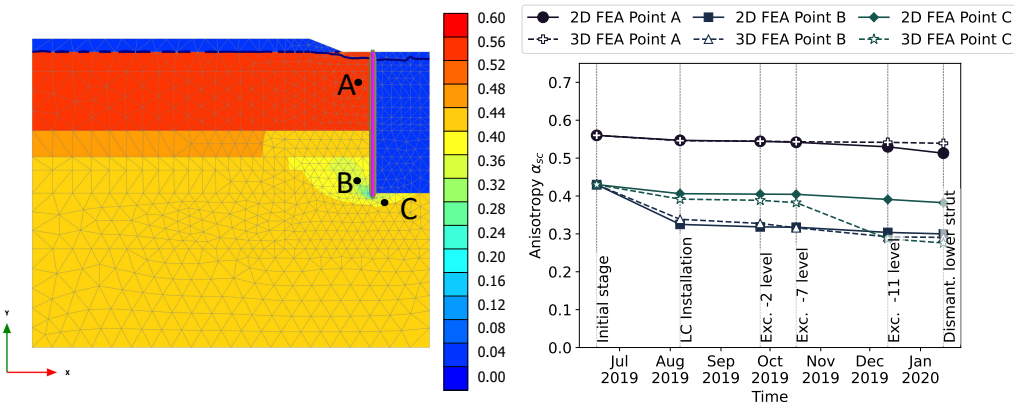

(a) (b)

Figure 3.12: *Change in anisotropy : (a) contour plot of column installation stage in the 2D analysis, (b) reduction in anisotropy in the 2D & 3D analyses.*

In Figure 3.13, the π-plane plots show the predicted stress paths for the 2D and the 3D analyses. The comparison results between the analyses revealed that the exposure of the external prescribed strain over the entire excavation volume, or limited application involving only LC columns, influences the untreated natural clay response. The 2D and the 3D simulation results indicate different behaviour for the representative sampling points which had an analogous initial stress-state. The limited application of the prescribed external strain application, only within the column volumes, resulted in different stress paths in the 3D analysis. Nonetheless, based on the predicted deformation behaviour, the 3D analysis appears to reflect the extreme conditions recorded by the short-span field measurements due to the varied spacing of the struts and the arching effect, whereas the 2D simulation depicted a more uniform stress distribution near the long-span measurements (for details, see **Paper A** and **Paper B**). Note that the postulated response in the passive side of the excavation could not be validated due to a lack of field monitoring data.

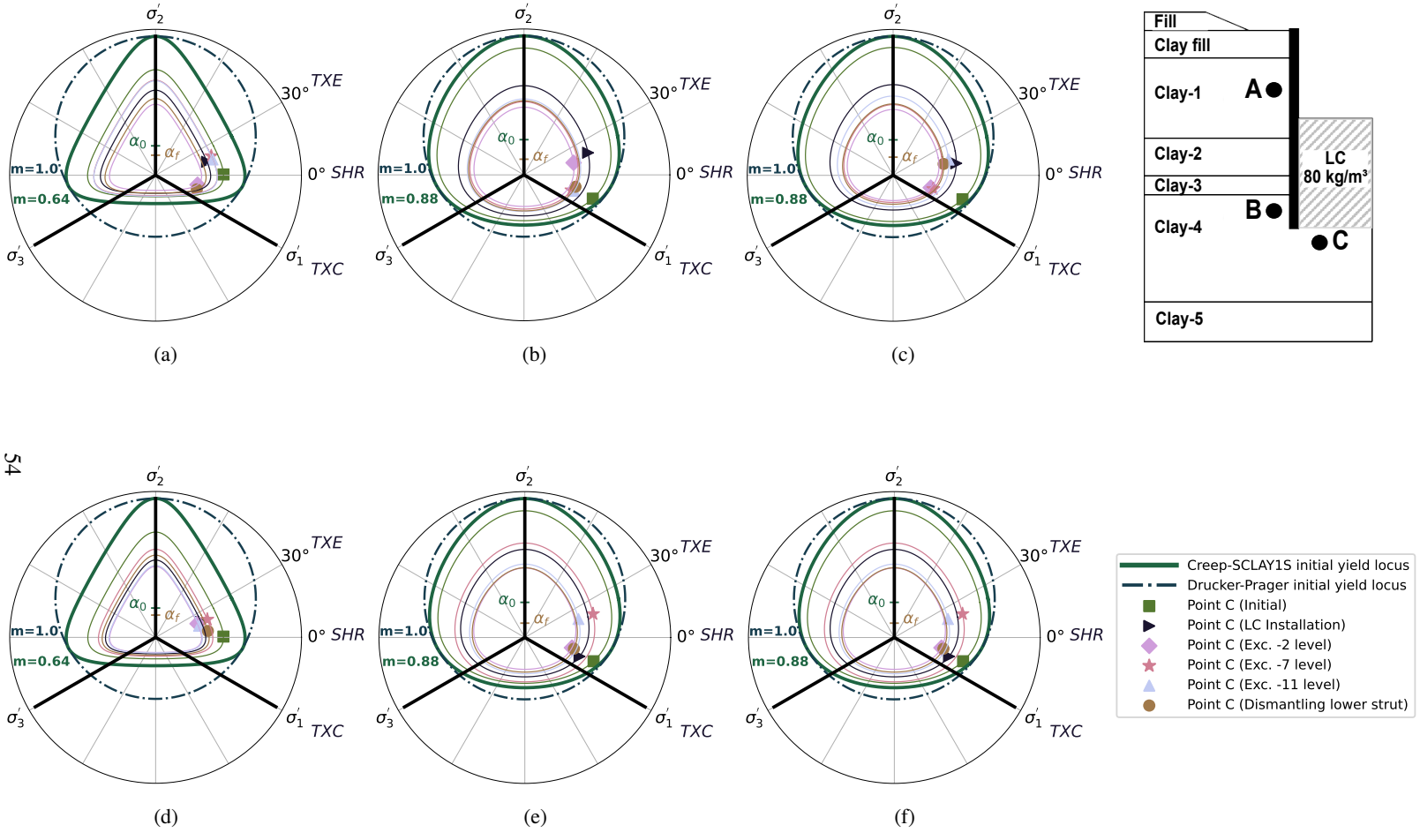

Figure 3.13: *Stress path in the π plane. The 2D FE analysis: (a) Point A, (b) Point B and (c) Point C, and the 3D FE analysis: (d) Point A, (e) Point B and (f) Point C.*

4 Summary of the appended papers

Overview of the papers

A schematic overview of the methodology development is presented in Figure 4.1. This starts with the coupled analysis of a real case of deep excavation and proceeds to the generalisation of the results of soil-column interaction. The latter includes the development, implementation and verification of VAT. Finally, sensitivity analyses of the system response for geostructures (i.e. embankments) constructed in soft natural clays stabilised with LC columns are performed. The methodology established comprises Stage I and Stage II, as further explained below.

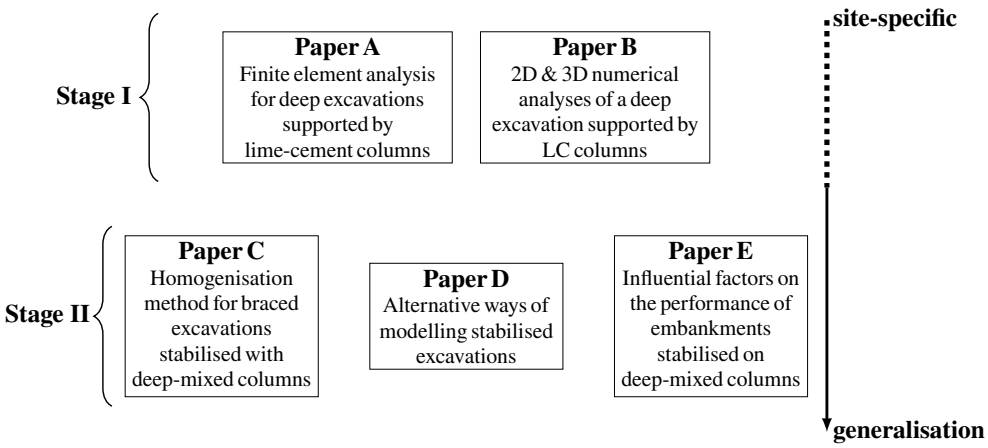

Figure 4.1: *Overview of the methodology in the appended papers through Stage I and II.*

Stage I comprises fully coupled numerical analyses of a well-documented case history involving a braced excavation supported with LC columns. The 2D and 3D FE simulations were benchmarked against the available field measurements. The simulations provided comprehensive insights into the soil–column interaction effects resulting from the installation of the columns produced by DSM. The framework, presented in **Papers A and B**, quantifies the installation effects and integrates these effects into numerical analyses in order to accurately predict the time-dependent stress-strain response of the excavation during both the construction and serviceability stages.

Stage II generalises the 3D soil–column interaction problem in stabilised clays with LC columns, and develops and implements an advanced numerical technique (i.e. VAT) to realistically evaluate the system performance, including the braced excavation, the soft natural clay, and the LC columns (**Papers C and D**).

In **Paper E**, VAT for embankments, developed by Vogler (2008), was employed in the system-level sensitivity analyses, aiming to identify the most influential factors affecting the hydromechanical response of stabilised clay with LC columns under embankment loading. The identified governing mechanisms, through a robust assessment using DOE, formed the basis for parametric studies in order to enhance computational efficiency and to reduce both material consumption (lime and cement) and related CO_2 emissions.

Paper A: "Finite element analysis for deep excavations supported by lime-cement columns: field performance in soft clay"

A section of the West Link railway project (an eight-kilometre-long double-track with a six-kilometre railway tunnel) in Gothenburg, Sweden, called E02 Central Station, is examined to evaluate the hydromechanical response of a temporary braced excavation during the eight-month construction period. The well-documented excavation in soft clay, stabilised with the dry mixing technique, is simulated using a two-dimensional plane strain (2D) model to benchmark its performance against the observed field response.

In the 2D analysis, extensive laboratory testing data including IL, CRS, CADC/E, and CAUC/E tests performed on deep-mixed column samples and on *in situ* natural clay were used. To monitor the soft clay response during the excavation, four different types of field instruments were installed at various locations. These devices recorded the pore pressure measurements through pore pressure probes, surface displacement via prisms, and strut forces using strain gauges assembled on the struts over the construction period. The authors were not involved in the programming of laboratory & field testing procedures, and the data were acquired from Swedish Transport Administration (2019), courtesy to NCC AB.

During the LC column construction stage, large deformations, in the order of 50 mm, were observed. These installation effects were incorporated into the simulation by using the prescribed external strain application. The magnitude and the direction of the prescribed strains were back-calculated and calibrated against the field monitoring data. The soft clay was modelled using the Creep–SCLAY1S model, whereas the soil behaviour of the stabilised soil with lime and cement (LC) columns was represented by the MNhard model. The weighted average of the soil moduli is used in the computation of the stabilised soil stiffness in the passive side of the excavation, considering a theoretical area replacement ratio.

A summary of some key results and conclusions is provided in the following:

(i) The experimental evidence of laboratory and field testing can be integrated to simulate the installation effects of the mixed columns based on the Observational Method (Peck 1969).

(ii) General deformation and strength parameters of the stabilised clay with LC columns exhibited similarities to those of partially saturated overconsolidated clays. The soil-mixed samples exhibited high apparent preconsolidation pressure resulting from cementation in the IL tests, whereas the CAUC/E tests demonstrated partial saturation of the samples under low confining stresses.

(iii) The inclinometers placed in the field indicated both expansive and contractive displacements caused by the construction of LC columns, before the main excavation stages. The field evidence suggests that the installation effects in relation to the high air-pressure application during the column construction and soil ageing (strength loss-regain) have a significant influence on the soil response.

(iv) The predicted deformations, pore pressure generation and structural forces caused by the excavation were in accordance with the field measurements throughout the construction period. Yet, due to the considerable difference in strut spacings, a cautious interpretation

of the results is necessary to account for potential three-dimensional effects which are not accounted for in a 2D simulation.

(v) Using a stress-dependent soil model for stabilised clay in combination with a conventional, simple stiffness-averaging method, along with a rate-dependent soil model for natural clay, can provide reasonable estimates of the time-dependent hydromechanical response of braced excavations stabilised with deep-mixed columns.

Paper B: 2D & 3D numerical analyses of a deep excavation supported by LC columns

Plane strain (2D) and three-dimensional (3D) finite element analyses of a braced excavation supported by deep-mixed columns constructed using the dry soil mixing method were performed. The results of the simulations were benchmarked against a case study in Gothenburg (see Paper A). In both analyses, elastoplastic soil models were utilised to describe the *in situ* natural clay and the lime-cement (LC) column behaviour. The stabilised clay, consisting of the soft clay and the columns, was simulated using the weighted average of the stiffness of the soft clay and the LC columns in the 2D analysis. In the 3D simulation, the overlapping columns were modelled separately and simplified into a rectangular arrangement, despite having circular cross-sections.

In order to represent the deformations caused by the construction of LC columns, prescribed strains in the horizontal directions were applied externally, which were calibrated using the field monitoring data. The values of the external strains were of the same order in both analyses. During the installation of the deep-mixed columns, significant deformations of approximately 50 mm, as monitored in the field, were simulated through external strain application.

The comparison results of the 2D and 3D simulations (PLAXIS 2D & 3D, version 22) of the excavation revealed different stress-strain responses with the excavation in progress. The arching effect in the 3D simulation created a significant difference compared to the 2D analysis, both in the predicted displacement profile and in the axial force distribution of the sheet-pile wall. The different deformation profiles can be attributed to the highly varied strut spacing in a range of 8.5–10.5 m for the upper struts.

A summary of some key results and conclusions is provided in the following:

(i) The numerical results indicate that accurate predictions of deformations and structural forces necessitate taking into account the installation effects and the 3D effects.

(ii) The deformation profiles of the 2D and the 3D analyses were compared, and significant differences were observed. A comparable deformation profile was projected in both simulations before reaching a level of -7. The ongoing excavation caused varied deformation profiles, and excessive deformations were observed in the 3D simulation.

(iii) The excess deformations projected in the 3D simulation were consistent with the measurements of the inclinometer located at the short-span. A more uniform stress distribution resulted in lower lateral deformation estimates, which were similar to the measurements of the long-span inclinometer.

Paper C: Homogenisation method for braced excavations stabilised with deep-mixed columns.

Ground improvement with deep soil mixing introduces a complex three-dimensional (3D) soil-structure interaction problem, involving soft clay and lime-cement (LC) columns arranged in a periodic grid pattern. Paper C examines the hydromechanical response of individual materials, and establishes a Volume Averaging Technique (VAT) for the accurate representation of the *in situ* clay and the columns in a plane strain analysis (2D).

The distinct responses of individual constituents (i.e. soft clay and the columns) were examined through a 3D simulation of a braced excavation supported by LC columns, using conventional separate soil clusters. Subsequently, a constitutive law for a 2D analysis, describing the response of an equivalent material, was established based on the 3D simulation. The law describes an anisotropic homogenised continuum through the averaging of the individual stress-strain responses of the constituents based on their representative volume fractions, for an unloading problem. Imposed constraints, which involve the local equilibrium and continuity of kinematics at the interface, form the basis for VAT. The soft clay was modelled using the S–CLAY1S model, whereas the soil behaviour of the LC columns was represented by the MNhard model. The stress-strain response of the individual materials as well as the horizontal deformations of the sheet-pile wall were compared between the 3D analysis and the 2D simulation with the VAT.

A summary of some key results and conclusions is provided in the following:

(i) The VAT was implemented into a 2D FE code for the numerical analysis of stabilised deep excavations with lime-cement columns.

(ii) The stress-strain responses of the soft clay and the columns were represented through an equivalent material using advanced soil models, thereby a realistic estimation of the soil response was achieved at the system level.

(iii) The 3D effects can be captured in a 2D analysis with a significantly reduced computational cost. The VAT enables the efficient incorporation of sensitivity analyses.

Paper D: Alternative ways of modelling stabilised excavations

The paper presents numerical analyses of a braced excavation in soft clay stabilised with lime-cement (LC) columns. The study compares the use of different constitutive models for stabilised clay with LC columns, as well as the 3D analysis and the 2D analysis with the Volume Averaging Technique (VAT), on the deformation and structural forces of the sheet-pile wall (SPW). In all simulations, the natural clay response was represented by the elastoplastic S–CLAY1S model.

Initially, the stabilised clay in the passive side of the excavation was simulated with a 2D model, using the averaged strength and stiffness properties based on current practice. Both linear-elastic perfectly-plastic (Mohr-Coulomb) and non-linear elastoplastic (MNhard) soil models were employed for the 2D analyses. The results showed that relying solely on unconfined compression tests for modelling the stabilised clay led to an underestimation of the deformations and structural forces of the SPW.

To account for the distinct hydromechanical response of the soft clay and LC columns, a 3D analysis was performed, in which the soft clay and LC columns were modelled separately using advanced constitutive models (the S–CLAY1S and MNhard models, respectively). Subsequently, the 2D analysis with VAT was performed to capture the 3D effects and the different responses of the individual materials. The 2D analysis with the technique provided results that closely matched the 3D simulation, demonstrating the potential of the proposed technique to efficiently capture the real soil behaviour in stabilised excavations.

A summary of some key results and conclusions is provided in the following:

(i) The 2D analyses using a simple averaging of stiffness/strength for the stabilised clay underestimated the deformations and structural forces of the sheet-pile wall compared to the 3D analysis.

(ii) Accounting for hardening/softening plasticity and stress-dependent stiffness when modelling the individual responses of natural clay and the column results in a more realistic representation of the stabilised clay compared to simple stiffness averaging.

(iii) The 2D analysis using VAT was able to better capture the 3D effects and the distinct responses of the soft clay and columns.

(iv) VAT proved to be a promising way to efficiently capture the real soil behaviour in plane strain analyses.

Paper E: Influential factors on the performance of embankments stabilised on deep-mixed columns.

Sensitivity analyses for an embankment stabilised with deep-mixed columns in soft natural clay were performed to examine time-dependent deformations for serviceability limit state. In the plane strain simulations, Volume Averaging Technique (VAT) by Vogler (2008) was employed. The robust assessment known as the Design of Experiments (DOE) adopted enhanced computational efficiency, while a range of model parameters, various stabilisation ratios and length configurations, including end-bearing and floating columns, were investigated. The system-level sensitivity analyses revealed the most influential factors governing the hydromechanical response of stabilised clay. Additionally, to minimise both material consumption (i.e. lime and cement) and associated CO_2 emissions, case-specific optimal deep-mixing configurations were examined.

A summary of some key results and conclusions is provided in the following:

(i) The time-dependent hydromechanical response of an embankment in soft clays, stabilised with deep-mixed columns, can be efficiently predicted with VAT in a plane strain analysis.

(ii) Incorporating DOE enabled identifying the governing mechanisms and related factors having the largest impact for floating and end-bearing columns.

(iii) The parameters of the soft clay have a considerable influence on the computed settlements and horizontal movements when using floating columns. The order of deformations and the magnitude of stress rotations decreased with increasing column length, while the column stiffness became more significant in the response for the end-bearing columns.

(iv) The link between the column length, stabilisation ratio (volume fraction), and the relative stiffness between the clay and the columns revealed the possibility of using less rigid columns to reduce the cost originating from the use of lime and cement, and associated anthropogenic greenhouse gas emissions.

5 Conclusions and recommendations

5.1 Conclusions

The time-dependent evolution of deformations in stabilised clay with deep-mixed columns was investigated at system-level for deep excavations and embankments, specifically for Serviceability Limit State (SLS), using the finite element framework. Traditional semi-empirical and numerical schemes for modelling the stress-strain response of stabilised clays were reviewed, and several shortcomings were identified, such as non-conservative predictions of displacements caused by the oversimplification of the constitutive response of the soil-column system, and the omission of the interaction effects inherent in the three-dimensional (3D) problem.

The methodology adopted consisted of two main stages. The first involved a site-specific investigation of a deep excavation stabilised with lime-cement (LC) columns in soft natural clay. The second extended the insights gained by generalising the response of stabilised clay for excavations using numerical modelling, including the development, implementation, and verification of the Volume Averaging Technique (VAT). Finally, VAT was applied in sensitivity analyses for embankments, using Design of Experiments (DOE).

To address the limitations of existing methodologies, the composite system of columns and clay was investigated through two-dimensional (2D) and 3D fully coupled numerical simulations of a well-documented reference excavation project in Gothenburg, Sweden. The mechanical properties of the *in situ* clay and LC columns were evaluated using data from incrementally loaded oedometer tests, vane tests, and anisotropically consolidated triaxial tests. In the 3D model, the hydromechanical response of each material, including stabilised clay and *in situ* soft clay, was represented using separate constitutive models: the creep-rate-dependent Creep–SCLAY1S (Sivasithamparam et al. 2013; Sivasithamparam et al. 2015; Gras et al. 2018) and hyperbolic MNhard (Benz et al. 2008) models, respectively. The weighted average of the soil moduli represented the stabilised region in the passive side of the excavation for the 2D simulation. The results of the simulations were benchmarked against the field measurements. The simulations revealed that accurate predictions of displacements and structural forces require accounting for installation effects and 3D geometrical effects.

Secondly, the boundary conditions between the clay and the column materials in the newly formulated VAT (i.e. strain compatibility and stress equilibrium conditions) were derived from fully coupled 3D consolidation analysis of braced excavations stabilised with densely spaced deep-mixed columns.

Subsequently, VAT was implemented into a 2D FE code (PLAXIS 2D, version 23) as a User Defined Soil Model (UDSM). The results of the 2D simulations using VAT were benchmarked and verified against the corresponding full 3D analysis. The current implementation of VAT accommodates different constitutive models for clay and column materials, specifically the anisotropic S–CLAY1S (Koskinen et al. 2002; Karstunen et al. 2005) and MNhard (Benz et al. 2008) models. The predicted horizontal and vertical displacements, along with effective principal stresses, were in close agreement with those from the computationally expensive 3D analysis throughout the consolidation stages. As a result, VAT offers an efficient alternative to 3D modelling, producing similar outcomes while significantly reducing computational costs for SLS. The technique also provided

realistic estimates of displacement profiles and moment distributions for the supporting structures (i.e. sheet pile walls), which are critical for the design of excavations in urban environments.

The study above demonstrates that advanced numerical modelling using VAT can overcome the limitations of 3D model creation, particularly the requirement for numerous soil clusters, while maintaining comparable accuracy. VAT is also well suited for integration with data-driven techniques to optimise deep mixing designs. For example, different column layouts can be assessed by adjusting a single model parameter, i.e. column fraction. Thus, the capabilities of VAT were shown through system-level sensitivity analyses of a benchmark embankment stabilised with LC columns, using the implementation of Vogler (2008) and Abed et al. (2025) for embankment loading. The fully coupled consolidation analyses combining VAT with factorial design (Box et al. 2005; Montgomery 2020) were systematically performed to examine key factors influencing the long-term deformations of the embankment, including different centre to centre spacings, stabilisation ratios, column length configurations (floating or end-bearing), and the full set of model parameters for both columns and surrounding *in situ* clay. Thereby, the possibility of using less rigid columns for material-efficient deep-mixing designs was examined to minimise lime and cement use and their associated environmental impacts.

5.2 Recommendations

(i) Soil improvement using deep soil mixing requires stabilised soil that meets the required engineering properties as function of space and time, thus guaranteeing the performance of geostructures during the design life span (Kitazume 2021). Under field conditions, achieving fully homogeneous deep-mixed columns is unlikely, if not impossible (Honjo 1982; Baker 2000; Porbaha et al. 2000; Larsson et al. 2005b; Wong et al. 2024). Therefore, incorporating probabilistic methods into numerical analyses using VAT, such as the Random Finite Element method (Vanmarcke 1977; Fenton and Vanmarcke 1990), enables to account for the spatial variability of the properties of both natural clay and deep-mixed columns in a computationally effective manner.

(ii) In infrastructure construction, especially for road & railway embankments, system-level analysis with VAT leads to a better prediction of soil response by integrating soil-structure interaction and accounting for individual material responses (clay and column), compared to semi-empirical methods. The VAT framework can, in principle, be implemented with any combination of suitable constitutive models for its constituents, such as the rate-dependent response of stabilised clay. The influence of creep for both LC columns and soft natural clays has not been fully explored at the system level as a boundary value problem, particularly for cases involving significant loading, such as embankments on soft clays. VAT can also be extended to study other key aspects, such as degradation of stiffness under dynamic loading, varying hydraulic conductivity in soft clay and LC columns (Baker 1999; Lorenzo and Bergado 2006), as well as secondary effects, such as temperature effects during curing, and partially saturated soil behaviour of the LC columns (Locat et al. 1996; Quang and Chai 2015).

(iii) The installation effects involve a multi-physics coupling problem (e.g. mechanical mixing with high air pressure, ion-exchange, pozzolanic reactions, volume change, heat transfer,

cementation, fluid flow, partial saturation, and deformations) in the time domain. Due to these complexities, back-analysis using field monitoring data as part of Observational Method to quantify the installation effects is recommended. This will improve the accuracy of predictions and enable responsive design decisions during and after the construction of geostructures. For a comprehensive investigation, numerical methods need to be combined with the thermo–hydro–mechanical–chemical (THMC) coupling framework, exploiting high-performance computing to deal with large deformations or computational challenges (e.g. frequent geometry updates).

(iv) More systematic inverse modelling strategies for updating the predicted magnitude and the extent of ground movements using data from wireless sensor networks, InSAR, and distributed fiber optic sensing (Apoji et al. 2023; Schweiger 2023; Amavasai et al. 2024) will greatly benefit from the computational efficiency of VAT.

References

Abed, A., Vogler, U., & Karstunen, M. (2025). Volume averaging technique for deep mixed columns under embankments: Verification and validation. *International Journal of Geomechanics*. https://doi.org/10.1061/IJGNAI/GMENG-11450 (cit. on pp. 4, 23, 64).

Adachi, T., Oka, F., & Zhang, F. (1998). An elasto-viscoplastic constitutive model with strain softening. *Soils and Foundations*, *38*(2), 27–35. https://doi.org/10.3208/SANDF.38.2_27 (cit. on p. 38).

Åhnberg, H., Bengtsson, P.-E., & Holm, G. (2001). Effect of initial loading on the strength of stabilised peat. *Proceedings of the Institution of Civil Engineers - Ground Improvement*, *5*(1), 35–40. https://doi.org/10.1680/grim.2001.5.1.35 (cit. on pp. 8, 9).

Åhnberg, H., & Holm, G. (1987). *On the influence of curing temperature on the shear strength of lime and cement stabilised soil* (Report No. 30). Swedish Geotechnical Institute (in Swedish). (Cit. on pp. 8, 11).

Åhnberg, H., & Holm, G. (1999). Stabilization of some Swedish organic soils with different types of binder. In H. Bredenberg, G. Holm, & B. B. Broms (Eds.), *Dry mix methods for deep soil stabilization: Proceedings of the International Conference on Dry Mix Methods for Deep Soil Stabilization, Stockholm, Sweden, 13–15 October 1999* (pp. 101–108). Routledge. https://doi.org/10.1201/9781315141466 (cit. on pp. 3, 8, 9).

Åhnberg, H. (2003). Measured permeabilities in stabilized Swedish soils. In L. F. Johnsen, D. A. Bruce, & M. J. Byle (Eds.), *Grouting and ground treatment: Proceedings of the Third International Conference on Grouting and Ground Treatment, Feb 10–12, 2003, New Orleans, Louisiana* (Vol. 1, pp. 622–633). American Society of Civil Engineers. https://doi.org/10.1061/40663(2003)34 (cit. on p. 9).

Åhnberg, H. (2004). Effects of back pressure and strain rate used in triaxial testing of stabilized organic soils and clays. *Geotechnical Testing Journal*, *27*(3), 250–259. https://doi.org/10.1520/gtj11453 (cit. on p. 8).

Åhnberg, H. (2006). *Strength of stabilised soil: A laboratory study on clays and organic soils stabilised with different types of binder* [Doctoral dissertation, Lund University]. Lund University Research Portal. https://portal.research.lu.se/en/publications/strength-of-stabilised-soil-a-laboratory-study-on-clays-and-organ. (Cit. on pp. 7, 8, 11).

Al-Naqshabandy, M. S., & Larsson, S. (2013). Effect of uncertainties of improved soil shear strength on the reliability of embankments. *Journal of Geotechnical and Geoenvironmental Engineering*, *139*(4), 619–632. https://doi.org/10.1061/(ASCE)GT.1943-5606.0000798 (cit. on pp. 16, 49).

Alamgir, M., Miura, N., Poorooshasb, H. B., & Madhav, M. R. (1996). Deformation analysis of soft ground reinforced by columnar inclusions. *Computers and Geotechnics*, *18*(4), 267–290. https://doi.org/10.1016/0266-352X(95)00034-8 (cit. on pp. 16, 17, 49).

Amavasai, A., Tahershamsi, H., Wood, T., & Dijkstra, J. (2024). Data assimilation for Bayesian updating of predicted embankment response using monitoring data. *Computers and Geotechnics*, *165*, 105936. https://doi.org/10.1016/j.compgeo.2023.105936 (cit. on p. 65).

Anderson, D. G., & Stokoe, K. H. (1978). Shear modulus: A time-dependent soil property. In M. L. Silver & D. Tiedemann (Eds.), *Dynamic geotechnical testing* (Vol. STP 654, pp. 66–90). ASTM International. https://doi.org/10.1520/STP35672S (cit. on p. 14).

Apoji, D., Sheil, B., & Soga, K. (2023). Shaping the future of tunneling with data and emerging technologies. *Data-Centric Engineering*, *4*, e29. https://doi.org/10.1017/dce.2023.24 (cit. on pp. 3, 65).

Ariyarathne, P., Liyanapathirana, D. S., & Leo, C. J. (2013). Comparison of different two-dimensional idealizations for a geosynthetic-reinforced pile-supported embankment. *International Journal of Geomechanics*, *13*(6), 754–768. https://doi.org/10.1061/(ASCE)GM.1943-5622.0000266 (cit. on p. 17).

Arroyo, M., Ciantia, M., Castellanza, R., Gens, A., & Nova, R. (2012). Simulation of cement-improved clay structures with a bonded elasto-plastic model: A practical approach. *Computers and Geotechnics*, *45*, 140–150. https://doi.org/10.1016/J.COMPGEO.2012.05.008 (cit. on p. 45).

Atkinson, J. H., Richardson, D., & Robinson, P. J. (1987). Compression and extension of K0 normally consolidated kaolin clay. *Journal of Geotechnical Engineering*, *113*(12), 1468–1482. https://doi.org/10.1061/(ASCE)0733-9410(1987)113:12(1468) (cit. on p. 18).

Atkinson, J. H. (1993). *An introduction to the mechanics of soils and foundations: Through critical state soil mechanics.* McGraw-Hill. (Cit. on p. 19).

Axelsson, M., & Larsson, S. (2003). Column penetration tests for lime-cement columns in deep mixing–experiences in Sweden. In L. F. Johnsen, D. A. Bruce, & M. J. Byle (Eds.), *Grouting and ground treatment: Proceedings of the Third International Conference on Grouting and Ground Treatment, Feb 10–12, 2003, New Orleans, Louisiana* (Vol. 1, pp. 681–694). American Society of Civil Engineers. https://doi.org/10.1061/40663(2003)39 (cit. on p. 8).

Bache, B. K. F., Wiersholm, P., Paniagua, P., & Emdal, A. (2022). Effect of temperature on the strength of lime–cement stabilized Norwegian clays. *Journal of Geotechnical and Geoenvironmental Engineering*, *148*(3), 04021198. https://doi.org/10.1061/(ASCE)GT.1943-5606.0002699 (cit. on p. 11).

Baker, S., Sällfors, G., & Alén, C. (2005). Deformation properties of lime/cement columns. Evaluation from in-situ full scale tests of stabilised clay. *Proceedings of the International Conference on Deep Mixing – Best Practice and Recent Advances, Deep Mixing'05, Stockholm, Sweden, May 23–25, 2005. Swedish Deep Stabilization Research Centre, c/o Swedish Geotechnical Institute (SD Report 13)*, *1*(1), 29–33 (cit. on p. 9).

Bak, H. M., Noorbakhsh, M., Halabian, A. M., Rowshanzamir, M., & Hashemolhosseini, H. (2021). Application of the Taguchi method to enhance bearing capacity in geotechnical engineering: Case studies. *International Journal of Geomechanics*, *21*(9), 04021167. https://doi.org/10.1061/(ASCE)GM.1943-5622.0002133 (cit. on p. 51).

Baker, S. (2000). *Deformation behavior of lime/cement column stabilized clay* [Doctoral dissertation, Chalmers University of Technology]. Chalmers Research. https://research.chalmers.se/en/publication/688. (Cit. on pp. 16, 17, 64).

Baker, S. (1999). Three dimensional consolidation settlement of stabilized soil using lime/cement columns. In H. Bredenberg, G. Holm, & B. B. Broms (Eds.), *Dry mix methods for deep soil stabilization: Proceedings of the International Conference on Dry Mix Methods for Deep Soil Stabilization, Stockholm, Sweden, 13–15 October 1999* (pp. 207–213). Routledge. https://doi.org/10.1201/9781315141466 (cit. on p. 64).

Balaam, N. P., & Booker, J. R. (1981). Analysis of rigid rafts supported by granular piles. *International Journal for Numerical and Analytical Methods in Geomechanics*, *5*(4), 379–403. https://doi.org/10.1002/nag.1610050405 (cit. on p. 16).

Balaam, N. P., & Booker, J. R. (1985). Effect of stone column yield on settlement of rigid foundations in stabilized clay. *International Journal for Numerical and Analytical Methods in Geomechanics*, *9*(4), 331–351. https://doi.org/10.1002/NAG.1610090404 (cit. on p. 16).

Barksdale, R. D., & Bachus, R. C. (1983). *Design and construction of stone columns* (Vol. I, Report No. FHWA/RD-83/026). Turner-Fairbank Highway Research Center, United States Federal Highway Administration. https://rosap.ntl.bts.gov/view/dot/25319. (Cit. on pp. 16, 17).

Barron, R. A. (1948). Consolidation of fine-grained soils by drain wells by drain wells. *Transactions of the American Society of Civil Engineers*, *113*(1), 718–742. https://doi.org/10.1061/TACEAT.0006098 (cit. on p. 16).

Becker, P., & Karstunen, M. (2013). Volume averaging technique in numerical modelling of floating deep mixed columns in soft soils. In M. A. Hicks, J. Dijkstra, M. Lloret-Cabot, & M. Karstunen (Eds.), *Installation effects in geotechnical engineering: Proceedings of the International Conference on Installation Effects in Geotechnical Engineering, Rotterdam, The Netherlands, 24–27 March 2013* (pp. 198–204). https://doi.org/10.1201/b13890 (cit. on pp. 23, 26).

Bell, F. G. (1996). Lime stabilization of clay minerals and soils. *Engineering Geology*, *42*(4), 223–237. https://doi.org/10.1016/0013-7952(96)00028-2 (cit. on pp. 7, 8).

Benz, T., Wehnert, M., & Vermeer, P. A. (2008). A lode angle dependent formulation of the hardening soil model. In *Proceedings of the 12th International Conference on Computer Methods and Advances in Geomechanics, Goa, India, 1–6 October, 2008* (Vol. 1, pp. 653–660). International Association for Computer Methods and Advances in Geomechanics. (Cit. on pp. 46–48, 63).

Benz, T. (2007). *Small-strain stiffness of soils and its numerical consequences* [Doctoral dissertation, University of Stuttgart]. Mitteilungen des Instituts für Geotechnik, Heft 55. https://www.igs.uni-stuttgart.de/institut/publikationen/mitteilungen/. (Cit. on pp. 6, 36, 44, 46, 47).

Bergado, D. T., Anderson, L. R., Miura, N., & Balasubramaniam, A. S. (1996). *Soft ground improvement in lowland and other environments*. American Society of Civil Engineers. (Cit. on p. 16).

Bergado, D. T., Ruenkrairergsa, T., Taesiri, Y., & Balasubramaniam, A. S. (1999). Deep soil mixing used to reduce embankment settlement. *Proceedings of the Institution of Civil Engineers - Ground Improvement*, *3*(4), 145–162. https://doi.org/10.1680/gi.1999.030402 (cit. on p. 17).

Bjerrum, L., & Eide, O. (1956). Stability of strutted excavations in clay. *Géotechnique*, *6*(1), 32–47. https://doi.org/10.1680/GEOT.1956.6.1.32 (cit. on p. 19).

Bjerrum, L., & Rosenqvist, I. T. (1956). Some Experiments With Artificially Sedimented Clays. *Géotechnique*, *6*(3), 124–136. https://doi.org/10.1680/geot.1956.6.3.124 (cit. on pp. 13, 14).

Bjerrum, L., & Lo, K. Y. (1963). Effect of aging of the shear-strength properties of a normally consolidated clay. *Géotechnique*, *13*(2), 147–157. https://doi.org/10.1680/geot.1963.13.2.147 (cit. on p. 12).

Bjerrum, L. (1967). Engineering geology of Norwegian normally-consolidated marine clays as related to settlements of buildings. *Géotechnique*, *17*(2), 83–118. https://doi.org/10.1680/geot.1967.17.2.83 (cit. on pp. 12, 14).

Bjerrum, L. (1973). Geotechnical problems involved in foundations of structures in the North Sea. *Géotechnique*, *23*(3), 319–358. https://doi.org/10.1680/GEOT.1973.23.3.319 (cit. on pp. 12–14, 16, 18, 19).

Boehm, D. W., Templeton, E., & Filz, G. M. (2005). Wet soil mixing to construct soilcrete columns for the transfer of large oil tank loads through highly compressible deltaic deposits. *Proceedings of the International Conference on Deep Mixing – Best Practice and Recent Advances, Deep Mixing'05, Stockholm, Sweden, May 23–25, 2005. Swedish Deep Stabilization Research Centre, c/o Swedish Geotechnical Institute (SD Report 13)*, *1*(2), 499–507 (cit. on p. 3).

Borror, C. M., Montgomery, D. C., & Myers, R. H. (2002). Evaluation of statistical designs for experiments involving noise variables. *Journal of Quality Technology*, *34*(1), 54–70. https://doi.org/10.1080/00224065.2002.11980129 (cit. on p. 51).

Box, G. E. P., Hunter, J. S., & Hunter, W. G. (2005). *Statistics for Experimenters: Design, Innovation, and Discovery* (2nd ed.). Wiley-Interscience. (Cit. on pp. 49, 51, 64).

Box, G. E., & Meyer, R. D. (1986). An analysis for unreplicated fractional factorials. *Technometrics*, *28*(1), 11–18. https://doi.org/10.1080/00401706.1986.10488093 (cit. on p. 51).

Bozkurt, S., Abed, A., & Karstunen, M. (2023a). 2D & 3D numerical analyses of a deep excavation supported by LC columns. In L. Zdravković, S. Kontoe, D. Taborda, & A. Tsiampousi (Eds.), *Proceedings of the 10th European Conference on Numerical Methods in Geotechnical Engineering* (pp. 1–6). International Society for Soil Mechanics and Geotechnical Engineering. https://doi.org/10.53243/NUMGE2023-188 (cit. on pp. 45, 115).

Bozkurt, S., Abed, A., & Karstunen, M. (2023b). Finite element analysis for a deep excavation in soft clay supported by lime-cement columns. *Computers and Geotechnics*, *162*, 105687. https://doi.org/10.1016/j.compgeo.2023.105687 (cit. on pp. 39, 93).

Bozkurt, S., Abed, A., & Karstunen, M. (2025a). Alternative ways of modelling stabilised excavations. *Proceedings of the 19th Nordic Geotechnical Meeting – Göteborg 2024 (SGF Report 1:2025)*, *1*, 160–173. Swedish Geotechnical Society. https://ngm2024.se/program/SGF%20R1-2025%20NGM%20volume%201.pdf (cit. on p. 141).

Bozkurt, S., Abed, A., & Karstunen, M. (2025b). Homogenisation method for braced excavations stabilised with deep-mixed columns. *Computers and Geotechnics*, *181*, 107095. https://doi.org/10.1016/j.compgeo.2025.107095 (cit. on p. 123).

Bozkurt, S., Dijkstra, J., & Karstunen, M. (2025c). Influential factors on the performance of embankments stabilised on deep-mixed columns. *Transportation Geotechnics*, *55*, 101643. https://doi.org/10.1016/j.trgeo.2025.101643 (cit. on p. 155).

Brandl, H. (1981). Alteration of soil parameters by stabilization with lime. In *Proceedings of the 10th International Conference on Soil Mechanics and Foundation Engineering, Stockholm, 15–19 June 1981* (Vol. 3, pp. 587–594). A.A. Balkema. (Cit. on pp. 7, 9).

Brady, N. C. (1984). *The nature and properties of soils* (9th ed.). MacMillan Publishing Company. (Cit. on p. 9).

Brinkgreve, R. B. J., & Vermeer, P. A. (2002). Plaxis finite element code for soil and rock analyses, Version 8. *Balkema, Rotterdam* (cit. on p. 25).

Broms, B. B., & Boman, P. (1979). Lime columns—A new foundation method. *Journal of the Geotechnical Engineering Division*, *105*(4), 539–556. https://doi.org/10.1061/AJGEB6.0000788 (cit. on pp. 7, 16).

Broms, B. B. (2004). Lime and lime/cement columns. In M. P. Moseley & K. Kirsch (Eds.), *Ground Improvement* (2nd ed., pp. 252–330). CRC Press. https://doi.org/10.1201/9780203489611 (cit. on pp. 9, 16).

Bruce, M. E. C., Berg, R. R., Filz, G. M., Terashi, M., Yang, D. S., & Collin, J. G. (2013). *Federal Highway Administration design manual: Deep mixing for embankment and foundation support*

(Report No. No. FHWA-HRT-13-046). United States Federal Highway Administration, Offices of Research & Development. Washington, D.C. https://rosap.ntl.bts.gov/view/dot/37379. (Cit. on pp. 3, 8, 16).

Burland, J. B. (1990). On the compressibility and shear strength of natural clays. *Géotechnique*, *40*(3), 329–378. https://doi.org/10.1680/geot.1990.40.3.329 (cit. on pp. 12, 13, 38).

Campolongo, F., Cariboni, J., & Saltelli, A. (2007). An effective screening design for sensitivity analysis of large models. *Environmental Modelling & Software*, *22*(10), 1509–1518. https://doi.org/10.1016/J.ENVSOFT.2006.10.004 (cit. on p. 49).

Canetta, G., & Nova, R. (1989). A numerical method for the analysis of ground improved by columnar inclusions [Special Issue on Soil Reinforcement]. *Computers and Geotechnics*, *7*(1), 99–114. https://doi.org/10.1016/0266-352X(89)90009-8 (cit. on pp. 4, 23, 25).

Carrillo, N. (1942). Simple two and three dimensional case in the theory of consolidation of soils. *Journal of Mathematics and Physics*, *21*(1-4), 1–5. https://doi.org/10.1002/SAPM19422111 (cit. on p. 16).

Carlsten, P. (1996). Lime and lime/cement columns. In J. Hartlén & W. Wolski (Eds.), *Embankments on Organic Soils* (Vol. 80, pp. 355-399). Elsevier. https://doi.org/10.1016/S0165-1250(96)80013-7 (cit. on p. 9).

Chai, J.-C., Shen, S.-L., Miura, N., & Bergado, D. T. (2001). Simple method of modeling PVD-improved subsoil. *Journal of Geotechnical and Geoenvironmental Engineering*, *127*(11), 965–972. https://doi.org/10.1061/(ASCE)1090-0241(2001)127:11(965) (cit. on p. 16).

Chai, J. C., Miura, N., Kirekawa, T., & Hino, T. (2010). Settlement prediction for soft ground improved by columns. *Proceedings of the Institution of Civil Engineers - Ground Improvement*, *163*(2), 109–119. https://doi.org/10.1680/grim.2010.163.2.109 (cit. on p. 17).

Chai, J. C., Shrestha, S., Hino, T., Ding, W. Q., Kamo, Y., & Carter, J. (2015). 2D and 3D analyses of an embankment on clay improved by soil–cement columns. *Computers and Geotechnics*, *68*, 28–37. https://doi.org/10.1016/J.COMPGEO.2015.03.014 (cit. on p. 17).

Chew, S. H., Kamruzzaman, A. H. M., & Lee, F. H. (2004). Physicochemical and engineering behavior of cement treated clays. *Journal of Geotechnical and Geoenvironmental Engineering*, *130*(7), 696–706. https://doi.org/10.1061/(ASCE)1090-0241(2004)130:7(696) (cit. on pp. 8–10).

Cheng, D., Reiner, D. M., Yang, F., Cui, C., Meng, J., Shan, Y., Liu, Y., Tao, S., & Guan, D. (2023). Projecting future carbon emissions from cement production in developing countries. *Nature Communications*, *14*(1), 8213. https://doi.org/10.1038/s41467-023-43660-x (cit. on p. 3).

Clare, K. E., & Pollard, A. E. (2015). The effect of curing temperature on the compressive strength of soil-cement mixtures. *Géotechnique*, *4*(3), 97–106. https://doi.org/10.1680/GEOT.1954.4.3.97 (cit. on p. 11).

Clough, G. W., & Lawrence, A. H. (1981). Clay anisotropy and braced wall behavior. *Journal of the Geotechnical Engineering Division*, *107*(7), 893–913. https://doi.org/10.1061/AJGEB6.0001168 (cit. on pp. 19, 20).

Crawford, C. B. (1960). The influence of rate of strain on effective stresses in sensitive clay. In *Papers on Soils 1959 Meetings*. ASTM International. https://doi.org/10.1520/STP44304S (cit. on p. 14).

Dafalias, B. F. Y., & Herrmann, L. R. (1986). Bounding surface plasticity. II: Application to isotropic cohesive soils. *Journal of Engineering Mechanics*, *112*(12), 1263–1291. https://doi.org/10.1061/(ASCE)0733-9399(1986)112:12(1263) (cit. on p. 45).

Davies, M., & Parry, R. (1985). Centrifuge modelling of embankments on clay foundations. *Soils and Foundations*, *25*(4), 19–36. https://doi.org/10.3208/sandf1972.25.4_19 (cit. on pp. 16, 18).

de Borst, R., & Heeres, O. M. (2002). A unified approach to the implicit integration of standard, non-standard and viscous plasticity models. *International Journal for Numerical and Analytical Methods in Geomechanics*, *26*(11), 1059–1070. https://doi.org/10.1002/nag.234 (cit. on p. 35).

Deb, K. (2008). Modeling of granular bed-stone column-improved soft soil. *International Journal for Numerical and Analytical Methods in Geomechanics*, *32*(10), 1267–1288. https://doi.org/10.1002/NAG.672 (cit. on p. 16).

Dennegård, B. (1984). *Late Weichselian and early Holocene stratigraphy in southwestern Sweden with emphasis on the Lake Vänern area* [Doctoral dissertation, University of Gothenburg]. GUPEA. https://gupea.ub.gu.se/handle/2077/17559. (Cit. on p. 12).

D'Ignazio, M., Länsivaara, T. T., & Jostad, H. P. (2017). Failure in anisotropic sensitive clays: finite element study of Perniö failure test. *Canadian Geotechnical Journal*, *54*(7), 1013–1033. https://doi.org/10.1139/cgj-2015-0313 (cit. on p. 16).

Duncan, J. M., & Chang, C. Y. (1970). Nonlinear analysis of stress and strain in soils. *Journal of the Soil Mechanics and Foundations Division*, *96*(5), 1629–1653. https://doi.org/10.1061/JSFEAQ.0001458 (cit. on p. 45).

Eades, J. L., & Grim, R. E. (1960). *Reaction of hydrated lime with pure clay minerals in soil stabilization* (Bulletin No. 262). Highway Research Board. (Cit. on p. 10).

Edefors, G., Larsson, F., & Lundgren, K. (2025). Computational homogenization for predicting the effective response of planar textile-reinforced concrete shells. *International Journal of Solids and Structures*, *320*, 113472. https://doi.org/10.1016/j.ijsolstr.2025.113472 (cit. on p. 4).

EN 14679. (2005). Execution of special geotechnical works–deep mixing. European Committee for Standardization. Brussels, Belgium. (Cit. on pp. 7, 16).

EN 1997-1. (2005). Eurocode 7: Geotechnical design - Part 1: General rules. European Committee for Standardization. Brussels, Belgium. (Cit. on pp. 3, 49).

EN 197-1. (2011). Cement – Part 1: Composition, specifications and conformity criteria for common cements. European Committee for Standardization. Brussels, Belgium. (Cit. on p. 7).

Eriksson, H., Gunther, J., & Ruin, M. (2005). MDM combines the advantages of dry and wet mixing. *Proceedings of the International Conference on Deep Mixing – Best Practice and Recent Advances, Deep Mixing'05, Stockholm, Sweden, May 23–25, 2005. Swedish Deep Stabilization Research Centre, c/o Swedish Geotechnical Institute (SD Report 13)*, *1*(2), 509–520 (cit. on p. 7).

Eriksson, H., Forsberg, T., & Hov, S. (2024). *Japanese Geotechnical Society Special Publication*, *11*(4), 72–79. https://doi.org/10.3208/JGSSP.VOL11.SL-2-03 (cit. on p. 7).

EuroSoilStab. (2002). Development of design and construction methods to stabilize soft organic soils: Design guide for soft soil stabilization. *CT97-0351. Project No. BE-96-3177. European Commission, Industrial and Materials Technologies Programme (Brite-EuRam III), Brussels* (cit. on pp. 3, 7, 8, 16).

Fenton, G. A., & Vanmarcke, E. H. (1990). Simulation of random fields via local average subdivision. *Journal of Engineering Mechanics*, *116*(8), 1733–1749. https://doi.org/10.1061/(ASCE)0733-9399(1990)116:8(1733) (cit. on p. 64).

Filz, G. M., Sloan, J. A., McGuire, M. P., Smith, M., & Collin, J. (2019). Settlement and vertical load transfer in column-supported embankments. *Journal of Geotechnical and Geoenvironmental*

Engineering, *145*(10), 04019083. https://doi.org/10.1061/(ASCE)GT.1943-5606.0002130 (cit. on p. 16).

Finno, R. J., Atmatzidis, D. K., & Nerby, S. M. (1988). Ground response to sheet pile installation in clay. *Proceedings of the Second Conference of the International Conference on Case Histories in Geotechnical Engineering*, *34*. https://scholarsmine.mst.edu/icchge/2icchge/2icchge-session6/34 (cit. on p. 21).

Finno, R. J., & Nerby, S. M. (1989). Saturated clay response during braced cut construction. *Journal of Geotechnical Engineering*, *115*(8), 1065–1084. https://doi.org/10.1061/(ASCE)0733-9410(1989)115:8(1065) (cit. on pp. 20, 21).

Flores, R. D. V., Emidio, G. D., & Impe, W. F. V. (2010). Small-strain shear modulus and strength increase of cement-treated clay. *Geotechnical Testing Journal*, *33*(1), 62–71. https://doi.org/10.1520/GTJ102354 (cit. on p. 8).

Forsman, J., Löfman, M., Ikävalko, J., & Korkiala-Tanttu, L. (2025). Low-carbon binders in six test deep mixing cases – variation of in-situ strength. *Transportation Geotechnics*, *53*, 101597. https://doi.org/10.1016/j.trgeo.2025.101597 (cit. on p. 3).

Freiseder, M. G. (1998). *Ein beitrag zur numerischen berechnung von tiefem baugrund in weichen böden (A contribution to the numerical calculation of deep excavations in soft soils)* [Doctoral dissertation, Graz University of Technology]. Mitteilungshefte der Gruppe Geotechnik Graz, Heft 3. https://www.tugraz.at/kooperationen/geotech/mitteilungshefte. (Cit. on p. 19).

Fritzson, H., Vesterberg, B., Holmén, M., & Lindh, P. (2024). Long-term properties of lime-cement treated clay. *Japanese Geotechnical Society Special Publication*, *11*(5), 96–101. https://doi.org/10.3208/JGSSP.VOL11.DS-1-01 (cit. on p. 11).

Gens, A., & Nova, R. (1993). Conceptual bases for a constitutive model for bonded soils and weak rocks. In *Proceedings of an International Symposium on Geotechnical Engineering of Hard Soils – Soft Rocks, Athens, Greece* (pp. 485–494). A.A. Balkema. (Cit. on pp. 42, 44, 45).

Ghadrdan, M., Shaghaghi, T., & Tolooiyan, A. (2020). Effect of negative excess pore-water pressure on the stability of excavated slopes. *Géotechnique Letters*, *10*(1), 20–29. https://doi.org/10.1680/jgele.19.00040 (cit. on p. 19).

Gras, J. P., Sivasithamparam, N., Karstunen, M., & Dijkstra, J. (2017). Strategy for consistent model parameter calibration for soft soils using multi-objective optimisation. *Computers and Geotechnics*, *90*, 164–175. https://doi.org/10.1016/J.COMPGEO.2017.06.006 (cit. on p. 43).

Gras, J. P., Sivasithamparam, N., Karstunen, M., & Dijkstra, J. (2018). Permissible range of model parameters for natural fine-grained materials. *Acta Geotechnica*, *13*, 387–398. https://doi.org/10.1007/S11440-017-0553-1 (cit. on pp. 6, 39, 43, 63).

Graham, J., Crooks, J. H., & Bell, A. L. (1983). Time effects on the stress-strain behaviour of natural soft clays. *Geotechnique*, *33*(3), 327–340. https://doi.org/10.1680/GEOT.1983.33.3.327 (cit. on p. 15).

Graham, J., & Houlsby, G. T. (1983). Anisotropic elasticity of a natural clay. *Géotechnique*, *33*(2), 165–180. https://doi.org/10.1680/geot.1983.33.2.165 (cit. on pp. 13, 19, 38).

Grimstad, G., Bujulu, P., & Nordal, S. (2008). A generalized constitutive model for stabilized quick clay. *Proceedings of the 15th Nordic Geotechnical Meeting, Sandefjord, September 4–6*, 187–194 (cit. on p. 45).

Grimstad, G., Degago, S. A., Nordal, S., & Karstunen, M. (2010). Modeling creep and rate effects in structured anisotropic soft clays. *Acta Geotechnica*, *5*(1), 69–81. https://doi.org/10.1007/S11440-010-0119-Y (cit. on p. 41).

Gunther, J., Holm, G., Westberg, G., & Eriksson, H. (2004). Modified Dry Mixing (MDM) – A new possibility in deep mixing. In *Geotechnical Engineering for Transportation Projects*. https://doi.org/10.1061/40744(154)127 (cit. on p. 7).

Hansbo, S. (1979). Consolidation of clay by band-shaped prefabricated drains. *Ground Engineering*, *12*(5), 16–25 (cit. on pp. 16, 17).

Hansbo, S. (1981). Consolidation of fine-grained soils by prefabricated drains. In *Proceedings of the 10th International Conference on Soil Mechanics and Foundation Engineering, Stockholm, 15–19 June 1981* (Vol. 3, pp. 677–682). A. A. Balkema. (Cit. on p. 16).

Hashin, Z. (1983). Analysis of composite materials—A survey. *Journal of Applied Mechanics*, *50*(3), 481–505. https://doi.org/10.1115/1.3167081 (cit. on p. 4).

Hayashi, H., Nishikawa, J., Ohishi, K., & Terashi, M. (2003). Field observation of long-term strength of cement treated soil, 598–609. https://doi.org/10.1061/40663(2003)32 (cit. on p. 11).

Hebib, S., & Farrell, E. R. (1999). Some experience of stabilising Irish organic soils. In H. Bredenberg, G. Holm, & B. B. Broms (Eds.), *Dry mix methods for deep soil stabilization: Proceedings of the International Conference on Dry Mix Methods for Deep Soil Stabilization, Stockholm, Sweden, 13–15 October 1999* (pp. 81–84). Routledge. https://doi.org/10.1201/9781315141466 (cit. on pp. 8, 9).

Helvacioglu, A., Sobocinski, R., & Thurner, R. (2024). Nearshore test field of wet deep soil mixing in Sweden. *Japanese Geotechnical Society Special Publication*, *11*(5), 108–113. https://doi.org/10.3208/jgssp.vol11.DS-1-03 (cit. on p. 7).

Hicher, P. Y., Wahyudi, H., & Tessier, D. (2000). Microstructural analysis of inherent and induced anisotropy in clay. *Mechanics of Cohesive-frictional Materials*, *5*(5), 341–371. https://doi.org/10.1002/1099-1484(200007)5:5<341::AID-CFM99>3.0.CO;2-C (cit. on p. 14).

Hight, D. W., Böese, R., Butcher, A. P., Clayton, C. R. I., & Smiths, P. R. (1992). Disturbance of the Bothkennar clay prior to laboratory testing. *Geotechnique*, *42*(2), 199–217. https://doi.org/10.1680/geot.1992.42.2.199 (cit. on p. 14).

Hill, R. (1963). Elastic properties of reinforced solids: Some theoretical principles. *Journal of the Mechanics and Physics of Solids*, *11*(5), 357–372. https://doi.org/10.1016/0022-5096(63)90036-X (cit. on p. 4).

Hird, C. C., Pyrah, I. C., & Russel, D. (1992). Finite element modelling of vertical drains beneath embankments on soft ground. *Géotechnique*, *42*(3), 499–511. https://doi.org/10.1680/geot.1992.42.3.499 (cit. on p. 16).

Holm, G., Andréasson, B., Bengtsson, P.-E., Bodare, A., & Eriksson, H. (2002). *Mitigation of track and ground vibrations by high speed trains at Ledsgard, Sweden* (Report No. 10). Swedish Deep Stabilization Research Centre. (Cit. on p. 7).

Honjo, Y. (1982). A probabilistic approach to evaluate shear strength of heterogeneous stabilized ground by deep mixing method. *Soils and Foundations*, *22*(1), 23–38. https://doi.org/10.3208/sandf1972.22.23 (cit. on pp. 49, 64).

Horpibulsuk, S., Miura, N., & Nagaraj, T. S. (2003). Assessment of strength development in cement-admixed high water content clays with Abrams' law as a basis. *Géotechnique*, *53*(4), 439–444. https://doi.org/10.1680/GEOT.2003.53.4.439 (cit. on p. 11).

Horpibulsuk, S., Miura, N., & Nagaraj, T. S. (2005). Clay–water/cement ratio identity for cement admixed soft clays. *Journal of Geotechnical and Geoenvironmental Engineering*, *131*(2), 187–192. https://doi.org/10.1061/(ASCE)1090-0241(2005)131:2(187) (cit. on p. 9).

Horpibulsuk, S., Liu, M. D., Liyanapathirana, D. S., & Suebsuk, J. (2010). Behaviour of cemented clay simulated via the theoretical framework of the Structured Cam Clay model. *Computers and Geotechnics*, *37*(1-2), 1–9. https://doi.org/10.1016/J.COMPGEO.2009.06.007 (cit. on p. 45).

Horpibulsuk, S., Chinkulkijniwat, A., Cholphatsorn, A., Suebsuk, J., & Liu, M. D. (2012). Consolidation behavior of soil–cement column improved ground. *Computers and Geotechnics*, *43*, 37–50. https://doi.org/10.1016/j.compgeo.2012.02.003 (cit. on p. 16).

Hov, S., Paniagua, P., Sætre, C., Rueslåtten, H., Størdal, I., Mengede, M., & Mevik, C. (2022). Lime-cement stabilisation of Trondheim clays and its impact on carbon dioxide emissions. *Soils and Foundations*, *62*(3), 101162. https://doi.org/https://doi.org/10.1016/j.sandf.2022.101162 (cit. on pp. 3, 7).

Hov, S., & Larsson, S. (2023). Strength and stiffness properties of laboratory-improved soft Swedish clays. *International Journal of Geosynthetics and Ground Engineering*, *9*(11). https://doi.org/10.1007/s40891-023-00432-3 (cit. on pp. 8, 9).

Hov, S., Meland, H., Helvacioglu, A., Thurner, R., & Amdal, Å. M. W. (2025). Distributed fiber-optic strain sensing in deep mixed columns. *Journal of Geotechnical and Geoenvironmental Engineering*, *151*(2), 05024015. https://doi.org/10.1061/JGGEFK.GTENG-12825 (cit. on p. 8).

Huang, J., Kelly, R., & Sloan, S. W. (2015). Stochastic assessment for the behaviour of systems of dry soil mix columns. *Computers and Geotechnics*, *66*, 75–84. https://doi.org/10.1016/j.compgeo.2015.01.016 (cit. on p. 49).

IEA. (2023). *Energy Technology Perspectives 2023* (Technical Report). International Energy Agency. France. https://www.iea.org/reports/energy-technology-perspectives-2023. (Cit. on p. 3).

Ignat, R., Baker, S., Liedberg, S., & Larsson, S. (2016). Behavior of braced excavation supported by panels of deep mixing columns. *Canadian Geotechnical Journal*, *53*(10), 1671–1687. https://doi.org/10.1139/cgj-2016-0137 (cit. on pp. 3, 20).

Ignat, R., Baker, S., Holmén, M., & Larsson, S. (2019). Triaxial extension and tension tests on lime-cement-improved clay. *Soils and Foundations*, *59*(5), 1399–1416. https://doi.org/10.1016/j.sandf.2019.06.004 (cit. on p. 8).

Ignat, R., Baker, S., Karstunen, M., Liedberg, S., & Larsson, S. (2020). Numerical analyses of an experimental excavation supported by panels of lime-cement columns. *Computers and Geotechnics*, *118*, 103296. https://doi.org/10.1016/j.compgeo.2019.103296 (cit. on pp. 3, 20, 22).

Inagaki, M., Abe, T., Yamamoto, M., Nozu, M., Yanagawa, Y., & Li, L. (2002). Behavior of cement deep mixing columns under road embankment. In P. Guo, R. Phillips, & R. Popescu (Eds.), *Physical modelling in geotechnics: Proceedings of the International Conference ICPGM '02, St John's, Newfoundland, Canada, 10–12 July 2002* (1st ed., pp. 967–972). Routledge. https://doi.org/10.1201/9780203743362-175 (cit. on p. 16).

Indraratna, B., Rujikiatkamjorn, C., Kelly, R., & Buys, H. (2010). Sustainable soil improvement via vacuum preloading. *Proceedings of the Institution of Civil Engineers - Ground Improvement*, *163*(1), 31–42. https://doi.org/10.1680/grim.2010.163.1.31 (cit. on p. 3).

Iorio, G., Marzano, I. P., & Panetta, G. (2024). Reinforced soil cement retaining walls for foundation pit excavation in Odessa (UA). *Japanese Geotechnical Society Special Publication*, *11*(4), 65–71. https://doi.org/10.3208/JGSSP.VOL11.SL-2-02 (cit. on p. 20).

Jamsawang, P., Boathong, P., Mairaing, W., & Jongpradist, P. (2016a). Undrained creep failure of a drainage canal slope stabilized with deep cement mixing columns. *Landslides*, *13*, 939–955. https://doi.org/10.1007/S10346-015-0651-9 (cit. on pp. 3, 20).

Jamsawang, P., Yoobanpot, N., Thanasisathit, N., Voottipruex, P., & Jongpradist, P. (2016b). Three-dimensional numerical analysis of a DCM column-supported highway embankment. *Computers and Geotechnics*, *72*, 42–56. https://doi.org/10.1016/j.compgeo.2015.11.006 (cit. on p. 17).

Jamsawang, P., Jamnam, S., Jongpradist, P., Tanseng, P., & Horpibulsuk, S. (2017). Numerical analysis of lateral movements and strut forces in deep cement mixing walls with top-down construction in soft clay. *Computers and Geotechnics*, *88*, 174–181. https://doi.org/10.1016/J.COMPGEO.2017.03.018 (cit. on p. 20).

Jamsawang, P., Voottipruex, P., Tanseng, P., Jongpradist, P., & Bergado, D. T. (2019). Effectiveness of deep cement mixing walls with top-down construction for deep excavations in soft clay: case study and 3D simulation. *Acta Geotechnica*, *14*(1), 225–246. https://doi.org/10.1007/s11440-018-0660-7 (cit. on p. 49).

Janbu, N. (1977). Slopes and excavations in normally and overconsolidated clays. *Proceedings of the 9th International Conference on Soil Mechanics and Foundation Engineering, Tokyo*, 549–566 (cit. on p. 20).

Jardine, R. J., Potts, D. M., Fourie, A. B., & Burland, J. B. (1986). Studies of the influence of non-linear stress–strain characteristics in soil–structure interaction. *Géotechnique*, *36*(3), 377–396. https://doi.org/10.1680/geot.1986.36.3.377 (cit. on pp. 18, 44).

Jellali, B., Bouassida, M., & de Buhan, P. (2005). A homogenization method for estimating the bearing capacity of soils reinforced by columns. *International Journal for Numerical and Analytical Methods in Geomechanics*, *29*(10), 989–1004. https://doi.org/10.1002/nag.441 (cit. on pp. 4, 23).

Jiang, Y., Han, J., & Zheng, G. (2013). Numerical analysis of consolidation of soft soils fully-penetrated by deep-mixed columns. *KSCE Journal of Civil Engineering*, *17*(1), 96–105. https://doi.org/10.1007/S12205-013-1641-X (cit. on p. 17).

Karstunen, M., Krenn, H., Wheeler, S. J., Koskinen, M., & Zentar, R. (2005). Effect of anisotropy and destructuration on the behavior of Murro test embankment. *International Journal of Geomechanics*, *5*(2), 87–97. https://doi.org/10.1061/(asce)1532-3641(2005)5:2(87) (cit. on pp. 6, 16, 19, 22, 36, 38, 63).

Karstunen, M., & Koskinen, M. (2008). Plastic anisotropy of soft reconstituted clays. *Canadian Geotechnical Journal*, *45*(3), 314–328. https://doi.org/10.1139/T07-073 (cit. on p. 38).

Karstunen, M., & Yin, Z. Y. (2010). Modelling time-dependent behaviour of Murro test embankment. *Géotechnique*, *60*(10), 735–749. https://doi.org/10.1680/geot.8.P.027 (cit. on pp. 13, 38).

Karlsson, M., Emdal, A., & Dijkstra, J. (2016). Consequences of sample disturbance when predicting long-term settlements in soft clay. *Canadian Geotechnical Journal*, *53*(12), 1965–1977. https://doi.org/10.1139/CGJ-2016-0129 (cit. on p. 14).

Kasama, K., Ochiai, H., & Yasufuku, N. (2000). On the stress-strain behaviour of lightly cemented clay based on an extended critical state concept. *Soils and Foundations*, *40*(5), 37–47. https://doi.org/10.3208/SANDF.40.5_37 (cit. on p. 45).

Kasama, K., Whittle, A. J., & Kitazume, M. (2019). Effect of spatial variability of block-type cement-treated ground on the bearing capacity of foundation under inclined load. *Soils and Foundations*, *59*(6), 2125–2143. https://doi.org/10.1016/j.sandf.2019.11.007 (cit. on p. 49).

Kawasaki, T., Niina, A., Saitoh, S., Suzuki, Y., & Honyo, Y. (1981). Deep mixing method using cement hardening agent. In *Proceedings of the 10th International Conference on Soil Mechanics and Foundation Engineering, Stockholm, 15–19 June 1981* (Vol. 3, pp. 721–724). A. A. Balkema. (Cit. on p. 9).

Khan, M. R. A., Hayano, K., & Kitazume, M. (2009). Behavior of sheet pile quay wall stabilized by sea-side ground improvement in dynamic centrifuge tests. *Soils and Foundations*, *49*(2), 193–206. https://doi.org/10.3208/SANDF.49.193 (cit. on p. 20).

Khaledi, K., Mahmoudi, E., Datcheva, M., König, D., & Schanz, T. (2016). Sensitivity analysis and parameter identification of a time dependent constitutive model for rock salt. *Journal of Computational and Applied Mathematics*, *293*, 128–138. https://doi.org/10.1016/J.CAM.2015.03.049 (cit. on p. 51).

Kitazume, M., & Maruyama, K. (2006). External stability of group column type deep mixing improved ground under embankment loading. *Soils and Foundations*, *46*(3), 323–340. https://doi.org/10.3208/sandf.46.323 (cit. on p. 16).

Kitazume, M., & Maruyama, K. (2007). Internal stability of group column type deep mixing improved ground under embankment loading. *Soils and Foundations*, *47*(3). https://doi.org/10.3208/sandf.47.437 (cit. on p. 16).

Kitazume, M., & Terashi, M. (2013). *The Deep Mixing Method* (1st ed.). CRC Press. https://doi.org/10.1201/b13873 (cit. on pp. 7, 8).

Kitazume, M. (2021). Recent development and future perspectives of quality control and assurance for the deep mixing method. *Applied Sciences*, *11*(19), 9155. https://doi.org/10.3390/app11199155 (cit. on p. 64).

Kitazume, M. (2024). Deep mixing technology – diversity and future development -. *Japanese Geotechnical Society Special Publication*, *11*(2), 1–16. https://doi.org/10.3208/JGSSP.VOL11.KL-1 (cit. on pp. 16, 49).

Kobayashi, I., Soga, K., Iizuka, A., & Ohta, H. (2003). Numerical interpretation of a shape of yield surface obtained from stress probe tests. *Soils and Foundations*, *43*(3), 95–103. https://doi.org/10.3208/SANDF.43.3_95 (cit. on p. 13).

Kolivand, F., & Rahmannejad, R. (2018). Estimation of geotechnical parameters using Taguchi's design of experiment (DOE) and back analysis methods based on field measurement data: Case study: Tehran Metro line no. 7. *Bulletin of Engineering Geology and the Environment*, *77*(4), 1763–1779. https://doi.org/10.1007/S10064-017-1042-3 (cit. on p. 51).

Kono, T., & Fujisawa, T. (2024). Application of high-slag cement for reducing CO2 emissions in grid-form deep cement mixing walls. *Japanese Geotechnical Society Special Publication*, *11*(3), 51–56. https://doi.org/10.3208/JGSSP.VOL11.SL-1-06 (cit. on p. 3).

Koskinen, M., Karstunen, M., & Wheeler, S. J. (2002). Modelling destructuration and anisotropy of a soft natural clay. In P. Mestat (Ed.), *Numerical Methods in Geotechnical Engineering: Proceedings of the 5th European Conference, Paris, 4–6 September* (pp. 11–19). Presses de l'ENPC. (Cit. on pp. 6, 22, 38, 42, 63).

Krenn, H., Karstunen, M., & Aalto, A. (2005). 2D and 3D Numerical Analyses of Deep-Stabilized Columns. *Proceedings of the International Conference on Deep Mixing – Best Practice and Recent Advances, Deep Mixing'05, Stockholm, Sweden, May 23–25, 2005. Swedish Deep*

Stabilization Research Centre, c/o Swedish Geotechnical Institute (SD Report 13), *1*(2), 547–554 (cit. on p. 17).

Krenn, H., & Karstunen, M. (2008). Numerical modelling of deep mixed columns below embankments constructed on soft soils. In M. Karstunen & M. Leoni (Eds.), *Geotechnics of Soft Soils: Focus on Ground Improvement: Proceedings of the 2nd International Workshop held in Glasgow, Scotland, 3–5 September 2008*. CRC Press. https://doi.org/10.1201/9780203883334 (cit. on pp. 16, 17).

Lacasse, S. M., Ladd, C. C., & Barsvary, A. K. (2011). Undrained behavior of embankments on New Liskeard varved clay. *10.1139/t77-041*, *14*(3), 367–388. https://doi.org/10.1139/T77-041 (cit. on p. 16).

Ladd, C. C., & Foott, R. (1974). New design procedure for stability of soft clays. *Journal of the Geotechnical Engineering Division*, *100*(7), 763–786. https://doi.org/10.1061/AJGEB6.0000066 (cit. on p. 16).

Lafifi, B., Rouaiguia, A., & Boumazza, N. (2019). Optimization of geotechnical parameters using Taguchi's Design of Experiment (DOE), RSM and desirability function. *Innovative Infrastructure Solutions*, *4*(1), 35. https://doi.org/10.1007/s41062-019-0218-z (cit. on p. 51).

Lagioia, R., & Nova, R. (1995). An experimental and theoretical study of the behaviour of a calcarenite in triaxial compression. *Géotechnique*, *45*(4), 633–648. https://doi.org/10.1680/geot.1995.45.4.633 (cit. on p. 44).

Lambe, T. W., & Whitman, R. V. (1991). *Soil mechanics*. John Wiley & Sons. (Cit. on p. 19).

Länsivaara, T., Mansikkamäki, J., & Lehtonen, V. (2014). Effective stress based stability analysis of normally consolidated clays. *Advances in Natural and Technological Hazards Research*, *36*, 317–328. https://doi.org/10.1007/978-94-007-7079-9_25 (cit. on p. 18).

Larsson, S., Dahlström, M., & Nilsson, B. (2005a). A complementary field study on the uniformity of lime-cement columns for deep mixing. *Proceedings of the Institution of Civil Engineers - Ground Improvement*, *9*(2), 67–77. https://doi.org/10.1680/grim.2005.9.2.67 (cit. on p. 51).

Larsson, S., Dahlström, M., & Nilsson, B. (2005b). Uniformity of lime-cement columns for deep mixing: a field study. *Proceedings of the Institution of Civil Engineers - Ground Improvement*, *9*(1), 1–15. https://doi.org/10.1680/grim.2005.9.1.1 (cit. on pp. 8, 51, 64).

Larsson, S., Stille, H., & Olsson, L. (2005c). On horizontal variability in lime-cement columns in deep mixing. *Géotechnique*, *55*(1), 33–44. https://doi.org/10.1680/geot.2005.55.1.33 (cit. on p. 51).

Larsson, S., & Kosche, M. (2005). A laboratory study on the transition zone around lime-cement columns. *Proceedings of the International Conference on Deep Mixing – Best Practice and Recent Advances, Deep Mixing'05, Stockholm, Sweden, May 23–25, 2005. Swedish Deep Stabilization Research Centre, c/o Swedish Geotechnical Institute (SD Report 13)*, *1*(1), 111–118 (cit. on pp. 9, 10).

Larsson, S., Rothhämel, M., & Jacks, G. (2009). A laboratory study on strength loss in kaolin surrounding lime–cement columns. *Applied Clay Science*, *44*(1), 116–126. https://doi.org/10.1016/j.clay.2008.12.009 (cit. on pp. 7, 9, 10).

Larsson, S., Malm, R., Charbit, B., & Ansell, A. (2012). Finite element modelling of laterally loaded lime–cement columns using a damage plasticity model. *Computers and Geotechnics*, *44*, 48–57. https://doi.org/10.1016/J.COMPGEO.2012.03.004 (cit. on pp. 20, 45).

Larsson, S. (2003). *Mixing processes for ground improvement by deep mixing* [Doctoral dissertation, Royal Institute of Technology]. DiVA. https://urn.kb.se/resolve?urn=urn:nbn:se:kth:diva-3667. (Cit. on p. 7).

Larsson, S. (2021). The Nordic dry deep mixing method: Best practice and lessons learned. *Deep Mixing – An Online Conference: Deep Mixing 2021, Best practice and legacy*. Deep Foundations Institute (cit. on p. 16).

Larsson, S. (1999). The mixing process at the dry jet mixing method. In H. Bredenberg, G. Holm, & B. B. Broms (Eds.), *Dry mix methods for deep soil stabilization: Proceedings of the International Conference on Dry Mix Methods for Deep Soil Stabilization, Stockholm, Sweden, 13–15 October 1999* (pp. 339–346). Routledge. https://doi.org/10.1201/9781315141466 (cit. on p. 7).

Law, K. T. (1978). Undrained strength anisotropy in embankment stability analysis. *Canadian Geotechnical Journal*, *15*(2), 306–309. https://doi.org/10.1139/T78-026 (cit. on p. 16).

Lee, K., Chan, D., & Lam, K. (2004). Constitutive Model for Cement Treated Clay in a Critical State Frame Work. *Soils and Foundations*, *44*(3), 69–77. https://doi.org/10.3208/SANDF.44.3_69 (cit. on p. 45).

Lee, F.-H., Lee, Y., Chew, S.-H., & Yong, K.-Y. (2005). Strength and modulus of marine clay-cement mixes. *Journal of Geotechnical and Geoenvironmental Engineering*, *131*(2), 178–186. https://doi.org/10.1061/(ASCE)1090-0241(2005)131:2(178) (cit. on p. 8).

Lee, J. S., & Pande, G. N. (1998). Analysis of stone-column reinforced foundations. *International Journal for Numerical and Analytical Methods in Geomechanics*, *22*(12), 1001–1020. https://doi.org/10.1002/(SICI)1096-9853(199812)22:12<1001::AID-NAG955>3.0.CO;2-I (cit. on pp. 4, 23, 25).

Lee, J., & Fenves, G. L. (1998). Plastic-Damage Model for Cyclic Loading of Concrete Structures. *Journal of Engineering Mechanics*, *124*(8), 892–900. https://doi.org/10.1061/(ASCE)0733-9399(1998)124:8(892) (cit. on p. 45).

Lehane, B. M., & Jardine, R. J. (2003). Effects of long-term pre-loading on the performance of a footing on clay. *Géotechnique*, *53*(8), 689–695. https://doi.org/10.1680/geot.2003.53.8.689 (cit. on p. 16).

Leonards, G. A., & Ramiah, B. K. (1960). Time effects in the consolidation of clays. In *Papers on Soils 1959 Meetings*. ASTM International. https://doi.org/10.1520/STP44309S (cit. on p. 12).

Leroueil, S., Roy, M., Rochelle, P. L., Brucy, F., & Tavenas, F. A. (1979). Behavior of destructured natural clays. *Journal of the Geotechnical Engineering Division*, *105*(6), 759–778. https://doi.org/10.1061/AJGEB6.0000823 (cit. on pp. 12, 13, 44).

Leroueil, S., Samson, L., & Bozozuk, M. (1982). Laboratory and field determination of preconsolidation pressures at Gloucester. *Canadian Geotechnical Journal*, *20*(3), 477–490. https://doi.org/10.1139/T83-056 (cit. on pp. 13, 14).

Leroueil, S., Kabbaj, M., Tavenas, F., & Bouchard, R. (1985). Stress-strain-strain rate relation for the compressibility of sensitive natural clays. *Géotechnique*, *35*(2), 159–180. https://doi.org/10.1680/geot.1985.35.2.159 (cit. on pp. 13–15, 38).

Leroueil, S., & Vaughan, P. R. (1990). The general and congruent effects of structure in natural soils and weak rocks. *Géotechnique*, *40*(3), 467–488. https://doi.org/10.1680/geot.1990.40.3.467 (cit. on pp. 12, 13).

Leroueil, S., Magnan, J.-P., & Tavenas, F. (1990). *Embankments on Soft Clays* [Chalmers Library Print Collection, EBSCOhost]. Ellis Horwood. (Cit. on p. 16).

Li, A. L., Rowe, R. K., & Asce, F. (2002). Some design considerations for embankments on rate sensitive soils. *Journal of Geotechnical and Geoenvironmental Engineering*, *128*(11), 885–897. https://doi.org/10.1061/(ASCE)1090-0241(2002)128:11(885) (cit. on p. 16).

Liu, M. D., Carter, J. P., Horpibulsuk, S., & Liyanapathirana, D. S. (2006). Modelling the behaviour of cemented clay. In *Ground Modification and Seismic Mitigation* (pp. 65–72). https://doi.org/10.1061/40864(196)10 (cit. on p. 45).

Liu, S. Y., Han, J., Zhang, D. W., & Hong, Z. S. (2008). A combined DJM-PVD method for soft ground improvement. *Geosynthetics International*, *15*(1), 43–54. https://doi.org/10.1680/gein.2008.15.1.43 (cit. on p. 10).

Lo, K. Y., & Morin, J. P. (1972). Strength anisotropy and time effects of two sensitive clays. *Canadian Geotechnical Journal*, *9*(3), 261–277. https://doi.org/10.1139/t72-030 (cit. on p. 14).

Locat, J., Bérubé, M.-A., & Choquette, M. (1990). Laboratory investigations on the lime stabilization of sensitive clays: shear strength development. *Canadian Geotechnical Journal*, *27*(3), 294–304. https://doi.org/10.1139/t90-040 (cit. on p. 7).

Locat, J., Tremblay, H., & Leroueil, S. (1996). Mechanical and hydraulic behaviour of a soft inorganic clay treated with lime. *Canadian Geotechnical Journal*, *33*(4), 654–669. https://doi.org/10.1139/T96-090-311 (cit. on pp. 9, 44, 64).

Löfroth, H. (2005). Properties of 10-year-old lime-cement columns. *Proceedings of the International Conference on Deep Mixing – Best Practice and Recent Advances, Deep Mixing'05, Stockholm, Sweden, May 23–25, 2005. Swedish Deep Stabilization Research Centre, c/o Swedish Geotechnical Institute (SD Report 13)*, *1*(1), 119–127 (cit. on p. 11).

Løken, T. (1970). Recent research at the Norwegian geotechnical institute concerning the influence of chemical additions on quick clay. *Geologiska Föreningen i Stockholm Förhandlingar*, *92*(2), 133–147. https://doi.org/10.1080/11035897009453673 (cit. on p. 13).

Lorenzo, G. A., & Bergado, D. T. (2003). New consolidation equation for soil-cement pile improved ground. *Canadian Geotechnical Journal*, *40*(2), 265–275. https://doi.org/10.1139/T02-114 (cit. on pp. 16, 17).

Lorenzo, G. A., & Bergado, D. T. (2006). Fundamental characteristics of cement-admixed clay in deep mixing. *Journal of Materials in Civil Engineering*, *18*(2), 161–174. https://doi.org/10.1061/(ASCE)0899-1561(2006)18:2(161) (cit. on pp. 11, 64).

Lubliner, J., Oliver, J., Oller, S., & Oñate, E. (1989). A plastic-damage model for concrete. *International Journal of Solids and Structures*, *25*(3), 299–326. https://doi.org/10.1016/0020-7683(89)90050-4 (cit. on p. 45).

Madhyannapu, R. S., Puppala, A. J., Nazarian, S., & Yuan, D. (2010). Quality Assessment and Quality Control of Deep Soil Mixing Construction for Stabilizing Expansive Subsoils. *Journal of Geotechnical and Geoenvironmental Engineering*, *136*(1), 119–128. https://doi.org/10.1061/(ASCE)GT.1943-5606.0000188 (cit. on p. 8).

Marte, R., Scharinger, F., & Lüftenegger, R. (2017). Panels Made by the Deep Mixing Method for a Building Pit Support in a Slope. In *Grouting 2017* (pp. 385–394). https://doi.org/10.1061/9780784480809.037 (cit. on p. 3).

Martinelli, M., Remmerswaal, G., & Reid, D. (2024). State parameter predictions based on cone penetration test simulated with MPM: an application to tailing deposits. *Géotechnique Letters*, *14*(4), 1–27. https://doi.org/10.1680/jgele.24.00025 (cit. on p. 51).

Massarsch, K. R., & Topolnicki, M. (2005). Regional Report: European Practice of Soil Mixing Technology. *Proceedings of the International Conference on Deep Mixing – Best Practice and Recent Advances, Deep Mixing'05, Stockholm, Sweden, May 23–25, 2005. Swedish Deep Stabilization Research Centre, c/o Swedish Geotechnical Institute (SD Report 13)*, *1*(1), R19–R45 (cit. on p. 7).

Massarsch, K. R. (2005). Deformation properties of stabilized soil columns. *Proceedings of the International Conference on Deep Mixing – Best Practice and Recent Advances, Deep Mixing'05, Stockholm, Sweden, May 23–25, 2005. Swedish Deep Stabilization Research Centre, c/o Swedish Geotechnical Institute (SD Report 13)*, *1*(1), 129–144 (cit. on p. 8).

Matsuoka, H., & Nakai, T. (1974). Stress-deformation and strength characteristics of soil under three different principal stresses. *Proceedings of the Japan Society of Civil Engineers*, *1974*(232), 59–70 (cit. on p. 46).

Matsuoka, H., & Nakai, T. (1982). A new failure criterion for soils in three dimensional stresses. *IUTAM Conference on Deformation and Failure of Granular Materials*, 253–263 (cit. on p. 46).

Matsuoka, H., & Nakai, T. (1985). Relationship among Tresca, Mises, Mohr-Coulomb and Matsuoka-Nakai failure criteria. *Soils and Foundations*, *25*(4), 123–128. https://doi.org/10.3208/sandf1972.25.4_123 (cit. on p. 47).

Miro, S., Hartmann, D., & Schanz, T. (2014). Global sensitivity analysis for subsoil parameter estimation in mechanized tunneling. *Computers and Geotechnics*, *56*, 80–88. https://doi.org/10.1016/j.compgeo.2013.11.003 (cit. on p. 51).

Mitchell, J. K., & Soga, K. (2005). *Fundamentals of Soil Behavior* (3rd ed.). John Wiley & Sons. (Cit. on pp. 12, 13).

Mitchell, J. K., Shen, C.-K., & Monismith, C. L. (1965). *Behavior of stabilized soils under repeated loading: Report 1: Background, equipment, preliminary investigations, repeated compression and flexure tests on cement-treated silty clay* (Contract Report No. 3-145). U.S. Army Engineer Waterways Experiment Station, Corps of Engineers, Vicksburg, Mississippi. (Cit. on p. 8).

Mitchell, J. K., & Dermatas, D. (1992). Clay soil heave caused by lime-sulfate reactions. *ASTM Special Technical Publication*, (1135), 41–64. https://doi.org/10.1520/stp15529s (cit. on p. 9).

Mitchell, J. K. (1956). The fabric of natural clays and its relation to engineering properties. *Proc. Highway Res. Board*, *35*, 693–713 (cit. on p. 12).

Miura, N., Horpibulsuk, S., & Nagaraj, T. S. (2001). Engineering behavior of cement stabilized clay at high water content. *Soils and Foundations*, *41*(5), 33–45. https://doi.org/10.3208/sandf.41.5_33 (cit. on pp. 8, 9).

Montgomery, D. C. (2020). *Design and Analysis of Experiments* (10th ed.). John Wiley & Sons. (Cit. on pp. 49, 51, 64).

Müthing, N., Zhao, C., Hölter, R., & Schanz, T. (2018). Settlement prediction for an embankment on soft clay [Ballina Embankment Prediction Symposium]. *Computers and Geotechnics*, *93*, 87–103. https://doi.org/10.1016/j.compgeo.2017.06.002 (cit. on p. 51).

Myers, R. H. (1999). Response surface methodology—Current status and future directions. *Journal of Quality Technology*, *31*(1), 30–44. https://doi.org/10.1080/00224065.1999.11979891 (cit. on p. 51).

Nagaraj, T. S., Yarigar, P., Miura, N., & Yamadera, A. (1998). Prediction of strength development in cement admixture based on water content. *Proceedings of the 2nd International Conference on Ground Improvement Geosystems*, *1*, 431–436 (cit. on p. 9).

Nakai, T., & Matsuoka, H. (1983). Shear behaviors of sand and clay under three-dimensional stress conditions. *Soils and Foundations*, *23*(2), 26–42. https://doi.org/10.3208/sandf1972.23.2_26 (cit. on p. 47).

Navin, M. P., & Filz, G. M. (2005). Statistical analysis of strength data from ground improved with DMM columns. *Proceedings of the International Conference on Deep Mixing – Best Practice and Recent Advances, Deep Mixing'05, Stockholm, Sweden, May 23–25, 2005. Swedish Deep Stabilization Research Centre, c/o Swedish Geotechnical Institute (SD Report 13)*, *1*(1), 145–154 (cit. on p. 8).

Navin, M. P., & Filz, G. M. (2006). Reliability of deep mixing method columns for embankment support. In *GeoCongress 2006* (pp. 1–6). https://doi.org/10.1061/40803(187)251 (cit. on pp. 16, 49).

Naylor, D. J., & Pande, G. N. (1981). *Finite elements in geotechnical engineering*. Pineridge Press, Swansea, UK. (Cit. on p. 35).

Nguyen, L., Fatahi, B., & Khabbaz, H. (2017). Development of a constitutive model to predict the behavior of cement-treated clay during cementation degradation: C3 model. *International Journal of Geomechanics*, *17*(7), 04017010. https://doi.org/10.1061/(ASCE)GM.1943-5622.0000863 (cit. on p. 45).

Nicholson, D. P., Tse, C., & Penny, C. (1999). *The observational method in ground engineering: Principles and applications* (Report No. R185). Construction Industry Research and Information Association (CIRIA). (Cit. on p. 49).

Nova, R., Castellanza, R., & Tamagnini, C. (2003). A constitutive model for bonded geomaterials subject to mechanical and/or chemical degradation. *International Journal for Numerical and Analytical Methods in Geomechanics*, *27*(9), 705–732. https://doi.org/10.1002/NAG.294 (cit. on pp. 13, 44).

Nova, R. (1986). Soil models as a basis for modelling the behaviour of geophysical materials. *Acta Mechanica*, *64*(1), 31–44. https://doi.org/10.1007/BF01180096 (cit. on p. 44).

Oates, J. A. H. (1998). Production of quicklime. In J. A. H. Oates (Ed.), *Lime and Limestone* (pp. 155–191). John Wiley & Sons. https://doi.org/10.1002/9783527612024.ch16 (cit. on p. 3).

Oka, F. (1985). Elasto/viscoplastic constitutive equations with memory and internal variables. *Computers and Geotechnics*, *1*(1), 59–69. https://doi.org/10.1016/0266-352X(85)90015-1 (cit. on p. 45).

Oliveira, P. J. V., Correia, A. A., & Lemos, L. J. (2017). Numerical prediction of the creep behaviour of an unstabilised and a chemically stabilised soft soil. *Computers and Geotechnics*, *87*, 20–31. https://doi.org/10.1016/J.COMPGEO.2017.02.006 (cit. on pp. 17, 45).

Omine, K., Ochiai, H., & Yoshida, N. (1998). Estimation of in-situ strength if cement-treated soils based on a two-phase mixture model. *Soils and Foundations*, *38*(4), 17–29. https://doi.org/10.3208/sandf.38.4_17 (cit. on pp. 23, 24).

Omine, K., Ochiai, H., & Bolton, M. D. (1999). Homogenization method for numerical analysis of improved ground with cement-treated soil columns. In H. Bredenberg, G. Holm, & B. B. Broms (Eds.), *Dry mix methods for deep soil stabilization: Proceedings of the International Conference on Dry Mix Methods for Deep Soil Stabilization, Stockholm, Sweden, 13–15 October 1999* (pp. 161–168). Routledge. https://doi.org/10.1201/9781315141466 (cit. on pp. 4, 23, 24).

O'Rourke, T. D., & McGinn, A. J. (2004). Case history of deep mixing soil stabilization for Boston Central Artery. In *Geotechnical Engineering for Transportation Projects* (pp. 77–136). https://doi.org/10.1061/40744(154)3 (cit. on pp. 8, 20).

O'Rourke, T. D., & O'Donnell, C. J. (1997). Field behavior of excavation stabilized by deep soil mixing. *Journal of Geotechnical and Geoenvironmental Engineering*, *123*(6). https://doi.org/10.1061/(asce)1090-0241(1997)123:6(516) (cit. on pp. 3, 9, 20, 21).

Ou, C.-Y., Teng, F.-C., & Wang, I.-W. (2008). Analysis and design of partial ground improvement in deep excavations. *Computers and Geotechnics*, *35*(4), 576–584. https://doi.org/10.1016/J.COMPGEO.2007.09.005 (cit. on pp. 3, 20, 22, 45).

Ou, C.-Y., Wu, T.-S., & Hsieh, H.-S. (1996). Analysis of deep excavation with column type of ground improvement in soft clay. *Journal of Geotechnical Engineering*, *122*(9), 709–716. https://doi.org/10.1061/(ASCE)0733-9410(1996)122:9(709) (cit. on p. 20).

Pan, Y., Shi, G., Liu, Y., & Lee, F.-H. (2018). Effect of spatial variability on performance of cement-treated soil slab during deep excavation. *Construction and Building Materials*, *188*, 505–519. https://doi.org/10.1016/J.CONBUILDMAT.2018.08.112 (cit. on p. 49).

Paniagua, P., Bache, B. K. F., Lund, A. K., & Karlsrud, K. (2021). Full-scale field-testing of lime-cement columns in a very sensitive clay. *IOP Conference Series: Earth and Environmental Science*, *710*(1), 012049. https://doi.org/10.1088/1755-1315/710/1/012049 (cit. on p. 8).

Pandey, B. K., Rajesh, S., & Chandra, S. (2022). Time-dependent behavior of embankment resting on soft clay reinforced with encased stone columns. *Transportation Geotechnics*, *36*, 100809. https://doi.org/10.1016/j.trgeo.2022.100809 (cit. on pp. 3, 49).

Paniagua, P., Falle, F. Å., Hov, S., Tekseth, K. R., Mirzaei, F., & Breiby, D. W. (2022a). Comparing laboratory and field samples of lime–cement-improved Norwegian clay. *Géotechnique Letters*, *12*(4), 265–271. https://doi.org/10.1680/jgele.22.00067 (cit. on p. 8).

Paniagua, P., Bache, B. K., Karlsrud, K., & Lund, A. K. (2022b). Strength and stiffness of laboratory-mixed specimens of stabilised Norwegian clays. *Proceedings of the Institution of Civil Engineers - Ground Improvement*, *175*(2), 150–163. https://doi.org/10.1680/jgrim.19.00051 (cit. on p. 8).

Patel, D. (2024). Observational Method. In M. Brown, J. Burland, T. Chapman, K. Higgins, H. Skinner, & D. Toll (Eds.), *ICE Manual of Geotechnical Engineering (2nd Edition), Volume I - Geotechnical Engineering Principles, Problematic Soils and Site Investigation* (pp. 1641–1653). ICE Publishing. (Cit. on p. 3).

Peck, R. B. (1969). Advantages and limitations of the observational method in applied soil mechanics. *Géotechnique*, *19*(2), 171–187. https://doi.org/10.1680/geot.1969.19.2.171 (cit. on pp. 3, 49, 56).

Perzyna, P. (1966). Fundamental problems in viscoplasticity. In G. G. Chernyi, H. L. Dryden, P. Germain, L. Howarth, W. Olszak, W. Prager, R. F. Probstein, & H. Ziegler (Eds.). Elsevier. https://doi.org/10.1016/S0065-2156(08)70009-7 (cit. on p. 39).

Phoon, K. K., Kulhawy, F. H., & Grigoriu, M. D. (2003). Multiple resistance factor design for shallow transmission line structure foundations. *Journal of Geotechnical and Geoenvironmental Engineering*, *129*(9), 807–818. https://doi.org/10.1061/(ASCE)1090-0241(2003)129:9(807) (cit. on p. 49).

Phoon, K.-K., & Kulhawy, F. H. (1999). Characterization of geotechnical variability. *Canadian Geotechnical Journal*, *36*(4), 612–624. https://doi.org/10.1139/t99-038 (cit. on p. 49).

Phutthananon, C., Jongpradist, P., Dias, D., Guo, X., Jamsawang, P., & Baroth, J. (2022). Reliability-based settlement analysis of embankments over soft soils reinforced with T-shaped deep cement mixing piles. *Frontiers of Structural and Civil Engineering*, *16*(5), 638–656. https://doi.org/10.1007/S11709-022-0825-1 (cit. on pp. 17, 49).

Pietruszczak, S., & Mróz, Z. (1982). Description of Anisotropic Consolidation of Clays. In J.-P. Boehler (Ed.), *Mechanical Behavior of Anisotropic Solids / Comportment Méchanique des Solides Anisotropes* (pp. 597–622). Springer Netherlands. (Cit. on p. 13).

Porbaha, A., Shibuya, S., & Kishida, T. (2000). State of the art in deep mixing technology. Part III: Geomaterial characterization. *Proceedings of the Institution of Civil Engineers - Ground Improvement*, *4*(3), 91–110. https://doi.org/10.1680/grim.2000.4.3.91 (cit. on pp. 7, 8, 10, 64).

Porbaha, A., Tanaka, H., & Kobayashi, M. (1998). State of the art in deep mixing technology: Part II. Applications. *Proceedings of the Institution of Civil Engineers - Ground Improvement*, *2*(3), 125–139. https://doi.org/10.1680/gi.1998.020303 (cit. on p. 7).

Pothiraksanon, C., Saowapakpiboon, J., Bergado, D. T., Voottipruex, P., & Abuel-Naga, H. M. (2010). Soft ground improvement with solar-powered drainage. *Proceedings of the Institution of Civil Engineers - Ground Improvement*, *163*(1), 23–30. https://doi.org/10.1680/grim.2010.163.1.23 (cit. on p. 3).

Potts, D. M., Dounias, G. T., & Vaughan, P. R. (1990). Finite element analysis of progressive failure of Carsington embankment. *Géotechnique*, *40*(1), 79–101. https://doi.org/10.1680/geot.1990.40.1.79 (cit. on p. 45).

Potts, D. M., & Zdravković, L. (1999). *Finite element analysis in geotechnical engineering: Volume One - Theory* [Chalmers Library Print Collection]. Thomas Telford. (Cit. on p. 35).

Puppala, A. J., Bhadriraju, V., Madhyannapu, R. S., Nazarian, S., & Williammee, R. (2006). Small strain shear moduli of lime-cement treated expansive clays. In *Geomechanics II* (pp. 58–70). https://doi.org/10.1061/40870(216)5 (cit. on p. 8).

Quang, N. D., & Chai, J. C. (2015). Permeability of lime- and cement-treated clayey soils. *Canadian Geotechnical Journal*, *52*(9), 1221–1227. https://doi.org/10.1139/CGJ-2014-0134 (cit. on pp. 9, 64).

Quiroga, A. J., Thompson, Z. M., Muraleetharan, K. K., Miller, G. A., & Cerato, A. B. (2017). Stress–strain behavior of cement-improved clays: testing and modeling. *Acta Geotechnica*, *12*(5), 1003–1020. https://doi.org/10.1007/s11440-017-0529-1 (cit. on p. 45).

Rampello, S., & Callisto, L. (2003). Predicted and observed performance of an oil tank founded on soil-cement columns in clayey soils. *Soils and Foundations*, *43*(4), 229–241. https://doi.org/10.3208/SANDF.43.4_229 (cit. on pp. 17, 18, 45).

Ramírez, A. L., & Korkiala-Tanttu, L. (2023). Stabilisation of Malmi soft clay with traditional and low-CO2 binders. *Transportation Geotechnics*, *38*, 100920. https://doi.org/10.1016/J.TRGEO.2022.100920 (cit. on pp. 3, 8).

Rankka, K., Andersson-Sköld, Y., Hultén, C., Larsson, R., Leroux, V., & Dahlin, T. (2004). *Quick clay in Sweden* (Report 65). Swedish Geotechnical Institute. (Cit. on p. 14).

Randolph, M. F., Carter, J. P., & Wroth, C. P. (1979). Driven piles in clay—the effects of installation and subsequent consolidation. *Géotechnique*, *29*(4), 361–393. https://doi.org/10.1680/GEOT.1979.29.4.361 (cit. on p. 21).

Reuss, A. (1929). Berechnung der Fließgrenze von Mischkristallen auf Grund der Plastizitätsbedingung für Einkristalle. *ZAMM - Journal of Applied Mathematics and Mechanics / Zeitschrift*

für Angewandte Mathematik und Mechanik, *9*(1), 49–58. https://doi.org/10.1002/zamm.19290090104 (cit. on p. 24).

Richardson, A. M., & Whitman, R. V. (1963). Effect of strain-rate upon undrained shear resistance of a saturated remoulded fat clay. *Géotechnique*, *13*(4), 310–324. https://doi.org/10.1680/geot.1963.13.4.310 (cit. on p. 14).

Rochelle, P. L., Sarrailh, J., Tavenas, F., Roy, M., & Leroueil, S. (1981). Causes of sampling disturbance and design of a new sampler for sensitive soils. *Canadian Geotechnical Journal*, *18*(1), 52–66. https://doi.org/10.1139/t81-006 (cit. on p. 14).

Roscoe, K. H., & Burland, J. B. (1968). On the generalized stress-strain behavior of "wet" clay. In *Engineering Plasticity: Papers for a Conference Held in Cambridge, March 1968* (pp. 535–609). Cambridge University Press. (Cit. on pp. 38, 45).

Rowe, P. W. (1962). The stress-dilatancy relation for static equilibrium of an assembly of particles in contact. *Proceedings of the Royal Society of London. Series A. Mathematical and Physical Sciences*, *269*(1339), 500–527. https://doi.org/10.1098/rspa.1962.0193 (cit. on p. 48).

Roy, R. K. (2010). *A primer on the Taguchi method* (2nd ed.). Society of Manufacturing Engineers. (Cit. on p. 51).

Ruff, C. G., & Ho, C. (1965). *Time-temperature-strength-reaction product relationships in lime-bentonite-water mixtures* [PhD dissertation, Iowa State University]. Iowa State University Digital Repository. https://doi.org/10.31274/rtd-180813-4545 (cit. on p. 11).

Saltelli, A., Ratto, M., Andres, T., Campolongo, F., Cariboni, J., Gatelli, D., Saisana, M., & Tarantola, S. (2008). *Global sensitivity analysis: The Primer*. John Wiley & Sons. (Cit. on p. 51).

Sargent, P., Hughes, P. N., & Rouainia, M. (2016). A new low carbon cementitious binder for stabilising weak ground conditions through deep soil mixing. *Soils and Foundations*, *56*(6), 1021–1034. https://doi.org/10.1016/J.SANDF.2016.11.007 (cit. on p. 3).

Savila, I.-M. E., Korkiala-Tanttu, L. K., Forsman, J. A., & Löfman, M. S. (2025). Mechanical properties of stabilized soil: study on recovered field samples from deep stabilization sites. *Transportation Geotechnics*, *51*, 101540. https://doi.org/10.1016/j.trgeo.2025.101540 (cit. on pp. 8, 11).

Schütz, R., Potts, D. M., & Zdravkovic, L. (2011). Advanced constitutive modelling of shotcrete: Model formulation and calibration. *Computers and Geotechnics*, *38*(6), 834–845. https://doi.org/10.1016/J.COMPGEO.2011.05.006 (cit. on p. 45).

Schädlich, B., & Schweiger, H. F. (2014). A new constitutive model for shotcrete. In M. A. Hicks, R. B. Brinkgreve, & A. Rohe (Eds.), *Numerical Methods in Geotechnical Engineering: Proceedings of the 8th European conference on numerical methods in geotechnical engineering, Delft, the Netherlands, 18–20 June 2014* (Vol. 1, pp. 103–108). https://doi.org/10.1201/b17017 (cit. on p. 45).

Schweiger, H. F., & Pande, G. N. (1986). Numerical analysis of stone column supported foundations. *Computers and Geotechnics*, *2*(6), 347–372. https://doi.org/10.1016/0266-352X(86)90030-3 (cit. on pp. 4, 23–25).

Schweiger, H. F., & Pande, G. N. (1988). Numerical analysis of a road embankment constructed in soft clay stabilised with stone columns. In G. Swoboda (Ed.), *Numerical Methods in Geomechanics: Proceedings of the Sixth International Conference on Numerical Methods in Geomechanics, Innsbruck, 11–15 April 1988* (Vol. 2, pp. 1329–1333). A. A. Balkema. (Cit. on pp. 23–25).

Schanz, T., Vermeer, P. A., & Bonnier, P. G. (1999). The hardening soil model: Formulation and verification. *Beyond 2000 in computational geotechnics. Ten Years of PLAXIS International. Proceedings of the international symposium, Amsterdam, March 1999*, 281–296. https://doi.org/10.1201/9781315138206-27 (cit. on pp. 22, 45, 46).

Schweiger, H. F. (2023). Numerical modelling of complex geotechnical problems — Three examples. In A. Zhussupbekov, Z. Sarsembayeva, & V. N. Kaliakin (Eds.), *Smart Geotechnics for Smart Societies* (pp. 190–201). CRC Press. https://doi.org/10.1201/9781003299127-17 (cit. on p. 65).

Schanz, T. (1998). *Zur modellierung des mechanischen verhaltens von reibungsmaterialen, habilitation (On the modeling of the mechanical behavior of friction materials, habilitation)* [Doctoral dissertation, University of Stuttgart]. Mitteilungen des Instituts für Geotechnik, Heft 45. https://www.igs.uni-stuttgart.de/institut/publikationen/mitteilungen/. (Cit. on p. 46).

SGF. (2000). *Lime and lime cement columns. Guide for design, construction and control* (Report 2:2000). Swedish Geotechnical Society, Linköping, Sweden (in Swedish). (Cit. on pp. 3, 8, 16).

Sheng, D., Sloan, S. W., & Yu, H. S. (2000). Aspects of finite element implementation of critical state models. *Computational Mechanics*, *26*, 185–196. https://doi.org/10.1007/s004660000166 (cit. on p. 41).

Shen, S.-L., Huang, X.-C., Du, S.-J., & Han, J. (2003a). Laboratory studies on property changes in surrounding clays due to installation of deep mixing columns. *Marine Georesources & Geotechnology*, *21*(1), 15–35. https://doi.org/10.1080/10641190306711 (cit. on pp. 7, 8, 10, 11).

Shen, S.-L., Miura, N., & Koga, H. (2003b). Interaction mechanism between deep mixing column and surrounding clay during installation. *Canadian Geotechnical Journal*, *40*(2), 293–307. https://doi.org/10.1139/t02-109 (cit. on pp. 10, 11).

Simoni, M., Wilkes, M. D., Brown, S., Provis, J. L., Kinoshita, H., & Hanein, T. (2022). Decarbonising the lime industry: State-of-the-art. *Renewable and Sustainable Energy Reviews*, *168*, 112765. https://doi.org/10.1016/J.RSER.2022.112765 (cit. on p. 3).

Sivasithamparam, N., Karstunen, M., Brinkgreve, R. B. J., & Bonnier, P. G. (2013). Comparison of two anisotropic creep models at element level. In M. A. Hicks, J. Dijkstra, M. Lloret-Cabot, & M. Karstunen (Eds.), *Installation Effects in Geotechnical Engineering - Proceedings of the International Conference on Installation Effects in Geotechnical Engineering, Rotterdam, The Netherlands, 24-27 March 2013* (pp. 72–78). https://doi.org/10.1201/b13890 (cit. on pp. 38, 39, 63).

Sivasithamparam, N., Karstunen, M., & Bonnier, P. (2015). Modelling creep behaviour of anisotropic soft soils. *Computers and Geotechnics*, *69*, 46–57. https://doi.org/10.1016/J.COMPGEO.2015.04.015 (cit. on pp. 6, 39, 63).

Skempton, A. W., & Northey, R. D. (1952). The sensitivity of clays. *Géotechnique*, *3*(1), 30–53. https://doi.org/10.1680/geot.1952.3.1.30 (cit. on p. 14).

Sloan, S. W. (1987). Substepping schemes for the numerical integration of elastoplastic stress–strain relations. *International Journal for Numerical Methods in Engineering*, *24*(5), 893–911. https://doi.org/10.1002/nme.1620240505 (cit. on p. 35).

Smith, I. M., & Hobbs, R. (1976). Biot analysis of consoidation beneath embankments. *Géotechnique*, *26*(1), 149–171. https://doi.org/10.1680/geot.1976.26.1.149 (cit. on p. 16).

Sobol', I. M. (1993). Sensitivity estimates for nonlinear mathematical models. *Mathematical Modelling and Computational Experiments*, *1*(4), 407–414 (cit. on p. 51).

Spross, J., Bergman, N., & Larsson, S. (2021). Reliability-based verification of serviceability limit states of dry deep mixing columns. *Journal of Geotechnical and Geoenvironmental Engineering*, *147*(3), 04020183. https://doi.org/10.1061/(ASCE)GT.1943-5606.0002458 (cit. on p. 49).

SS-EN ISO 14067:2018. (2018). *Greenhouse gases — Carbon footprint of products — Requirements and guidelines for quantification*. International Organization for Standardization. https://www.sis.se. (Cit. on p. 3).

Stevens, R. L., Rosenbaum, M. S., & Hellgren, L. G. (1991). Origins and engineering hazards of Swedish glaciomarine and marine clays. *Geological Society, London, Engineering Geology Special Publications*, *7*(1), 257–264. https://doi.org/10.1144/GSL.ENG.1991.007.01.24 (cit. on p. 12).

Stevens, R. L., & Bayard, E. (1994). Clay mineralogy of agricultural soils (Ap horizon) in Västergötland, SW Sweden. *GFF*, *116*(2), 87–91. https://doi.org/10.1080/11035899409546163 (cit. on p. 12).

Stroh, D. (1974). *Berechnung verankerter Baugruben nach der Finite-Element-Methode (Design of Anchored Walls with the Finite Element Method)* [Doctoral dissertation, Technical University of Darmstadt]. Mitteilungsheft 13, Versuchsanstalt für Bodenmechanik und Grundbau der Technischen Hochschule Darmstadt. ULB Darmstadt. (Cit. on p. 19).

Suebsuk, J., Horpibulsuk, S., & Martin, D. L. (2010). Modified Structured Cam Clay: A generalised critical state model for destructured, naturally structured and artificially structured clays. *Computers and Geotechnics*, *37*(7), 956–968. https://doi.org/10.1016/J.COMPGEO.2010.08.002 (cit. on p. 45).

Swedish Transport Administration. (2018). *Fullskaleförsök DDM (Dry Deep Mixing) i passivzon, delprojekt E02 Centralen, Västlänken* (tech. rep. No. TRV 2015/74805). Swedish Transport Administration (Trafikverket). (Cit. on p. 11).

Swedish Transport Administration. (2019). *Redogörelse för konstruktionsarbetets förutsättningar och metoder (RKFM) – Temporär geokonstruktion: 4.1, 4.3, 4.4 och 5.3* (Report No. E02-16-015-2400-0_0-2201). Swedish Transport Administration (Trafikverket). (Cit. on p. 56).

Taguchi, G. (1987). *System of experimental design: Engineering methods to optimize quality and minimize Costs*. UNIPUB, Kraus International Publications. (Cit. on p. 51).

Tahershamsi, H., & Dijkstra, J. (2022). Using experimental design to assess rate-dependent numerical models. *Soils and Foundations*, *62*(6), 101244. https://doi.org/10.1016/J.SANDF.2022.101244 (cit. on p. 51).

Tahershamsi, H. (2023). *On cyclic accumulation models for degradation of railway foundations* [Doctoral dissertation, Chalmers University of Technology]. Chalmers Research. https://research.chalmers.se/en/publication/534868. (Cit. on p. 38).

Takahashi, H., Morikawa, Y., Fujii, N., & Kitazume, M. (2018). Thirty-seven-year investigation of quicklime-treated soil produced by deep mixing method. *Proceedings of the Institution of Civil Engineers: Ground Improvement*, *171*(3), 135–147. https://doi.org/10.1680/JGRIM.17.00044 (cit. on p. 11).

Tanaka, H. (1993). Behavior of braced excavations stabilized by deep mixing method. *Soils and Foundations*, *33*(2), 105–115. https://doi.org/10.3208/sandf1972.33.2_105 (cit. on p. 20).

Tatsuoka, F., & Kobayashi, A. (1983). Triaxial strength characteristics of cement-treated soft clay. In H. G. Rathmayer & K. H. O. Saari (Eds.), *Proceedings of the Eighth European Conference on Soil Mechanics and Foundation Engineering: Improvement of Ground, Helsinki, 23–26 May 1983* (Vol. 1, pp. 421–426). A. A. Balkema. (Cit. on p. 10).

Tatsuoka, F., Uchida, K., Imai, K., Ouchi, T., & Kohata, Y. (1997). Properties of cement-treated soils in Trans-Tokyo Bay Highway project. *Proceedings of the Institution of Civil Engineers - Ground Improvement*, *1*(1), 37–57. https://doi.org/10.1680/gi.1997.010105 (cit. on p. 8).

Tavenas, F., & Leroueil, S. (1980). The behaviour of embankments on clay foundations. *Canadian Geotechnical Journal*, *17*(2), 236–260. https://doi.org/10.1139/t80-025 (cit. on p. 16).

Tavenas, F., & Leroueil, S. (1985). Structural effects on the behaviour of natural clays. In M. Jamiolkowski, C. C. Ladd, J. T. Germaine, & R. Lancellotta (Eds.), *Proceedings of the Eleventh International Conference on Soil Mechanics and Foundation Engineering* (pp. 2693–2694). A.A. Balkema. (Cit. on p. 13).

Taylor, H. F. W. (1997). *Cement chemistry* (Vol. 2). Thomas Telford. London. (Cit. on pp. 3, 11).

Terzaghi, K. (1943). Theoretical Soil Mechanics. *John Wiley & Sons* (cit. on p. 19).

Trafikverket. (2014). Trafikverkets tekniska krav för geokonstruktioner, TK Geo 13 - ver 1.0. (Cit. on p. 8).

Uddin, K., Balasubramaniam, A. S., & Bergado, D. T. (1997). Engineering behavior of cement-treated Bangkok soft clay. *Geotechnical Engineering*, *28*(1), 89–119 (cit. on pp. 8, 9).

Unwin, W. C. (1886). On the rate of hardening of cement and cement mortars. *Minutes of the Proceedings of the Institution of Civil Engineers*, *84*(1886), 399–411. https://doi.org/10.1680/imotp.1886.21336 (cit. on p. 11).

Van Impe, W., Verastegui Flores, R., Mengé, P., & Van den Broeck, M. (2005). Considerations on laboratory test results of cement stabilised sludge. *Proceedings of the International Conference on Deep Mixing – Best Practice and Recent Advances, Deep Mixing'05, Stockholm, Sweden, May 23–25, 2005. Swedish Deep Stabilization Research Centre, c/o Swedish Geotechnical Institute (SD Report 13)*, *1*(1), 163–168 (cit. on p. 8).

van der Sluis, O., Schreurs, P. J. G., & Meijer, H. E. H. (1999). Effective properties of a viscoplastic constitutive model obtained by homogenisation. *Mechanics of Materials*, *31*(11), 743–759. https://doi.org/10.1016/S0167-6636(99)00028-9 (cit. on p. 4).

Vanmarcke, E. H. (1977). Reliability of earth slopes. *Journal of the Geotechnical Engineering Division*, *103*(11), 1247–1265. https://doi.org/10.1061/AJGEB6.0000518 (cit. on p. 64).

Vatsala, A., Nova, R., & Murthy, B. R. S. (2001). Elastoplastic model for cemented soils. *Journal of Geotechnical and Geoenvironmental Engineering*, *127*(8), 679–687. https://doi.org/10.1061/(ASCE)1090-0241(2001)127:8(679) (cit. on p. 45).

van Dijk, N. P. (2016). Formulation and implementation of stress-driven and/or strain-driven computational homogenization for finite strain. *International Journal for Numerical Methods in Engineering*, *107*(12), 1009–1028. https://doi.org/10.1002/nme.5198 (cit. on p. 4).

Vervoorn, R. R. E., & Barros, A. A. S. (2021). Deep soil mixing for stabilising deep excavations. *IOP Conference Series: Earth and Environmental Science*, *710*(1), 012060. https://doi.org/10.1088/1755-1315/710/1/012060 (cit. on p. 11).

Vermeer, P. A., & Brinkgreve, R. B. J. (1998). PLAXIS finite element code for soil and rock analysis. *Balkema, Rotterdam-Brookfield, Netherlands*, 1–114 (cit. on p. 46).

Vogler, U., & Karstunen, M. (2008). Application of volume averaging technique in numerical modelling of deep mixing. In M. Karstunen & M. Leoni (Eds.), *Geotechnics of Soft Soils: Focus*

on Ground Improvement: Proceedings of the 2nd International Workshop on Geotechnics of soft soils, Glasgow, Scotland, 3 – 5 September 2008 (1st ed., pp. 189–195). CRC Press. https://doi.org/10.1201/9780203883334 (cit. on pp. 4, 23, 25, 26, 45).

Vogler, U. (2008). *Numerical Modelling of Deep Mixing with Volume Averaging Technique* [Doctoral dissertation, University of Strathclyde]. University of Strathclyde repository. (Cit. on pp. 4, 17, 23, 25, 26, 35, 47, 55, 61, 64).

Voigt, W. (1889). Ueber die Beziehung zwischen den beiden Elasticitätsconstanten isotroper Körper. *Annalen der Physik*, *274*(12), 573–587. https://doi.org/10.1002/andp.18892741206 (cit. on p. 24).

Voottipruex, P., Bergado, D. T., Suksawat, T., Jamsawang, P., & Cheang, W. (2011). Behavior and simulation of deep cement mixing (DCM) and stiffened deep cement mixing (SDCM) piles under full-scale loading. *Soils and Foundations*, *51*(2), 307–320. https://doi.org/10.3208/SANDF.51.307 (cit. on p. 17).

Waichita, S., Jongpradist, P., Patawanit, P., Jamsawang, P., Arangelovski, G., & Likitlersuang, S. (2020a). Deformation and failure mechanism of deep cement mixing walls: experimental study using physical model tests. *Archives of Civil and Mechanical Engineering*, *21*(3), 1–17. https://doi.org/10.1007/S43452-021-00287-3 (cit. on p. 20).

Waichita, S., Jongpradist, P., & Schweiger, H. F. (2020b). Numerical and experimental investigation of failure of a DCM-wall considering softening behaviour. *Computers and Geotechnics*, *119*, 103380. https://doi.org/10.1016/J.COMPGEO.2019.103380 (cit. on pp. 20, 45).

Wang, D., & Tanttu, L. K. (2018). 1-D compressibility behaviour of cement-lime stabilized soft clays. *European Journal of Environmental and Civil Engineering*, *24*(7), 1013–1031. https://doi.org/10.1080/19648189.2018.1440633 (cit. on pp. 8, 9).

Wang, Z. Z., & Whittle, A. J. (2024). Effects of movement induced by ground improvement on the performance of an excavation support system in underconsolidated clay. *Journal of Geotechnical and Geoenvironmental Engineering*, *150*(2), 05023008. https://doi.org/10.1061/JGGEFK.GTENG-11588 (cit. on pp. 3, 20).

Wheeler, S. J., Näätänen, A., Karstunen, M., & Lojander, M. (2003). An anisotropic elastoplastic model for soft clays. *Canadian Geotechnical Journal*, *40*(2), 403–418. https://doi.org/10.1139/t02-119 (cit. on pp. 13, 38).

Wijerathna, M., Liyanapathirana, D. S., & Leo, C. J. (2017). Analytical Solution for the Consolidation Behavior of Deep Cement Mixed Column–Improved Ground. *International Journal of Geomechanics*, *17*(9), 04017065. https://doi.org/10.1061/(ASCE)GM.1943-5622.0000954 (cit. on pp. 16, 17).

Wijerathna, M., & Liyanapathirana, D. S. (2019). Significance of spatial variability of deep cement mixed columns on reliability of column-supported embankments. *International Journal of Geomechanics*, *19*(8), 04019087. https://doi.org/10.1061/(ASCE)GM.1943-5622.0001473 (cit. on p. 49).

Wiltafsky, C. (2003). *S-clay1s, User Defined Soil Model Documentation* (Report). University of Glasgow. UK. (Cit. on p. 35).

Wissa, A. E. Z., Ladd, C. C., & Lamb, T. W. (1965). Effective stress strength parameters of stabilized soils. *Proceedings of the Sixth International Conference on Soil Mechanics and Foundation Engineering, Montreal, 8–15 September, 1965*, *1*, 412–416 (cit. on p. 10).

Wong, D. Y.-C., Sadasivan, V., Isaksson, J., Karlsson, A., & Dijkstra, J. (2024). Trans-scale spatial variability of lime-cement mixed columns. *Construction and Building Materials*, *417*, 135394. https://doi.org/10.1016/j.conbuildmat.2024.135394 (cit. on pp. 8, 64).

Wood, D. M. (2004). *Geotechnical modelling*. CRC press. https://doi.org/10.1201/9781315273556 (cit. on p. 45).

Worrell, E., Price, L., Martin, N., Hendriks, C., & Meida, L. O. (2001). Carbon dioxide emissions from the global cement industry. *Annual Review of Environment and Resources*, *26*, 303–329. https://doi.org/10.1146/annurev.energy.26.1.303 (cit. on p. 3).

Wu, S.-H., Ching, J., Asce, M., & Ou, C.-Y. (2014). Simplified reliability-based design of wall displacements for excavations in soft clay considering cross walls. *Journal of Geotechnical and Geoenvironmental Engineering*, *141*(3), 06014017. https://doi.org/10.1061/(ASCE)GT.1943-5606.0001258 (cit. on p. 49).

Wu, C. F. J., & Hamada, M. (2021). *Experiments: Planning, Analysis, and Optimization*. John Wiley & Sons. https://doi.org/10.1002/9781119470007 (cit. on p. 49).

Xiao, H., Lee, F. H., & Liu, Y. (2017). Bounding surface Cam-Clay model with cohesion for cement-admixed clay. *International Journal of Geomechanics*, *17*(1), 04016026. https://doi.org/10.1061/(ASCE)GM.1943-5622.0000671 (cit. on p. 45).

Yang, I. C.-Y., Li, Y., Park, J. K., & Yen, T. F. (1993). The use of slime-forming bacteria to enhance the strength of the soil matrix. In E. T. Premuzic & A. Woodhead (Eds.), *Microbial enhancement of oil recovery—recent advances* (Vol. 39, pp. 89–96). Elsevier. https://doi.org/https://doi.org/10.1016/S0376-7361(09)70052-4 (cit. on p. 20).

Yao, K., Yao, Z., Song, X., Zhang, X., Hu, J., & Pan, X. (2016). Settlement evaluation of soft ground reinforced by deep mixed columns [Sustainability on Pavement Engineering]. *International Journal of Pavement Research and Technology*, *9*(6), 460–465. https://doi.org/10.1016/j.ijprt.2016.07.003 (cit. on p. 16).

Yao, K., Chen, Q., Xiao, H., Liu, Y., & Lee, F. H. (2020). Small-strain shear modulus of cement-treated marine clay. *Journal of Materials in Civil Engineering*, *32*(6), 04020114. https://doi.org/10.1061/(ASCE)MT.1943-5533.0003153 (cit. on p. 8).

Yapage, N. N. S., Liyanapathirana, D. S., Kelly, R. B., Poulos, H. G., & Leo, C. J. (2014). Numerical modeling of an embankment over soft ground improved with deep cement-mixed columns: Case history. *Journal of Geotechnical and Geoenvironmental Engineering*, *140*(11), 04014062. https://doi.org/10.1061/(ASCE)GT.1943-5606.0001165 (cit. on pp. 17, 18, 45).

Yin, J.-H., & Cheng, C.-M. (2006). Comparison of strain-rate dependent stress–strain behavior from K_0-consolidated compression and extension tests on natural Hong Kong marine deposits. *Marine Georesources & Geotechnology*, *24*(2), 119–147. https://doi.org/10.1080/10641190600704780 (cit. on pp. 13, 38).

Yin, Z.-Y., Karstunen, M., Chang, C. S., Koskinen, M., & Lojander, M. (2011). Modeling time-dependent behavior of soft sensitive clay. *Journal of Geotechnical and Geoenvironmental Engineering*, *137*(11), 1103–1113. https://doi.org/10.1061/(ASCE)GT.1943-5606.0000527 (cit. on pp. 13, 38, 41).

Yin, J.-H., & Graham, J. (1994). Equivalent times and one-dimensional elastic viscoplastic modelling of time-dependent stress–strain behaviour of clays. *Canadian Geotechnical Journal*, *31*(1), 42–52. https://doi.org/10.1139/T94-005 (cit. on p. 13).

Yong, D. M., Hayashi, K., & Chia, B. H. (1996). Jet grouting for the construction of a RC canal in soft marine clay. In R. Yonekura, M. Terashi, & M. Shibazaki (Eds.), *Grouting and*

Deep Mixing: Proceedings of IS–Tokyo '96: The Second International Conference on Ground Improvement Geosystems, Tokyo, 14–17 May 1996 (Vol. 1, pp. 375–380). A. A. Balkema. (Cit. on p. 10).

Yoshikuni, H., & Nakanodo, H. (1974). Consolidation of soils by vertical drain wells with finite permeability. *Soils and Foundations*, *14*(2), 35–46. https://doi.org/10.3208/sandf1972.14.2_35 (cit. on p. 16).

Yu, Y., Pu, J., & Ugai, K. (1997). Study of mechanical properties of soil–cement mixture for a cutoff wall. *Soils and Foundations*, *37*(4), 93–103. https://doi.org/10.3208/sandf.37.4_93 (cit. on p. 8).

Zdravkovic, L., Potts, D. M., & Hight, D. W. (2002). The effect of strength anisotropy on the behaviour of embankments on soft ground. *Géotechnique*, *52*(6), 447–457. https://doi.org/10.1680/GEOT.2002.52.6.447 (cit. on p. 16).

Zdravković, L., Potts, D. M., & Taborda, D. M. G. (2021). Integrating laboratory and field testing into advanced geotechnical design. *Geomechanics for Energy and the Environment*, *27*, 100216. https://doi.org/10.1016/J.GETE.2020.100216 (cit. on p. 18).

Zhang, W., Li, Y., Goh, A. T. C., & Zhang, R. (2020). Numerical study of the performance of jet grout piles for braced excavations in soft clay. *Computers and Geotechnics*, *124*, 103631. https://doi.org/10.1016/J.COMPGEO.2020.103631 (cit. on pp. 20, 49).

Zienkiewicz, O. C., & Cormeau, I. C. (1974). Visco-plasticity—plasticity and creep in elastic solids—a unified numerical solution approach. *International Journal for Numerical Methods in Engineering*, *8*(4), 821–845. https://doi.org/10.1002/NME.1620080411 (cit. on p. 14).

Zöhrer, A., Wehr, W., & Stelte, M. (2010). Is ground engineering environmentally friendly? Ecological balance of foundation engineering methods. *Proceedings of the 11th International EFFC-DFI Conference: Session 3 – Sustainability in the Foundation Industry* (cit. on p. 3).